6-2015

Lithologic Properties of the Upper Ordovician Utica Formation, Michigan Basin, USA: A Geological Characterization and Assessment of Carbon Dioxide Confinement Potential

Frank Richard Sattler
Western Michigan University

LITHOLOGIC PROPERTIES OF THE UPPER ORDOVICIAN UTICA FORMATION, MICHIGAN BASIN, USA: A GEOLOGICAL CHARACTERIZATION AND ASSESSMENT OF CARBON DIOXIDE CONFINEMENT POTENTIAL

by

Frank Richard Sattler

A thesis submitted to the Graduate College
in partial fulfillment of the requirements
for the degree of Master of Science
Geosciences
Western Michigan University
June 2015

Thesis Committee:

David Barnes, Ph.D., Chair
William B. Harrison III, Ph.D.
Peter Voice, Ph.D.

LITHOLOGIC PROPERTIES OF THE UPPER ORDOVICIAN UTICA FORMATION, MICHIGAN BASIN, USA: A GEOLOGICAL CHARACTERIZATION AND ASSESSMENT OF CARBON DIOXIDE CONFINEMENT POTENTIAL

Frank Richard Sattler, M.S.

Western Michigan University, 2015

The Utica/Maquoketa Shale is considered to be the primary confining layer for Cambro-Ordovician CO_2 sequestration targets in the Midwest in the Michigan and Illinois basins, respectively. Prospective regional geologic seals in mudrock formations possess a combination of lithologic properties including nanometer scale pore space, elevated breakthrough pressures for non-wetting fluid phases and ductile mechanical deformation. Mineralogical composition is related to and typically controls these properties.

The objective of this study is to investigate the geological controls on stratigraphic and lithologic variability in the Utica/Collingwood in the Michigan basin. Twelve conventional cores and hundreds of modern well logs from the Michigan basin were analyzed in order to correlate/calibrate wire-line log signatures with whole rock mineral composition (from X-ray diffraction analysis) and mechanical properties (from core analysis) to identify brittle, fracture-prone zones, and to validate the Utica Shale as a regional geologic seal. Analysis using scanning electron microscopy with Quantitative Evaluation of Minerals by Scanning Electron Microscope (QEMSCAN®) software was employed to image pores and for quantitative analysis of mineralogy, texture, and porosity. Mercury Injection Capillary Pressure test (MICP) and Triaxial Strength Testing were conducted in order to assess petrophysical and mechanical response. Spatial and stratigraphic distributions of lithological properties were mapped, documenting the distribution of lithologic properties of the Utica Shale in the Michigan basin.

ACKNOWLEDGMENTS

I would like to begin by acknowledging my thesis committee for answering my questions, supporting me, and remaining patient with me throughout this project. A special thanks to Dr. Dave Barnes for his direction and insight throughout this project as well as giving me the freedom to organize and control the project myself. The entire MGRRE facility was crucial to this project, including the staff: Bill and Linda Harrison and Jennifer Trout were especially helpful.

Secondly I would like to thank Dr. David Cole, Dr. Julie Sheets, and Alex Swift at The Ohio State University for allowing me access to the SEMCAL lab and directing me during my time in Columbus. I would also like to acknowledge Dr. Dennis Eberl for advice and help running the RockJock program.

Lastly, I would like to thank my friends and family. The graduate students at WMU have always been extremely approachable and helpful. A special thanks to the MGRRE students. We are always pushing each other on every class project and with thesis work, which has made me both a much better scientist and person. I thank you all very much. I would like to thank my Mom and Dad for supporting me and pushing me to be the best I can be. I would like to thank my brother Mike for getting me interested in science and teaching me so much along the way, and my brother Eric for constantly reminding me what an inquisitive mind really is. This thesis project is dedicated to my late Opa, who unfortunately was not able to see me finish my degree.

Frank Richard Sattler

TABLE OF CONTENTS

LIST OF TABLES

LIST OF FIGURES

List of Figures-Continued

1. INTRODUCTION

Study Objective

The objective of this study is geological characterization of the Upper Ordovician Utica Shale in the Michigan basin in order to assess CO_2 sequestration caprock (seal) potential, including petrophysical properties and mechanical fracture response. Detailed observations of mineralogical and textural variations in the Utica, from conventional core samples were compared to petrophysical and mechanical properties determined using a variety of analytical methodologies. The upper Ordovician Utica Shale is thought to be the primary hydrocarbon source rock, but also the ultimate seal for important, Ordovician Trenton-Black River hydrocarbon reservoirs in the Midwest. In the Northeast, the Utica Shale is known to be an unconventional hydrocarbon reservoir. In nearby states including Maryland, New York, Ohio, Pennsylvania, Virginia, and West Virginia the Utica Shale is estimated to contain as much as 38 trillion cubic feet of undiscovered, technically recoverable natural gas, 940 million barrels of oil and 208 million barrels of natural gas liquids (USGS, 2012). The Utica Shale formation in Michigan has received little attention as an unconventional reservoir, although significant production from unconventional hydrocarbon reservoirs in neighboring states is currently ongoing.

The Utica and Maquoketa Shale formations are considered to be the primary confining layer for Cambro-Ordovician CO_2 sequestration targets in the Midwest in the Michigan and Illinois basins (figure 1-1). Important saline aquifer, geological carbon sequestration reservoir targets in the Knox Supergroup and St. Peter Sandstone in Michigan, Illinois, Kentucky and Indiana have less laterally persistent, generally thinner and less reliable secondary confining zones but lateral continuity of the Utica Shale, dense mudrock lithology and thickness in excess of 100 ft. is noteworthy. The Utica Shale overlies the Trenton Formation and is overlain by the Queenston Shale in the Michigan basin. Although the Utica Shale is a prospective, unconventional hydrocarbon reservoir, there is currently little, publically available geological characterization

information related to the Utica Shale in the Michigan basin. This study establishes the spatial and stratigraphic distribution of lithological properties of the Utica Shale in the Michigan basin that may control regional confining layer integrity.

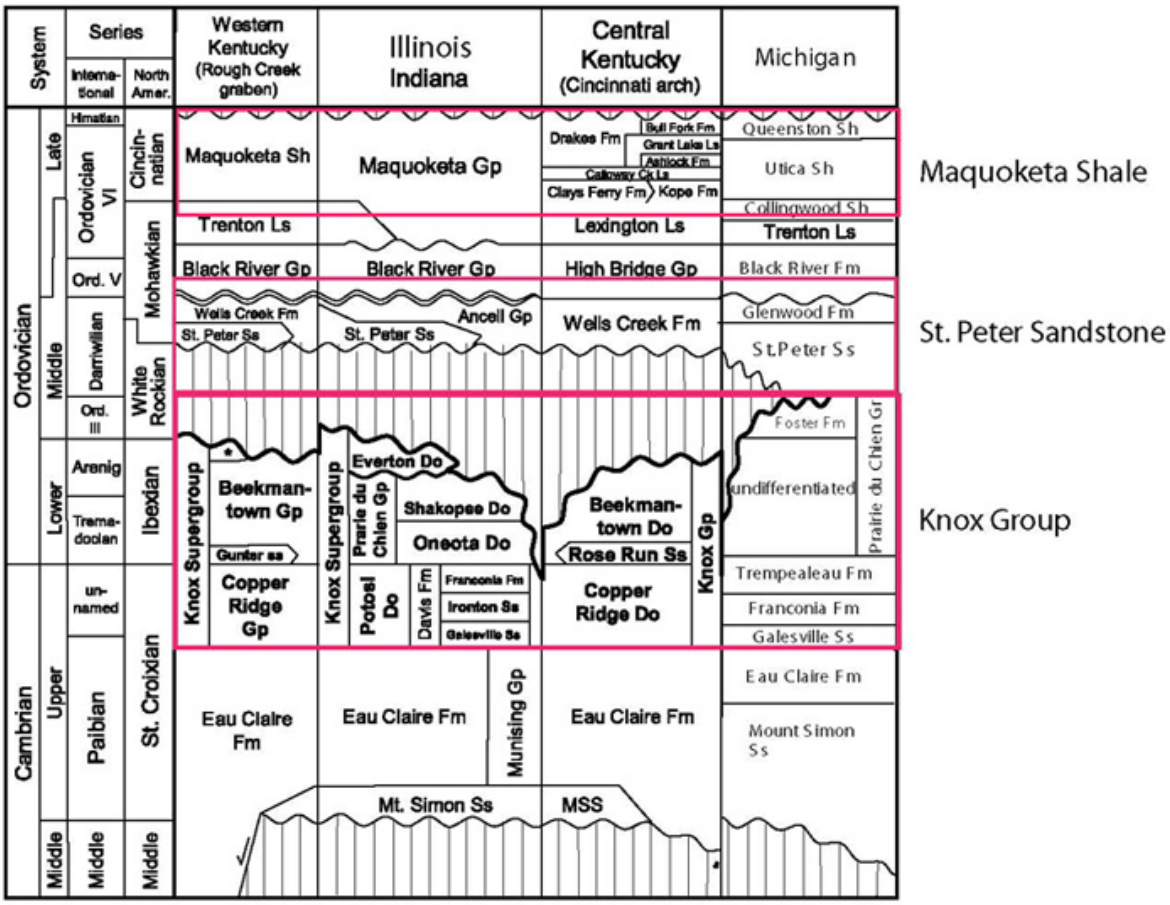

Figure 1-1: Utica Shale (and related strata) stratigraphy in the Illinois and Michigan basins.

Modified from Barnes, D.A. (knoxstp.org/mi-strat.htm)

The upper Ordovician Utica Shale underlies much of the northeastern United States and southern Canada. In Michigan, the Utica Shale is typically 200-400 ft. thick but thickens to greater than 475 ft. in the southeastern part of the Michigan basin (figure 1-2). The increased thickness observed in the southeastern part of the basin will be referred to as the "southeastern subbasin" in this study. The widespread geographical extent, generally dense and impermeable lithology, and thickness of the

Utica Shale make it a prospective confining zone for Cambro-Ordovician, regional geological carbon sequestration injection targets. Regional seal integrity is required for secure and permanent storage of CO_2,to ensure buoyant supercritical fluid confinement with no leakage of injected CO2 into overlying strata, underground sources of drinking water (USDW), soils or the atmosphere.

Whole rock mineralogy relates to rock ductility or brittleness and other mechanical properties, which affects rock strength and the development of permeability through fractures. Strata with high clay content will have relatively low strength, but will be less likely to develop fractures due to a high ductility. In contrast, increasing carbonate or silica content increases strength and will result in higher tendency to develop fractures due to an increase in rock brittleness (IEAGHG, 2011). The geological controls on lithological and mineralogical variability and corresponding mechanical properties are therefore a fundamental aspect of comprehensive seal integrity evaluation.

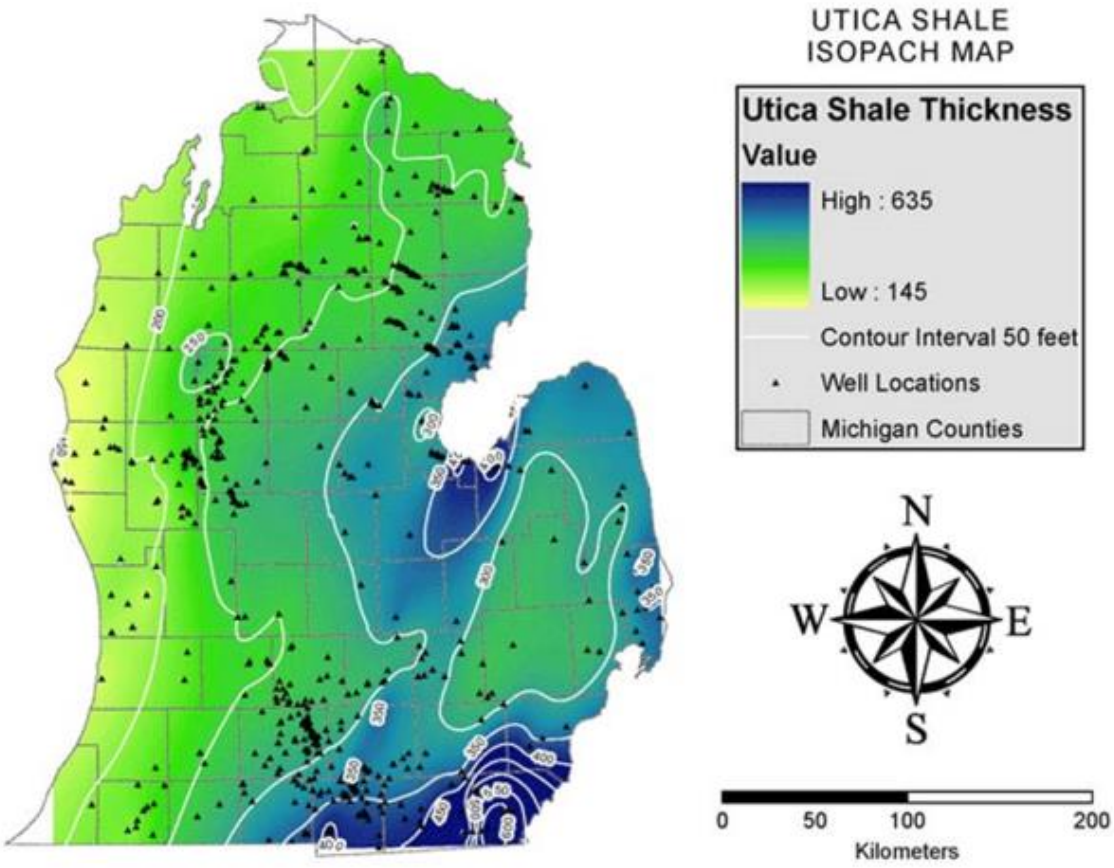

Figure 1-2: Utica (Shale) Formation Isopach. The widespread geographic extent of the Utica Formation makes it a potential seal for Cambro-Ordovician CO_2 sequestration targets.
Contour interval shown in gray
Modified from Barnes, D.A. (knoxstp.org/mi-strat.htm)

Michigan Basin Geology

Figure 1-3: Regional structural features related to the Michigan basin and proximity to proposed source terrain (Appalachian highlands)
Modified from Rupp, 1997

The Michigan basin is an intracratonic, bowl shaped basin centered in the lower peninsula of Michigan comprising up to 16,000 feet (4,900 m.) of sedimentary rock strata. It is slightly elongated in the N-S direction and approximately 300 miles (480 km.) in diameter (Banas, 2011; Howell & van der Pluijm 1990, 1999). The Michigan basin also includes parts of eastern Wisconsin; southwestern Ontario, Canada; northwestern Ohio; northeastern Illinois; and northern Indiana (Harrison III et al., 2009). Basin geodynamics include periods of basin-centered subsidence as well as regional, eastward tilting (Howell & van der Pluijm, 1999). The basin lies in-board in an intra-cratonic setting relative to the Appalachian basin and is bounded by the Kankakee and Findlay Arches (figure 1-3). Michigan basin bedrock geology at outcrop and the Pleistocene cub-crop

consists of Precambrian basement rocks around the margins and Paleozoic rocks of Cambrian through Pennsylvanian age up to as recent as Jurassic sedimentary strata in the basin center.

The Taconic orogeny refers to the North American mountain building episodes that occurred during the Ordovician (Faill, 1997). The Taconic orogeny was a complex series of orogenic episodes spread over the entire Ordovician period along what are now the Appalachian Mountains (Rodgers, 1971). Modern, eastern North America (Laurentia) was located south of the equator (figure 1-4) during the early Ordovician and was separated from the newly forming Taconic Island Arc by the Iapetus Ocean (Howell and Van der Pluijm, 1999). Late Ordovician Taconic orogenesis along proto-eastern North America caused the Iapetus Ocean to narrow and eventually closed the Laurentian-Taconic seaway (Faill, 1997). A convergent plate boundary developed and continental crust was uplifted. The uplifted igneous and sedimentary rocks were folded, faulted and eroded.

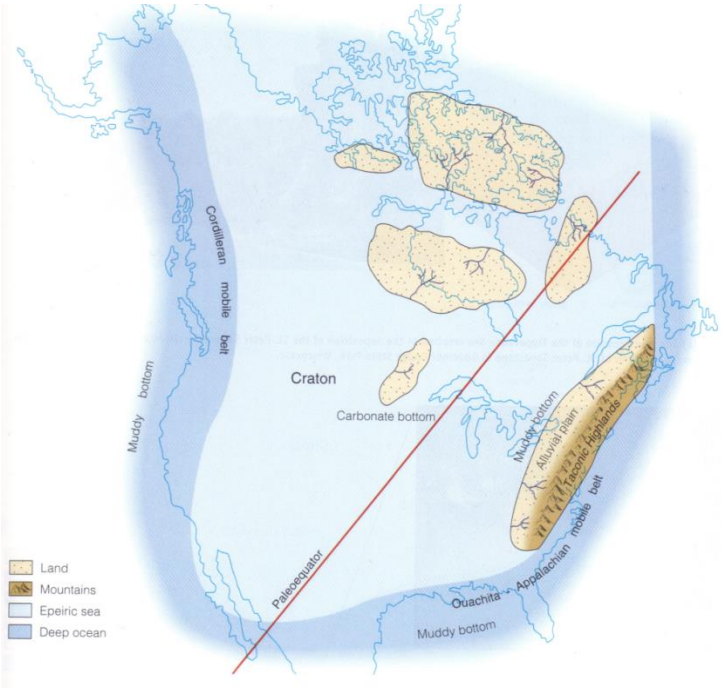

Figure 1-4: Michigan basin during the late Ordovician. Michigan is situated south of the equator with sediment being supplied from the southeast and east.
Modified from Wicander and Monroe, 2000.

Carbonate sedimentation dominated the Michigan basin during the early Ordovician. A vast carbonate platform spanned much of the eastern Laurentian continent and carbonate production on this platform kept pace with subsidence and sea-level rise, forming a thick succession of shallow marine, platform carbonate deposits of the Trenton/Black River now underlying the Utica Shale (Howell and Van der Pluijm, 1999). Fine-grained, organic-rich carbonate dominated strata of the Collingwood Shale (a member of the Trenton Formation) underlies the Utica Shale in the northern Michigan basin and is capped by a phosphatic lag deposit and hardground suggesting a long period of marine non-deposition (condensed interval) [Hiatt, 1985]. This contact is interpreted as a diastem. The Collingwood is a fine-grained organic rich member of the Trenton Formation. The Collingwood was observed to be a finely laminated calcareous biomicrite. The Collingwood is rich in organic content and has been an unconventional self-sourced reservoir target with organic carbon content as high as 4%. The phosphatic cap is found at the top of the Collingwood, separating the Collingwood from the Utica Shale.

Craton derived clastics were then initially deposited in the Taconic foreland basin with sediment being supplied from the newly uplifted Taconic highlands (Howell and Van der Pluijm, 1999). The locus of siliciclastic deposition migrated to the northwest and the middle Ordovician, shallow marine carbonate platform was drowned (Howell and Van der Pluijm, 1999). As a result of a regional sea level rise and transgression coincident with uplift in the Taconic highlands to the east, fine-grained siliciclastic sediments flooded the eastern interior platform and the Michigan, Illinois, and Appalachian basins and comprise the bulk of the Utica Shale. Spillover from the filled Taconic foreland basin resulted in the deposition of fine-grained clastics of the Utica Shale in the Michigan basin (Howell and Van der Pluijm, 1999).

The Utica Shale contact with underlying carbonate rocks of the Trenton Formation signifies an abrupt change in sedimentation. This observation is in support of a “drowning ramp scenario”, supported by Howell and Van der Pluijm (1999), in which relative sea level was rising through the late Ordovician. Taconian orogenic events

caused a shift in ocean currents, water oxygenation, and sediment sources. This change in depositional environment is shown by the sharp contact of the Utica Formation over Trenton-Black River carbonate deposits (Banas, 2011). This contact is marked by a sudden gamma-ray spike (GR) and a marked increase in the neutron porosity (NPHI) and decrease in photoelectric (PEF) log curves. These relationships make the top of the Trenton a widely traceable stratigraphic boundary in the Michigan basin, easily distinguishable on both petrophysical and lithologic logs.

The Utica Shale isopach shows a thickening in the southeastern part of the state. Fine-grained, argillaceous clastics of the Utica Shale were deposited with varying regional thickness and lithofacies (Hiattt, 1985; Banas, 2011; Howell & Van der Pluijm, 1990, 1999; Sharma et al., 2003; Sharma, 2004; Rancourt, 2009). Howell & Van der Pluijm, (1990) suggest the varying thicknesses observed in the Utica Shale isopach are the result of the infilling of bathymetric lows in the Michigan basin. This clastics-dominated succession is now found superjacent to Trenton/Black River strata that was deposited in a laterally extensive carbonate platform (Banas, 2011; Sharma et al., 2003). After the deposition of the Utica Shale, late Ordovician regional regression resulted in the return of shallow water conditions, and deposition of the mixed terrigenous-carbonate Queenston Formation (Brogly et al., 1998).

The Queenston Formation is poorly sampled and poorly understood in the Michigan basin. Wire-line log analysis shows a mixed system with interfingered clastic and carbonate units. The Utica is differentiated from the Queenston Formation by a shift in the wire-line log signature to a more carbonate-rich rock. The Queenston Formation is not sampled in this study but difficulty differentiating the Utica from the Queenston should be noted.

The Utica-Trenton contact is suggested to be a maximum flooding surface (MFS) and the Utica Shale was deposited during a high-stand systems tract, in an open marine environment. The upper interval of the Utica Shale was deposited in shallower water, and therefore is classified as a high stand systems tract where the Utica then transitions into the Queenston Formation.

2. METHODOLOGY

Conventional Core and Geophysical Well-Log Analysis

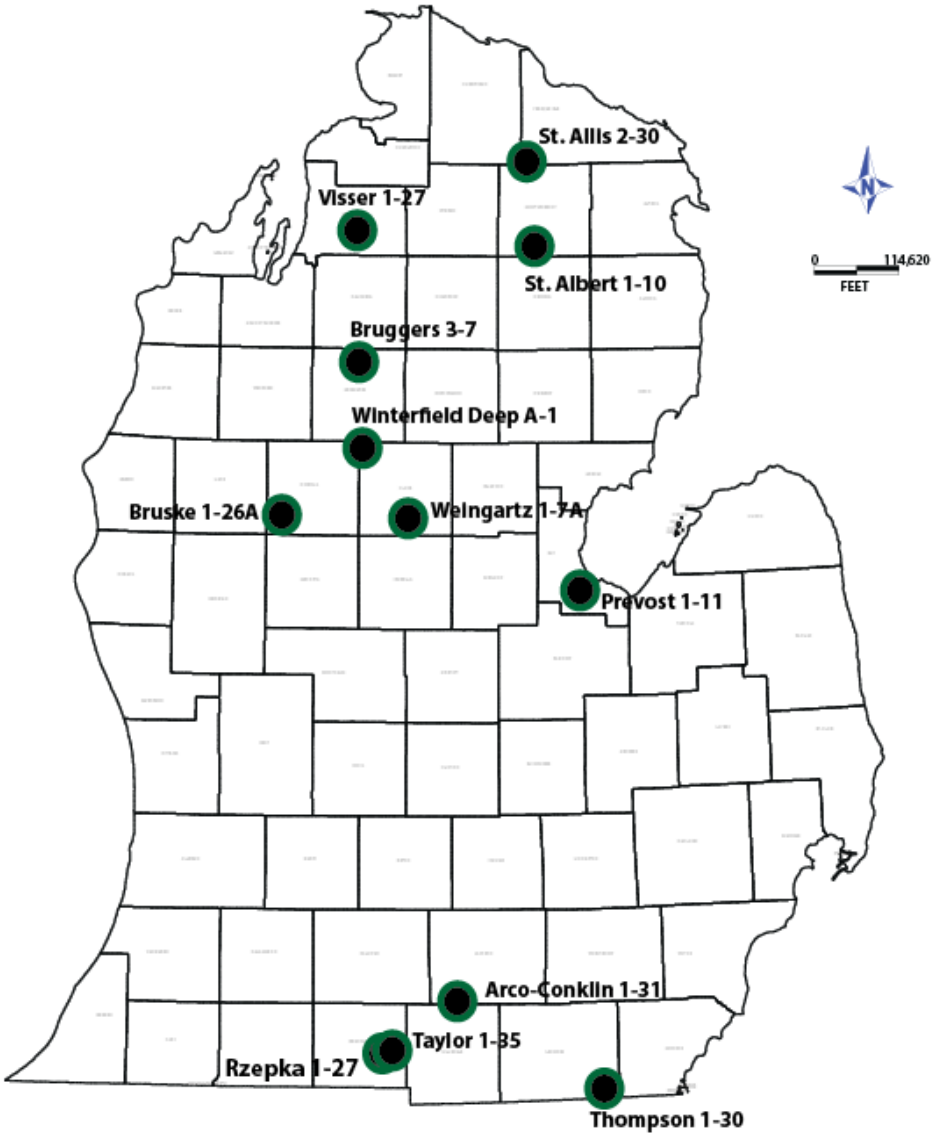

Figure 2- 1: Location of Utica Shale core used in this study.

Subsurface geophysical well-logs were used extensively in this study. The IHS Petra software is the primary software application used in this study for well log

analysis, subsurface mapping, and isopach contouring of the Utica Shale in the Michigan basin. Digital logs were used for interpretation and regional subsurface mapping in order to understand the subsurface distribution of lithofacies in the Michigan basin. Subsurface geophysical well-log analysis was conducted using subsurface data curated at the Michigan Geologic Repository for Research and Education (MGRRE), Kalamazoo, MI. The MGRRE facility houses more than 500,000 linear feet of conventional core from the Michigan basin as well as various software and petrographic tools that were utilized throughout this study. Twelve Utica Shale cores totaling over 500 ft. from the Michigan basin were analyzed in this study. Locations for Utica Shale cores used in this study are shown in figure 2-1. The Utica Shale has a relatively homogenous log signature throughout the Michigan basin (figure 2-2). The signature is characterized by an elevated gamma ray log response (generally > 150 gapi), as well as a low photoelectric factor (PEF), high neutron porosity (NPHI) and a (higher) bulk density (RHOB) log response than the underlying Trenton Formation. The NPHI and PEF curves overlie one another around 3,200 ft on the type log. This relationship (high NPHI and PEF ≈3.0) is indicative of a dolomitic mudrock and is persistent for roughly 200 ft in the type log.

Anomalous log signatures are observed in the basin around the Saginaw Bay area (figure 2-3). This signature makes it impossible to differentiate between log curves and therefore the Utica has not been mapped extensively in this region. Anomalous log signatures in the Saginaw Bay area are coincident with an isopach thick and the raster log files cannot be reliably digitized. The gamma-ray log response is not affected but the RHOB, NPHI, PE and caliper curves cannot be reliably digitized. The consistent mineralogy of the Utica in this area, inferred from the gamma-ray log compared to more reliable well logs elsewhere, does not support a shift in facies and there are no observable differences in the rock in core. The anomalous signature has a limited extent and is observed (at least partially) in Arenac, Gladwin, Midland, Bay, Saginaw and Tuscola counties. The signature roughly corresponds with the increased Utica Shale thickness observed in the isopach in the Saginaw Bay area, shown in figure 1-2.

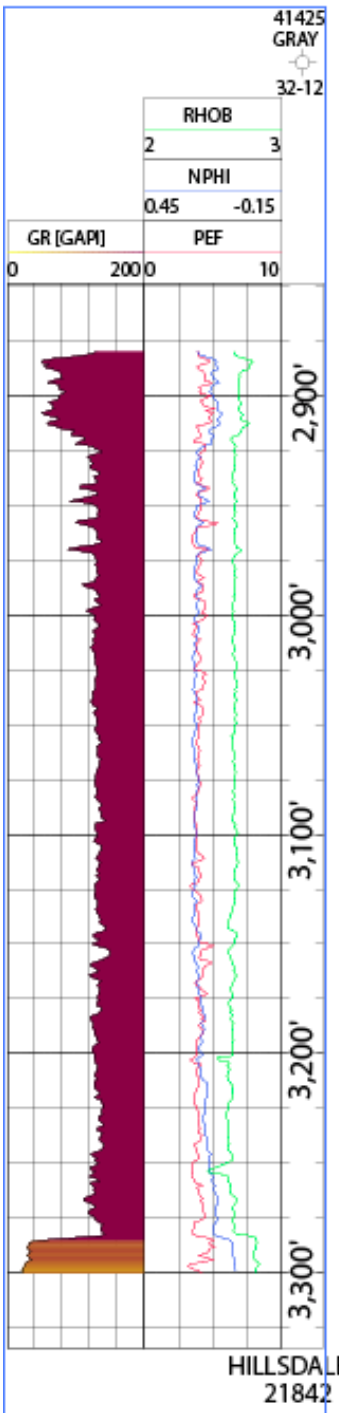

Figure 2- 2: Type log for the Utica Shale in the Michigan basin. The log response is typical of dense mudrock lithologies.

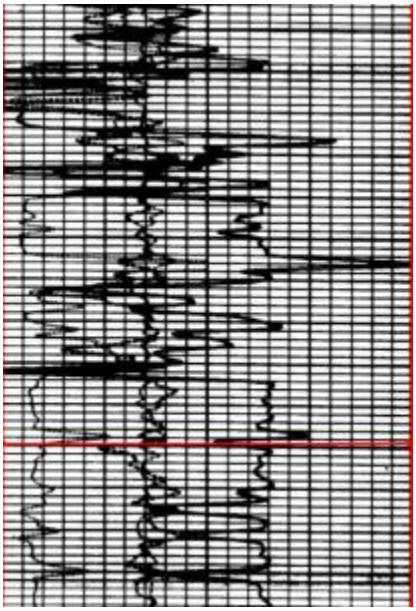

Figure 2- 3: Anomalous log signature found in the Saginaw Bay area. The gamma ray curve is unaffected but the NPHI, RHOB, PE and caliper curves cannot be digitized with confidence.

X-Ray Diffraction

Powder X-ray diffraction (XRD) is currently the best and most widely available technique for the identification and quantification of minerals present in clay-rich rocks (Środoń et al., 2001). Quantitative XRD analysis is used to determine the relative proportions of different minerals from a powdered, whole-rock sample. Quantitative XRD was used to evaluate the relative proportions of minerals present in the Utica Shale, in order to characterize the rock for both petrophysical and mechanical response. Clay minerals with variable chemical compositions and crystal structures dominate mudrocks and make the XRD analysis of clay-rich samples difficult. A wide range of intensities may be present for XRD reflections of different samples of the same clay mineral species, and furthermore clay mineral crystallites may differentially orientate in sample holders causing variability in sample intensities (Środoń et al., 2001). The platy nature of clay mineral crystallites results in a tendency for preferred orientation (Środoń et al., 2001). Randomly orientated samples may be used to avoid orientation-related problems, and can be used to determine the relative proportions of distinct clay

minerals within the clay-sized fraction. For these reasons errors amounting to ±10% are not uncommon for major components and ±20% for minor constituents.

Sample Preparation Procedure

Sample preparation is a fundamental aspect of accurate quantitative XRD analysis. Samples were ground with a mortar and pestle, mixed with an internal corundum standard and ground in a laboratory grinding mill with 4 ml of methanol. Samples were then dried and packed onto a holder and inserted into the Rigaku X-Ray Diffractometer at Western Michigan University.

X-rays are generated in a Cr- tube (wavelength 2.2909 Å) by a current measuring 15 mA. This current heats a tungsten filament, which liberates electrons that hit a Cr target. Cr- tubes have higher diffraction resolution at low 2θ angles than do Cu- tubes and are especially suitable for this study since clay minerals have low 2θ reflection peaks (large d-spacing). X-ray wave length emissions are then accelerated by a 30kV potential and passed through a Be window. The incident beam leaves the tube and passes through two slits (divergence and scattering) before coming into contact with the sample. The width and angle of the incident beam is determined by the size of the slits. Wider slits will provide more energy, but have wider peaks. Smaller slits provide less energy, but give better peak resolution. Clay minerals, especially detrital clays, have intrinsically broad peaks due to crystal defects, and the use of smaller slit sizes helps distinguish peaks from background (Moore and Reynolds, 1989). Arriving at an angle (Θ), x-rays are reflected from internal crystal planes separated by a distance (d). Bragg's Law refers to the equation $n\lambda = (2d)\sin\Theta$, where λ is the wavelength of the x-rays (2.2909 Å), Θ is the angle between the incident rays and the surface of the crystal and constructive interference occurs when n is an integer. The angle between the incident beam and the sample must be equal to the angle between the sample and the diffracted beam for Bragg's Law to apply (Moore and Reynolds, 1989). Bragg's Law explains the interaction of the beam and the sample, and provides unequivocal evidence for the structures of crystals, making XRD possible. Crystals will be orientated at random angles

when x-rays contact the sample. When the x-ray beam, crystal orientation and detector are orientated to satisfy Bragg's equation, a characteristic peak will be generated that represents the presence of a certain mineral. The detector rotates over a range of angles (minimum 5-65^{o}) to ensure sampling at all possible crystal orientations. X-rays diffracting a crystal pass through a receiving slit before ultimately arriving at the detector.

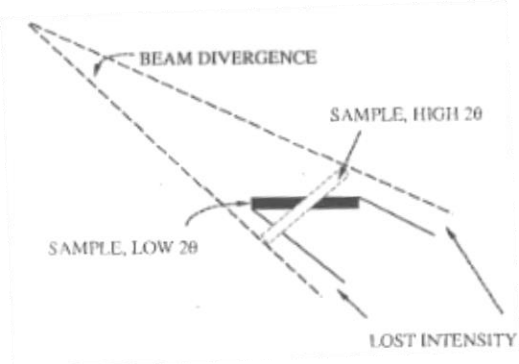

Figure 2- 4: Incident intensity loss at low diffraction angles
Modified from Moore and Reynolds, 1989

Characteristic peaks of diffracted x-rays are proportional to the volume of sample exposed to radiation, although the sample must be wider than the spread of the incoming beam at the lowest diffraction angles for this relationship to be reliable (Moore and Reynolds, 1989). Sample and divergence slit width must be known in order to ensure intensity is not lost at low diffraction angles (figure 2-4). At the highest diffraction angles the sample must be infinitely thick to incident x-rays (Moore and Reynolds, 1989). Samples may lose intensity at high reflection angles when the powder has not met the minimum thickness requirement. To ensure adequate sample thickness, petroleum jelly was placed on a glass slide and the samples were pushed into the jelly. A glass cover slide was used to push down on the sample and ensure an infinitely thick sample with a flat surface. Samples must be ground so there is little particle-size variation found within a single sample.

X-ray diffraction pattern fitting methods use measured diffraction patterns for analysis. The RockJock program (Eberl, 2003, using the Solver function in Microsoft

Excel) fits the sum of stored XRD pattern libraries of pure minerals to the unknown sample pattern measured by varying the fraction of each mineral standard pattern. The pure mineral standards are selected from a list of minerals thought to be present in the sample. The intensity of each mineral is determined from the proportion of each mineral standard pattern required to give the best fit (Eberl, 2003). Sample preparation techniques used in this study were consistent with those used in the RockJock user's guide (Eberl, 2003).

SEM/Petrographic Analysis

Scanning Electron Microscopy (SEM) imaging was used in this study to evaluate mineral composition and textural information including pore size, pore type and distribution of pores on the nanometer scale. Additional, quantitative mineralogy analysis by employing SEM QEMSCAN® software provided further confidence of the accuracy of XRD techniques, as well as evaluating relationships between grain types. Detrital grains and authigenic cements were identified and interpretations were made on the basis of high resolution imaging provided by the SEM.

Imaging and energy dispersive x-ray analysis of mineral composition for Utica Shale samples in this study were conducted at the Subsurface Energy Materials Characterization and Analysis Laboratory (SEMCAL), School of Earth Sciences, Ohio State University. Images were obtained with an FEI Quanta 250 Field Emission Gun (FEG). Imaging parameters were an accelerating voltage of 15 KeV, an emission current of 130 μA, and a working distance of 13 mm. Total field size of 9 mm^2 was obtained for images in this study (3 mm x 3 mm). Nine fields, each measuring 1 mm x 1 mm are generated and then stitched together to create a single 3 mm x 3 mm back scattered election (BSE) image mosaic. Images were stitched together using the Stitching plugin (described in Preibisch et al., 2009) for the ImageJ software (Fiji distribution). Uncertainties and limitations of software capabilities during the stitching process may cause a slight error during processing, however this error is considered negligible and not thought to affect

quantitative mineralogical results. The FEI QEMSCAN® analytical platform (hardware and software) uses backscattered electron (BSE) signals along with characteristic X-ray energy emissions to yield average atomic number contrast and individual elemental signal intensity (Swift et al., 2014). The energy-dispersive X-ray spectrum provides characteristic information of mineral composition and, using a point count spacing of 1 micron provides mineral composition and textural information. The iDiscover software package is used to manage the mineral database and for data processing.

Mercury Injection-Capillary Pressure Testing

Petrophysical properties; including porosity, permeability, and pore geometry, must be assessed in order to understand CO_2 entrapment and migration potential. Mercury injection-capillary pressure tests can be used to determine the potential for non-wetting fluid phases to permeate through a pore system at various pressure conditions. Porosity and permeability may be correlated to pore throat aperture sizes corresponding to different mercury saturations. Relationships developed between porosity, permeability and pore throat radii can be used to estimate fluid flow responses to injection of a buoyant non-wetting fluid (such as CO_2) into underlying strata. The identification of lithofacies with breakthrough pore throat aperture sizes capable of readily transferring non-wetting fluids under pressure conditions expected in the subsurface, along with the 3D stratigraphic and spatial distribution of these prospective confining layers can be evaluated. The entrapment and migration potential of injected CO_2 depends on the pore structure and regional geometry of the caprock. Special core analyses using mercury injection-capillary pressure tests have established the relationships between porosity, permeability, modal pore-throat size and relative permeability. Evaluation of these relationships establishes lithofacies that may be vulnerable to migration of non-wetting fluid phases, such as supercritical CO_2, under temperature/pressure regimes expected in subsurface environments. Understanding the regional stratigraphic and lateral distribution relationships amongst distinct

lithofacies is crucial to evaluating the seal integrity of the Utica Shale in the Michigan basin.

Mercury Injection-Capillary Pressure(MICP) analysis was conducted at the Ohio State University SEMCAL facility on a Micromeretics AutoPore IV 9500 (software version 1.09). Samples were degassed under vacuum at 50 ^{o}C overnight before being returned to ambient pressure and temperature and loaded for MICP analysis. Rock pieces taken from core were used and varied in size from 9 g to 16 g. Larger sized samples yielded better data but in order to fit into the 15 mL sample cup, two pieces of rock were used instead of one for some of the samples. Using two pieces of rock for some samples allowed for a sufficient volume of rock to be analyzed when a single piece did not satisfy volumetric requirements. A single piece of core was difficult to obtain and cut to an acceptable size due to the weakness inherit to clay-rich samples. Samples were cut from core or taken as core plugs and cut to shape in order to fit inside the sample cup. Equilibration times for the low pressure (<30 psia) runs were 10 seconds because no intrusion was observed to occur during these pressure steps, and low pressure analysis is done primarily to fill the sample holding cup for the high pressure cycle. Equilibration times for the high pressure runs were 1000 seconds to ensure a slow, steady increase in pressure and an accurate depiction of breakthrough pressures.

Mechanical Testing

Mechanical properties analysis in mudrock formations provides a fundamental characterization tool important for basin modeling, seismic response, and wellbore stability. The correlation of mechanical rock properties to gross lithofacies discriminated on the basis of mineral composition was used to predict the regional distribution of rock mechanical properties for the Utica Shale, regionally, in the Michigan basin.

Mineral composition and lithology are intrinsic controls on the development of naturally occurring fractures in mudrocks (Ding et al., 2012). Mudrock is a general lithologic term used for fine-grained sedimentary rocks composed of 50% or greater clay

minerals (grain size diameter less than 4μm) [Tucker, 2001]. Mudrocks with grain size variations include clay-rich, sand-rich, or carbonate-rich units. Each lithologic variation possesses distinct mechanical behavior. Quartz, feldspar and calcite are known to increase brittleness, while increasing clay mineral content results in higher ductility (Ding et al., 2012). Shales rich is quartz tends to be more brittle than shales rich in calcite, which tend to deform in a more plastic (ductile) fashion (Ding et al., 2012). Where mineralogical composition is similar, finer-grained rocks tend to be more conducive to fracturing (Ding et al., 2012).

Young's modulus and Poisson's ratio are the parameters associated with rock tensile strength and lateral compressibility, respectively. Young's modulus is defined as the stress on a material divided by the strain of that material along a given axis. Elevated Young's modulus corresponds to rigidity. Materials with an elevated Young's modulus will be more brittle than materials with a low Young's modulus.

When a material is compressed along a single axis, it will tend to expand in the other two axis planes. The measurement of the percent of expansion divided by the percent of compression is called Poisson's ratio. Materials with a low Poisson's ratio (0.0-0.2) will show limited lateral expansion when compressed, while materials with a higher Poisson's ratio (0.2-0.5) show limited compressibility. Poisson's ratio decreases with an increase in brittleness. Several authors (Buller et al., 2010; Rickman, et al., 2008; Mullen et al., 2007; Horsrud, 2001) suggest mechanical properties testing to be a fundamental geological characterization tool, particularly in mudrocks, where an increasingly large percentage of wells are now drilled. Interbedded silt, carbonate, or fine-grained sandstone may be conducive to fracture development, enhancing permeability in mudrock formations (Ding et al., 2012). It is further suggested by Ding et al., (2012) that organic content (TOC) is an important factor affecting fracture development, where rocks with high TOC values have less tensile strength, and are prone to produce natural fractures as a result of increased brittleness.

Properties of clay-rich rocks may be dependent on the direction of maximum principle stress. When rock properties change with respect to direction, the rock may

be considered anisotropic. Mudrocks may exhibit variations in compressive strength relative to bedding plane orientations (Kier et al., 2011). Anisotropic formations (particularly mudrock formations) may exhibit a loss of strength of up to 85% when tested at 45-55^{o} to bedding planes (Kier et al., 2011). Two core plugs in this study are taken at orientations parallel and 45^{o} to bedding. The loss of rock strength at various orientations to bedding planes quantifies anisotropy for the formation.

Weatherford laboratory conducted triaxial strength testing on six samples in this study. All of the samples tested are from the Bruske 1-26A or Thompson 1-30 wells. Core plugs which could not be taken of sufficient length were deemed unsuitable for mechanical analysis. The six suitable samples were cut to length and their dimensions and mass were recorded. After samples were cut to length they were made square and parallel by being fitted into a precision machinist's v-block and end-ground with 80-grit sandpaper before being finished with 220-grit paper. Samples were determined to be ready for testing when the ends were flat to a precision of ±0.001 inch. Once prepared for testing, samples were jacketed using fluorinated ethylene propylene (FEP) heat-shrink tubing in order to isolate the sample from confining oil during testing. After being jacketed the samples were affixed to the loading platens and sealed to them using rubber O-rings and a stainless steel wire tourniquet. When the sample is affixed to the loading platens, axial and circumferential deformation transducers were fitted onto the assembly. Once the sample assembly was built, it was fitted inside of the load frame and the pressure cell was lowered over the sample, filled with silicone oil, and pressurized to experimental conditions (0.5*depth(ft.) ≈ confining pressure in psi for all samples in this study) at a rate of 1000 psi/min. At this point the sample was allowed to stabilize under constant confining pressure until such time as the circumferential deformation transducer indicated a rate of deformation less than 0.005 mm/minute. Following stabilization the axial ram was brought into contact with the sample assembly and the sample was deformed at an axial strain rate of ~$5x10^{-6}$ mm/s until it fractured. During this period of deformation axial load, axial deformation, and radial deformation were recorded at a rate of 1 Hz. Following fracture of the sample the assembly was unloaded

at a rate of 0.25 inch/minute for 1 minute, the confining pressure brought down at a rate of 1000 psi/minute, and the pressure cell subsequently emptied. At the end of the stabilization period (differential stress: $\sigma_D = 0$) and during the initial stages of axial loading ($\sigma_D \approx$ 1000, 2000, and 3000 psi) P- and S-waves were passed through the sample and the waveforms were recorded in order to determine the P- and S-wave velocities for samples Bruske 1-26A #3, #4, and Thompson 1-30 #5.

Sonic logs measure seismic wave transit time. Sonic measurements are created using transducers to produce spherically symmetrical outgoing electrically charged compressional waves in the borehole fluid, exciting compressional and shear waves in the formation. In an anisotropic media, shear waves will split into a fast and slow component, with the fast component polarized along the direction of maximum stress (parallel to fracture strike) (Brie et al., 1998). The transit time (velocity) for both p-waves (V_p) and s-waves (V_s) is measured by the time it takes for each wave to travel through the formation and meet the receiver. The generated shear waves measure sonic compressional and shear slowness data, valuable for lithology interpretations and porosity distribution (Brie et al., 1998). Sedimentary rocks, particularly mudrocks, are known to exhibit significant intrinsic velocity, strength, and permeability anisotropy (Kuila et al., 2010; Brie et al., 1998; Donald et al., 2009; Kier et al., 2011; Miller et al., 2012). Anisotropy in mudrocks may be the result of intrinsic properties such as aligned natural fractures, platy clay mineral particle orientation, or unequal stress states within the formation (Brie et al., 1998; Donald et al., 2009; Kier et al., 2011). Density logs, along with the arrival times for p- and s- waves, can be used to calculate elastic properties such as Poisson's ratio and Young's modulus (Nygaard, 2010). Poisson's ratio (V_d) is calculated from the relationship between the p- and s- wave velocities as:

$$v_d = \frac{V_P^2 - 2V_S^2}{2(V_P^2 - V_S^2)}$$

Young's modulus (E_d) can then be calculated from velocity and density logs where:

$$E_d = 2\rho * V_S^2 | 1 - \upsilon_d |$$

(Nygaard, 2010). Sonic logs with V_p/V_s values can be evaluated for Poisson' ratio, Young's modulus, shear and bulk modulus. These predictive, in-situ mechanical rock properties were measured in the Bruske 1-26A well as seen in figure 2-5.

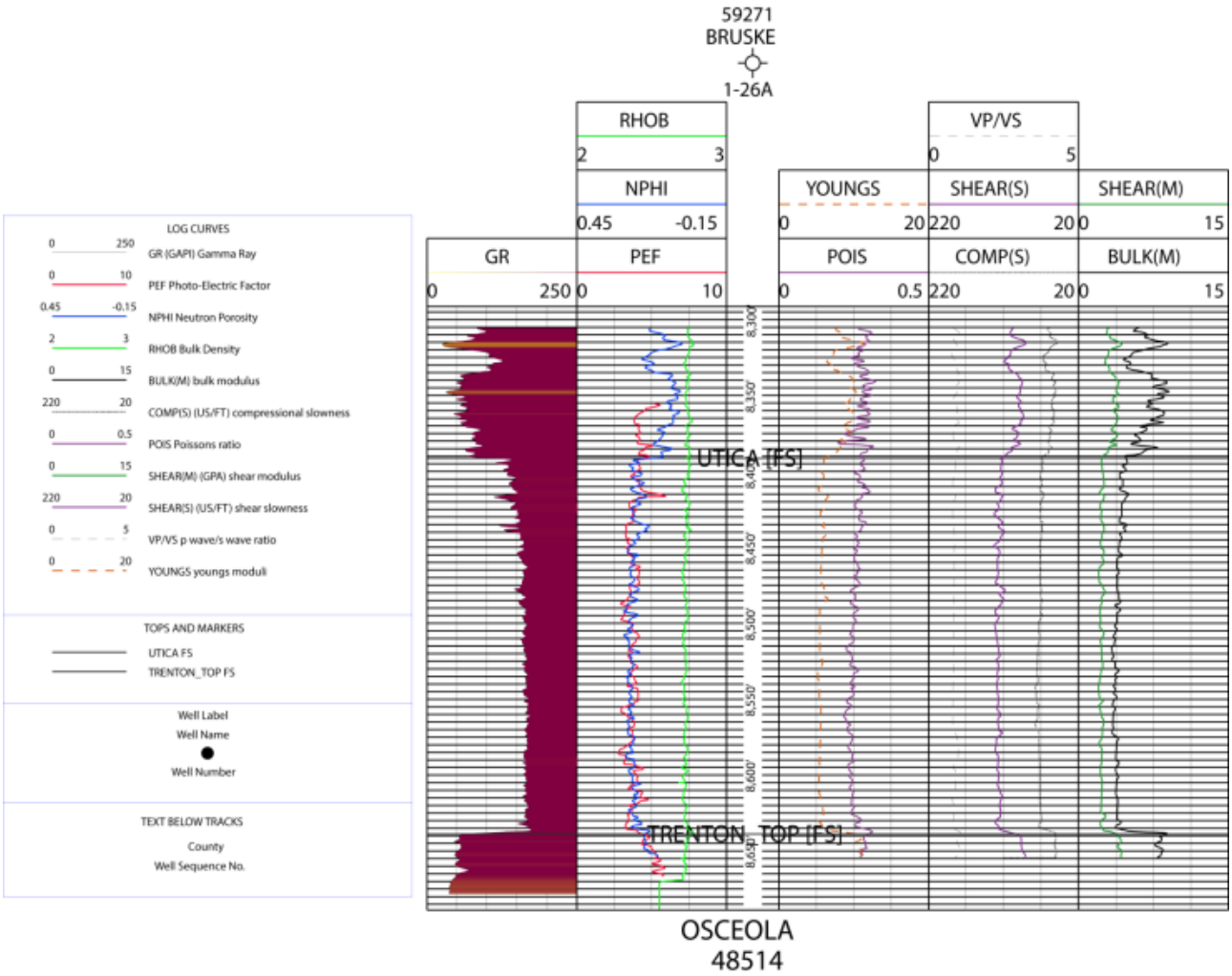

Figure 2- 5: Predictive rock mechanical properties calculated from dipole sonic logs in Bruske 1-26A.

Figure 3- 1: Weingartz 1-7A box. The Utica Shale is a grey to black, structureless mudrock with bedding parallel fractures. Some vertical fractures are observed and typically cemented with calcite, or gypsum/anhydrite.

3. CONVENTIONAL CORE AND GEOPHYSICAL WELL-LOG ANALYSIS

The Utica Shale cores used in this study are primarily cored in the lower interval of the Utica Shale, near the Collingwood (where present) or Trenton

unconformity. The Utica Shale is a grey to black mudstone, with some cemented vertical fractures and calcareous lenses (figure 3-1). The Utica/Trenton unconformity is easily distinguished in both wire-line logs and in core. In core an abrupt change is observed above fossiliferous lime mudstone with scattered shell fragments and intense bioturbation and below black to gray mudstone devoid of bedding structures with multiple bedding parallel (induced) fractures. This contact is observed in the Prevost 1-11 well at a depth of 9,363.5 ft in figure 3-2. X-Ray diffraction analysis confirms the presence of a phosphatic hardground at the contact, interpreted to be associated with a long period of sub-marine non-deposition. The vertical fracture present in the Utica Shale in this photo is cemented with calcite. Underlying the Utica Shale, the Collingwood (where present) or the Trenton Formation has abundant shell fragments, rip-up clasts, and pyrite rich lenses.

Core from the St. Allis 2-30 and the St. Albert 1-10 (located in Presque Isle County and Montmorency County, respectively) wells contain the contact with the Collingwood Shale. Both the St. Allis and St. Albert exhibit a thin (< 5 cm) layer of volcanic ash around 20 ft above the contact with the Collingwood. The presence of this volcanic ash bed and the locations it is found (figure 2-1) suggests volcanism occurred to the east or northeast. Ash beds are not found in the Prevost well core or any other wells cored in the same interval anywhere else in the Michigan basin.

Graptolites, cephalopods, brachiopods and trilobites are observed in the Utica Shale. Pyrite is common throughout the Utica and particularly common in the southeastern subbasin, where fossils are often replaced with pyrite (figure 3-3). These fossils are primarily disarticulated and are present in silty-carbonate lenses. The lenses typically occur in scour contact above the underlying mudrock suggesting alternating energy conditions and scour of muddy, suspension sediment during deposition. The disarticulated nature of the fossils indicates some amount of transport prior to deposition. Less commonly these fossils are found intact in the Utica Shale, suggesting infaunal benthic organisms were present during Utica Shale deposition. Bedding is mostly parallel laminates or structureless, with minor burrowing/bioturbation.

Figure 3- 2: The Utica/Trenton unconformity (9,363.5 ft) as observed in the Prevost 1-11 well located in Bay County. Note the abrupt change from a fossiliferous limestone with burrows and stylolite to a gray/black mudstone. The contact shown is confirmed to contain substantial calcium fluorophosphate. The vertical fracture observed in the Utica Shale is calcite cemented.

Figure 3- 3: Graptolites replaced with pyrite in the Thompson 1-30 core. This core was not slabbed for observation and therefor images are from a top down view of the rock. Core is 4 inches in diameter.

The Thompson 1-30 core is located in Lenawee County (see figure 2-1). The core is a total of 105 ft including about 5 ft of the Trenton Formation. The contact is abrupt as the gray limestone of the Trenton Formation suddenly changes into the black, structureless mudrock of the Utica Shale. Throughout the Thompson 1-30 core the Utica Shale is a black, structureless mudrock with pyrite replaced fossils. Graptolites are the most common biota found in this core and represent the pelagic fauna that lived in the water column during the time the Utica Shale was deposited. Benthic organisms are extremely rare in the Thompson 1-30 core, which suggests that there may have been poor bottom water circulation and oxygen deficiencies. The Thompson core was extensively studied because it is a full core and does not have many bedding parallel fractures to complicate plugging and sampling. Core plugs at high angle to bedding were taken from the Thompson well for more comprehensive mechanical testing. Other cores were not amenable to this sampling method. In addition, thin section observations indicate that the Thompson core is generally more completely cemented with abundant (relative to other samples) carbonate. This property results in a stronger rock allowing for the additional analysis.

The wire-line log signature for the Thompson 1-30 well is shown in figure 3-4. The core corresponding to the log signature was sampled for XRD analysis, thin section, MICP tests, and for mechanical testing. The XRD results (table 3-1) show elevated clay

content for the well at 2,307 and 2,311 ft consistent with increased gamma ray log signature. At shallower depths, the Thompson 1-30 well has a lower gamma ray signature and slightly higher PEF and RHOB signature. Based on the XRD and QEMSCAN® results and relationships to wire-line logs, this signature likely corresponds to increased dolomite and quartz content. The wire-line log signature for the Thompson 1-30 well will be discussed in detail in Chapter 4. This section of the well was not available for sampling so the seal integrity in the upper parts of the formation cannot be directly evaluated. However the underlying Utica Shale strata, in excess of 200 ft in thickness is shown to have ideal seal capacity.

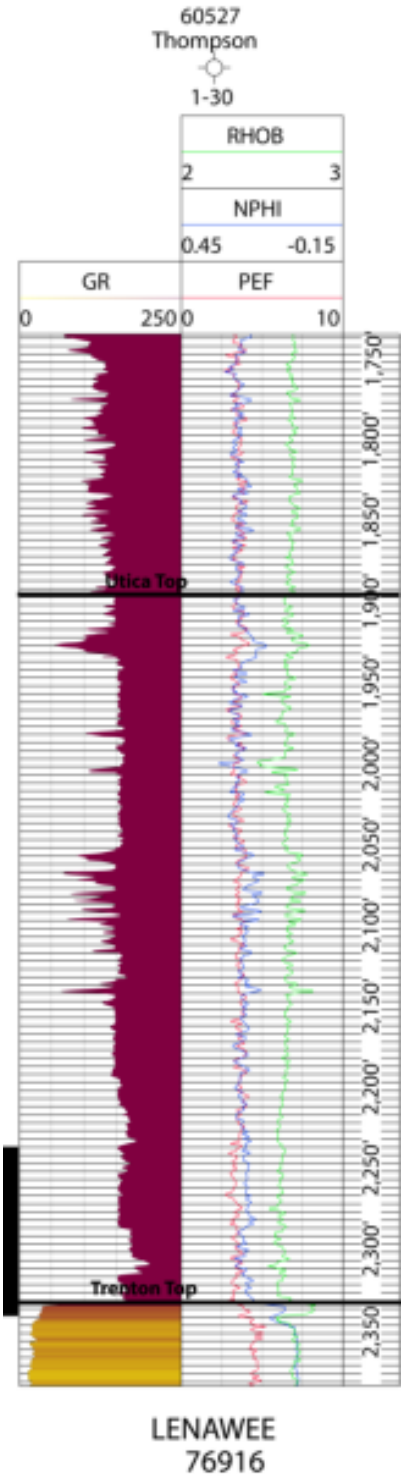

Figure 3- 4: Wire-line log for the Thompson 1-30 well in Lenawee County. The black bar to the left of the gamma ray signature shows the cored interval. The wire-line log signature becomes less consistent shallow to the cored interval and may represent a facies not yet described in this study.

The Arco-Conklin well used in this study is located in the south-central part of Jackson County (figure 3-2). The core is a dull gray mudrock with bedding parallel microfractures. There are some brachiopods both disarticulated and intact found in the gray mudrock. The unconformity with the Trenton Formation is once again abrupt both in core and on wire-line logs (figure 3-5). Five feet above the unconformity there is a 4 inch bed of brown to gray, cross-bedded siltstone. This segment of core was sampled for MICP analysis and thin section. The results indicate a quartz and dolomite dominated mineralogy. MICP analysis of this sample indicates nano-scale pore throats. On either side of this lens gray mudrock comprises 70% illite clay.

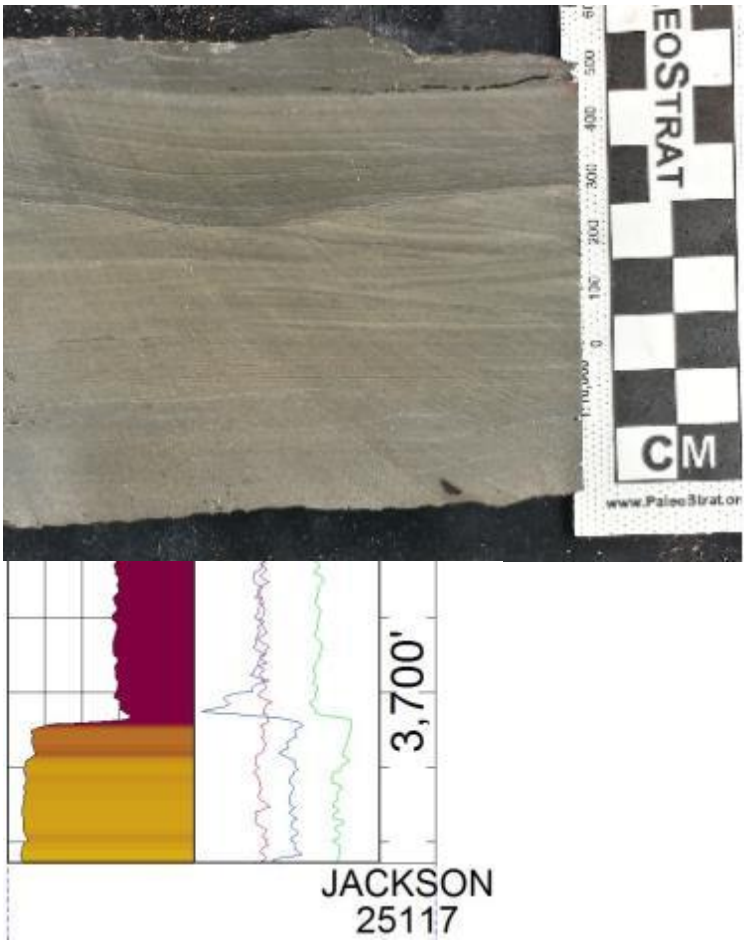

Figure 3- 5: The Arco-Conklin well in Jackson County at a depth of 3,695 ft. The convex downward silty lens observed in core corresponds to an elevated NPHI signature in wire-line log analysis.

The Bruske 1-26A core is located in the southwestern corner of Osceola County (figure 2-1) and is the only core in this study to capture the upper interval of the Utica. The cored interval is a light, to medium gray, Silty Claystone to Silty Marl with siltstone in light gray lenses throughout the core. The lenses in the core are composed of primarily quartz and dolomite grains (as observed in petrographic analysis), and contain skeletal fragments from brachiopods, trilobites, and cephalopods. The fossiliferous limestone lenses in the upper interval of the Utica are the result of higher energy currents and a possible return to shallower water conditions, suggesting overall upwards shoaling, perhaps the result of regional regression. To the east in Ontario, the deeper shelf settings of the Utica Shale (Georgian Bay Formation) contain well-developed hummocky cross-stratification, grading upward to a rapidly prograding muddy shore with silty limestone storm layers (Brogly et al., 1998). The upper interval of the Utica Shale (as observed in the Bruske 1-26A core) shows coarser grains and reworked carbonate fossil fragments and clastic lenses. These observations show a distinct difference in water depth from other Utica Shale cores. Storm deposited lenses and early cemented rip-up clasts are observed in the Bruske 1-26A well core (figure 3-6). Silt sized grains fine upwards into clay sized particles. The lenses produce cm-scale ball and pillow structures, dewatering structures, and load casts. The presence of these structures suggests that rapid sediment accumulation compacted the underlying sediment prior to lithification resulting in the development of soft sediment deformation. Burrows are observed and infilled with coarse grains, indicating oxygenated sediments for benthic organisms. The evidence observed in the Bruske 1-26A core suggests periodic, storm-induced events above storm wave base. The Bruske 1-26A well plots as both a Silty Claystone and a Silty Marl with XRD data.

The wire-line log for the Bruske 1-26A well is shown in figure 3-7. When compared to the Thompson 1-30 well the wire-line log signature for the Bruske 1-26A well is more consistent. The Utica Shale interval from the top of the Trenton Formation to the base of the cored interval is homogeneous in log response. From the bottom of the cored interval up to the top of the Utica Shale the wire-line log signature is observed

to have thin, low gamma ray intervals. The drop in the gamma ray signature is caused by a drop in the relative abundance of clay minerals. The percentage of clay minerals decreases upwards as the core shallows (table 1, Ch. 4) and the expected drop in the gamma ray signature is observed in the log. The decrease in clay mineral abundance is only observed in the upper interval of the Utica Shale in the northern part of the Michigan basin. Core observation and XRD results indicate that the drops in the gamma ray signature (and corresponding lower NPHI signature) correspond to large storm beds composed of primarily quartz and dolomite. The log signature that is observed in the upper part of the Bruske 1-26A well is observed in most other wells located in the northern part of the Michigan basin, as will be discussed further below.

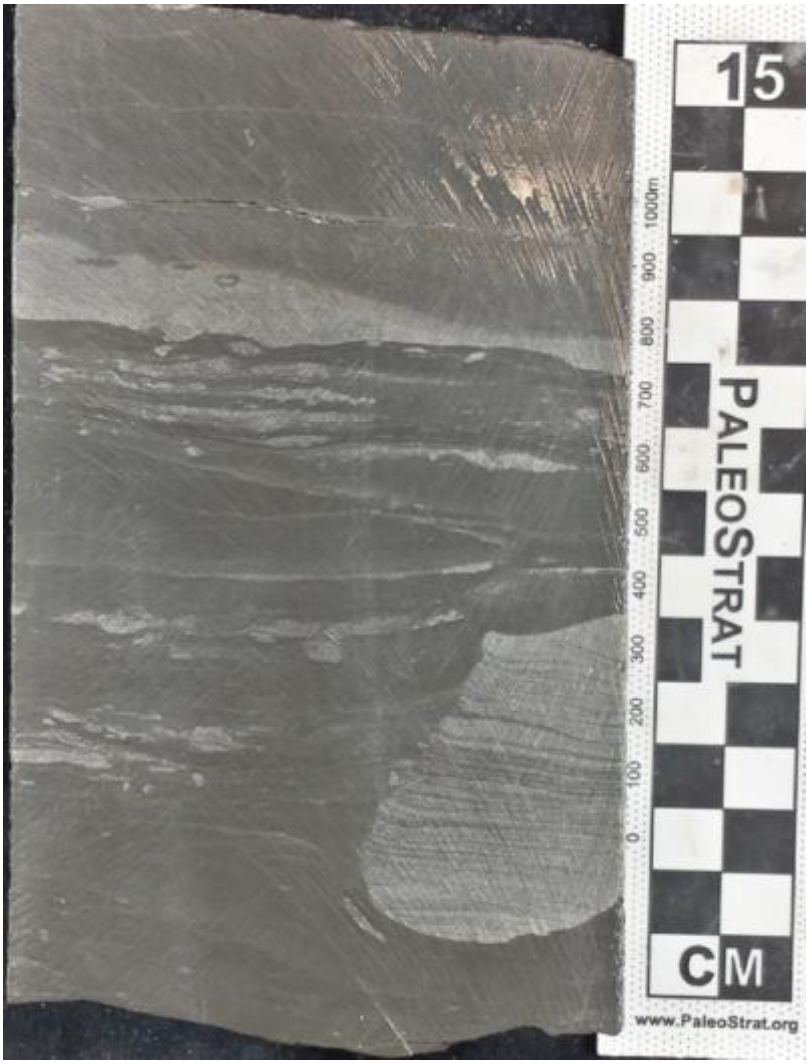

Figure 3- 6: The Bruske 1-26A core is shown (8,448.4 ft.) with silt-infilled burrows and ball and pillow structures. The cross bedding in the burrow is evidence of higher energy storm sediment. The carbonate lens in this photo is gradational at the top, suggesting higher energy currents. The fining upwards grain size that is observed in the lens can be attributed to the waning part of a storm event.

The upper part of the Utica Shale has been shown through core analysis, thin section analysis and XRD results to be rich in carbonate and siliciclastic content in the Bruske 1-26A well (relative to other Utica Shale wells used in this study). Wire-line logs have been used to trace the extent of a lower NPHI signature within the upper part of the Utica Shale. The logs show that in the north and eastern part of the basin the upper interval of the Utica Shale has a lower gamma ray signature and lower NPHI signature,

but the signature is not laterally persistent through the entire basin. The relative drop in the NPHI signature is not associated with organic matter because the mineralogy changes to a more carbonate and siliciclastic rich rock in sections. The overlying Queenston Formation is a mixed carbonate/siliciclastic system and the upper part of the Utica Shale discussed here is transitional to the Queenston. Figure 3-8 shows a cross-section from the northern part of the Michigan basin trending W-E. The upper part of the Utica Shale is labelled CBNT, and is shaded green to blue with respect to the NPHI signature. The westernmost wells are shaded green which corresponds to a higher NPHI signature, while to the east as the NPHI signature is lower, the wells are shaded blue. The stratigraphic thickness of the shaded unit is thickest to the east, thinning to the west. The top is picked based on the point where the gamma ray signature begins to drop, and the NPHI signature begins to lower. This point marks a shift to a more carbonate and siliciclastic rich rock, with core observations (albeit limited) suggesting a shift in depositional environment to above the storm weather wave base.

Figure 3-9 shows a north-south trending cross-section where the carbonate and siliciclastic content in the upper part of the Utica Shale disappears in the southern and western ends of the basin. The Utica Shale is thicker in the southern part of the basin, but the lenses of carbonate and siliciclastic content are not observed in the upper part of the log signature. The southeastern sub-basin is observed to have elevated carbonate/siliciclastic content in the lower part of the Utica Shale, with no clear differentiation of contacts separating the carbonate rich sections from the primarily clay rock that is present throughout the Utica Shale (figure 3-10). A map showing the locations of wells used in the previous cross-sections is shown in figure 3-11.

The Utica Shale is thickest in the southeastern subbasin of the Michigan basin with 300-500 ft thick shale deposits. Lenses of silt-sized siliciclastic/carbonate content are observed in the subbasin but do not extend outside of the subbasin in the lower interval of the Utica Shale. The wells located in the southeastern subbasin include the Thompson 1-30, Arco-Conklin 1-31, Rzepka 1-27 and Taylor 1-35 wells. All of the XRD results from these wells plot in the Silty Claystone facies, with the exception of the

Thompson 1-30 well, which plots as both a Silty Claystone and a Silty Marl (classification scheme provided in chapter 5). The log response for all of these wells is very similar, with no clear difference denoting a shift in mineralogy. The Thompson 1-30 well and the Arco-Conklin 1-31 well were studied extensively through QEMSCAN® analysis, and are shown to be clay rich, with some quartz and dolomite.

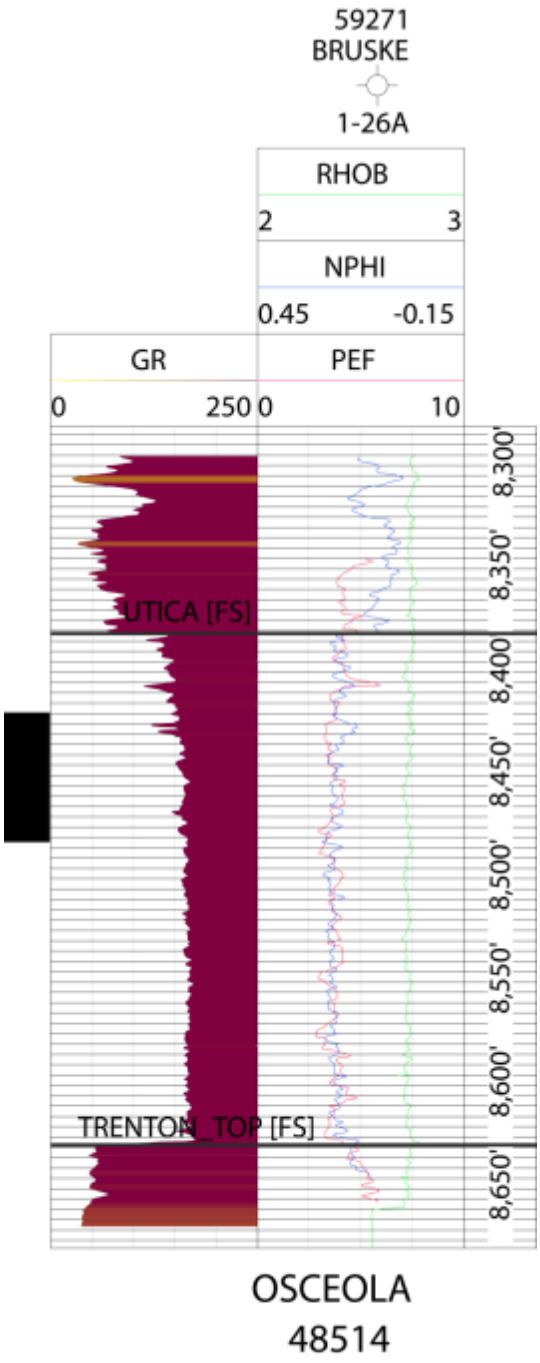

Figure 3- 7: Wire-line log for the Bruske 1-26A well in Osceola County. The black bar to the left of the gamma ray signature shows the cored interval. The increase in carbonate lenses observed in core (and documented by XRD results) is also observed in wire-line logs, where small drops in the NPHI signature correspond to a drop in the GR signature.

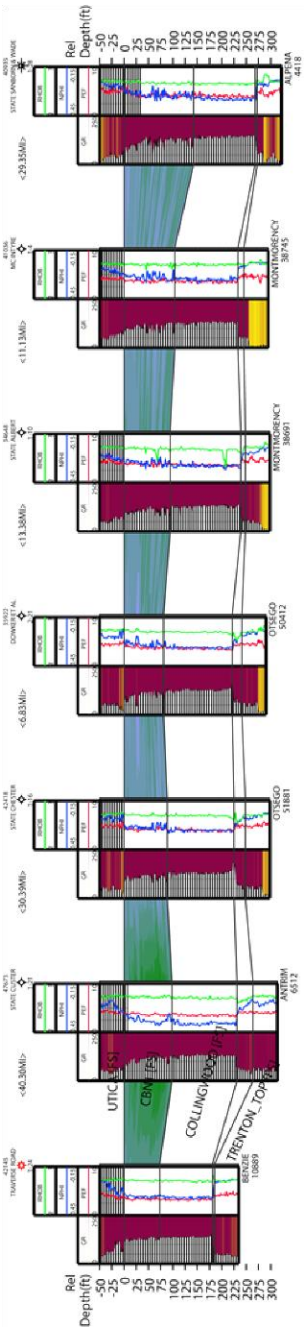

Figure 3- 8: W-E trending cross-section in the northern part of the Michigan basin. The upper interval of the Utica is shaded green-blue depending on the NPHI signature. Decreased NPHI signatures are observed in the eastern part of the basin, where carbonate content is increased.

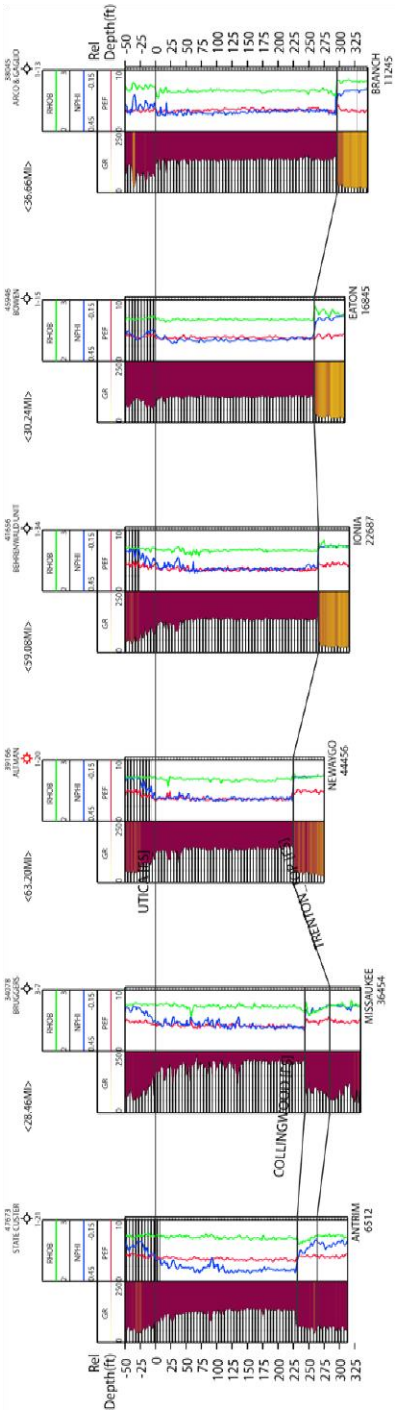

Figure 3- 9: N-S trending cross-section on the western part of the Michigan basin. The carbonate rich upper interval of the Utica Shale does not extend to the southern part of the basin, where the Utica is primarily a Silty Claystone throughout.

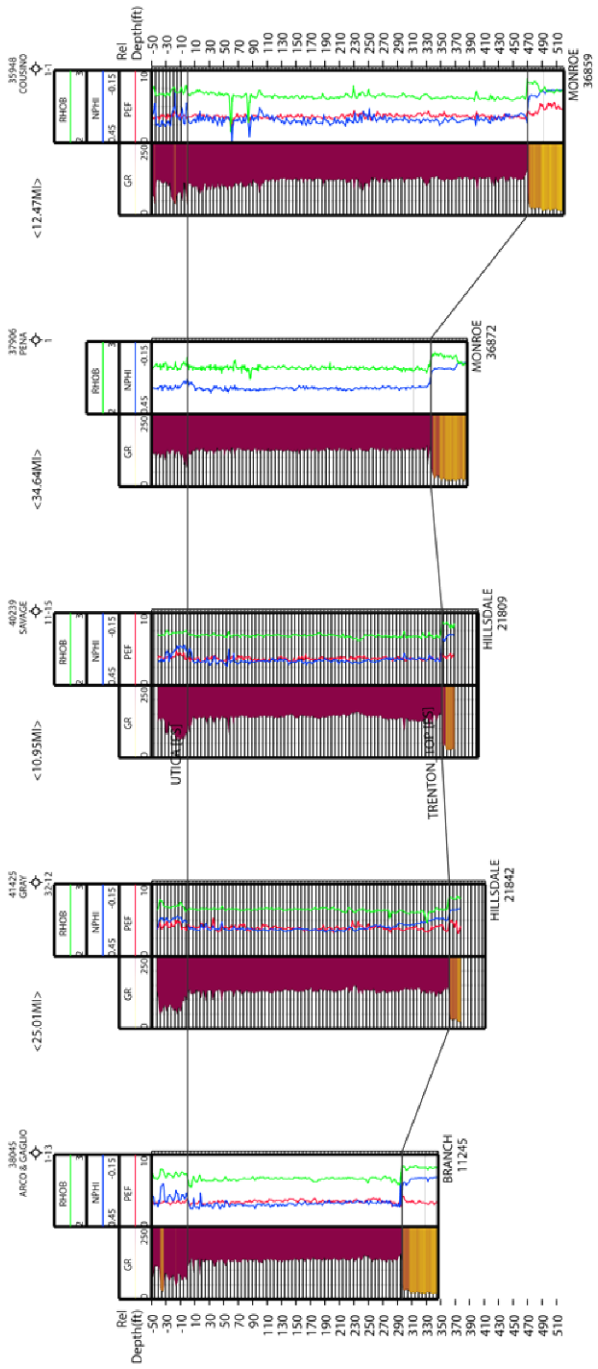

Figure 3- 10: W-E trending cross-section in the southern part of the state. Note the increased thickness of the Utica Shale in the southeastern sub-basin.

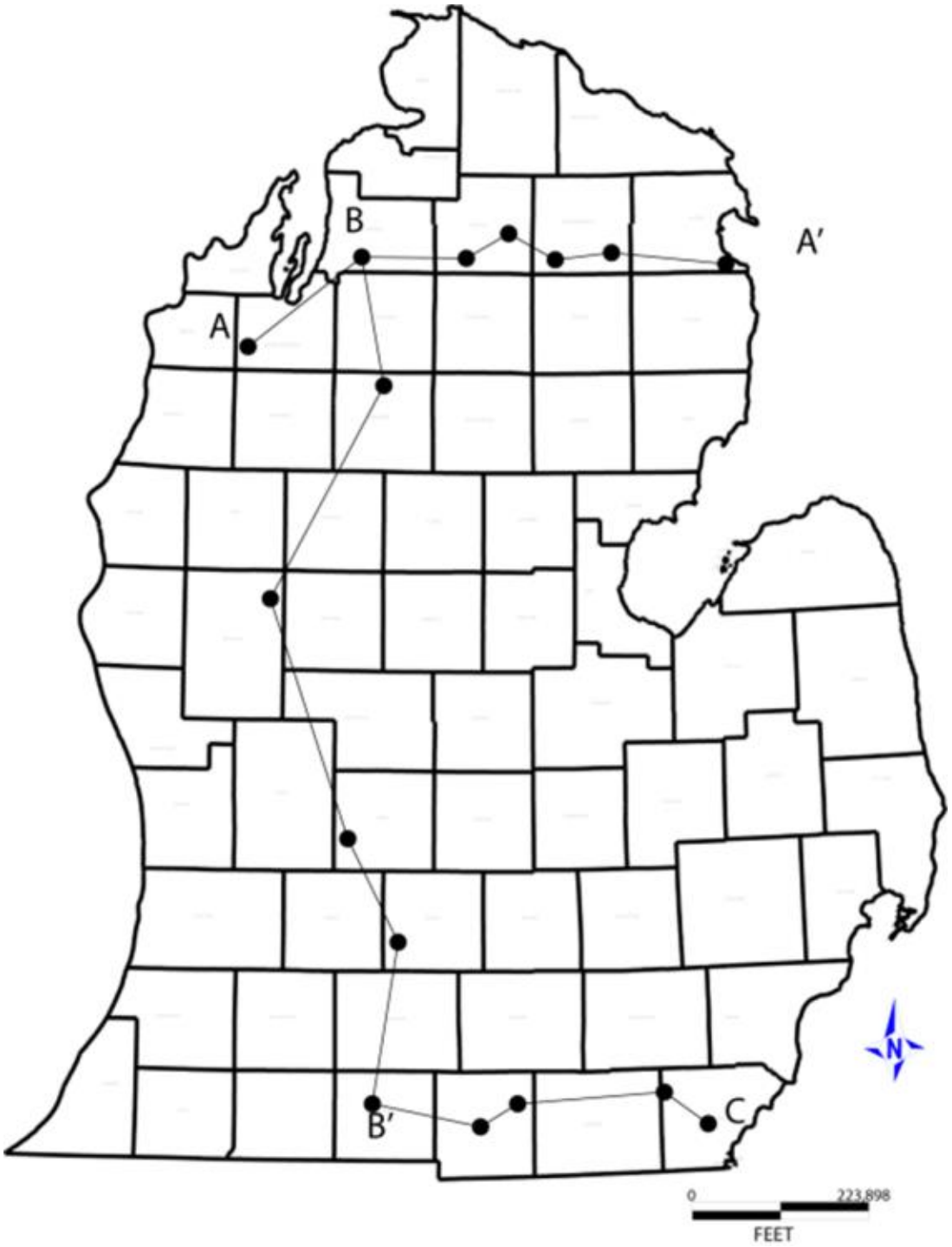

Figure 3- 11: Locations of wells used in cross-sections from figures 3-8, 3-9, 3-10.

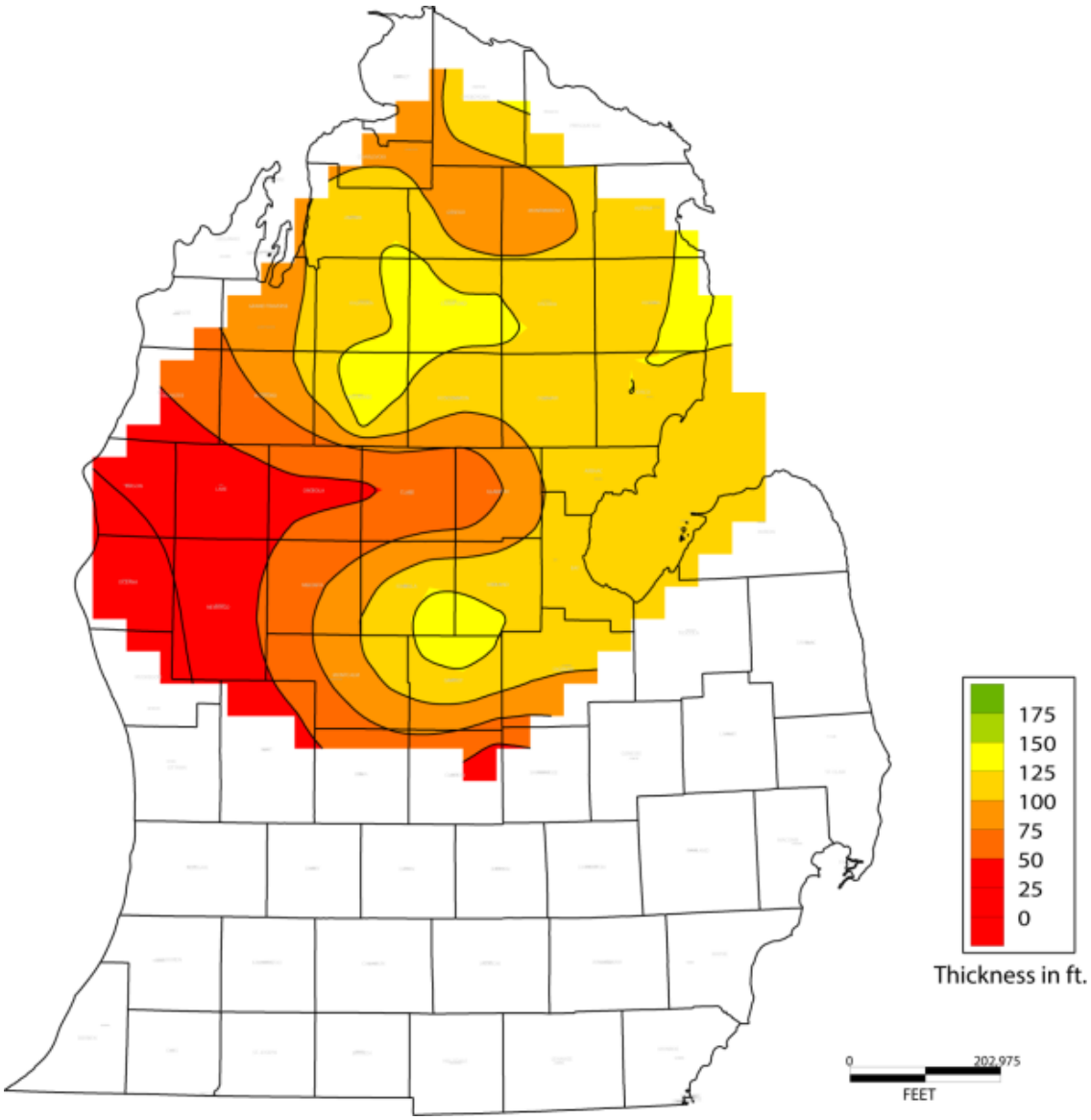

Figure 3- 12: Isopach map of the carbonate rich upper interval in the Utica Shale. The extent of the carbonate lens suggests the northern portion of the Michigan basin was the first affected by a regressing sea level.

Well-log analysis confirms the identification of two distinct lithofacies within the Utica Shale. The thick shale deposits are observed to have been deposited in the basin after the initial maximum flooding surface that marks the beginning of the Utica. As regression and restricted, shallower water conditions evolved upsection, there is a marked increase in carbonate content, but only in the north-eastern part of the basin. Carbonate lenses and increased carbonate content is not observed in the Utica Shale in

the western part of the basin. This relationship is observed in figure 3-8, where the upper interval is shaded blue-to-green indicating a decrease in apparent porosity to the east. The decrease in the NPHI curve corresponds to increase in the RHOB curve as well as a decrease in the gamma ray curve.

The carbonate-rich interval interpreted from well-logs in the upper part of the Utica Shale extends south only about half way across the basin. Figure 3-12 is an isopach thickness map created for the interval containing the increased carbonate content. The results indicate that the carbonate-rich interval is less than 150 ft thick, thinning to the west, northwest. Increased carbonate content in the upper part of the Utica Shale suggests a more restricted environment in the northern part of the basin during the deposition of the upper Utica Shale. Fossil fragments and carbonate stringers found within the mud matrix shows increased carbonate productivity as a result of basin restriction and limited clastic input. The carbonate rich interval is not present at all in the southwestern or southeastern part of the basin. The locus of carbonate production is in the northeastern part of the basin, suggesting restriction from the siliciclastic input in present to the south and shows the first indication of basin restriction that is present during the deposition of the overlying Queenston Formation. Limited, reliable wire-line log data is available around the thumb area and was not used to construct figure 3-12.

4. X-RAY DRIFFRACTION RESULTS AND ANALYSIS

X-Ray diffraction analysis conducted at Western Michigan University was completed on over 50 Utica Shale samples from 12 conventional cores. Samples were analyzed using the RockJock program in MS-Excel. The output file for the RockJock program is an excel table with individual mineral abundances given as a weight percentage of whole rock mineralogy. The mineralogy was then lumped into a non-clay siliciclastic, carbonate, clay mineral and other categories in this study. The minerals that comprise the majority of the non-clay siliciclastic fraction include quartz, K-feldspar and plagioclase. The carbonate fraction is primarily calcite or dolomite, while illite is by far the most commonly observed clay mineral. The "other" category is represented primarily by pyrite or gypsum/anhydrite. The results are shown in table 1 below. The x-ray diffraction results indicate that clay content dominates a large portion of the mineralogy in the Utica Shale in the Michigan basin. The data points taken from the formation labelled Utica/Collingwood or Utica/Trenton are taken from the contact representing the unconformity between the underlying carbonate units and the Utica Shale. The Prevost (4) sample has a more precise depth because it was taken right at the unconformity. The "other" category making up the majority of these samples is primarily fluorapatite, or calcium fluorophosphate. The presence of a phosphatic deposit at an interpreted unconformity suggests submarine weathering and a prolonged period of non-deposition before the deposition of the Utica Shale.

			Whole Rock Mineralogy			
			Weight %			
Well	**Formation**	**Depth (ft.)**	**Clastic**	**Carbonate**	**Clay**	**Other**
Arco-Conklin 1-31 (1)	Utica Shale	3,695	14.6	8.5	70.1	6.8
Arco-Conklin 1-31 (2)	Utica Shale	3,698	20.3	6.8	69.2	3.7
Arco-Conklin 1-31 (3)	Utica Shale	3,704	22.1	15.4	59.7	2.8
Bruggers 3-7 (1)	Utica Shale	9,649	46	0	53	1
Bruggers 3-7 (2)	Utica Shale	9,657	55	0	43	2
Bruggers 3-7 (3)	Collingwood	9,660	1	78.2	11.4	9.6
Bruske 1-26A (1)	Utica Shale	8,426	29	25	43.3	2.7
Bruske 1-26A (2)	Utica Shale	8,432	0	94	0	6
Bruske 1-26A (3)	Utica Shale	8,438	28	15	56	1
Bruske 1-26A (4)	Utica Shale	8,443	3.5	96.5	0	0
Bruske 1-26A (5)	Utica Shale	8,450	18	39	31	2
Bruske 1-26A (6)	Utica Shale	8,457	19	10	71	0
Bruske 1-26A (7)	Utica Shale	8,461	27	24	43	4
Bruske 1-26A (8)	Utica Shale	8,465.5	19	11	68	2
Bruske 1-26A (9)	Utica Shale	8,471.5	26	14	60	0
Bruske 1-26A (10)	Utica Shale	8,478	26	8	65	1
Bruske 1-26A (11)	Utica Shale	8,486	22	12	66	0
Prevost 1-11 (1)	Utica Shale	9,347	13	5.9	75.5	5.6
Prevost 1-11 (2)	Utica Shale	9,349	18.4	7.3	67	7.3
Prevost 1-11 (3)	Utica Shale	9,362	15.7	8.7	73	2.6
Prevost 1-11 (4)	Utica/Trenton	9,363.50	0	7.2	0	92.8
Rzepka 1-27 (1)	Utica Shale	3,110	11.2	8.4	77.6	2.8
Rzepka 1-27 (2)	Utica Shale	3,114	17.3	8.7	71.8	2.2
Rzepka 1-27 (3)	Utica Shale	3,119	25.5	12.2	53.9	8.4
Rzepka 1-27 (4)	Utica Shale	3,126	22.1	28.3	46.7	2.9

Table 1: Quantitative mineralogy based on x-ray diffraction results.

			Whole Rock Mineralogy Weight %			
Well	Formation	Depth (ft.)	Clastic	Carbonate	Clay	Other
St. Albert 1-10 (1)	Utica Shale	7,719	11.7	4.4	78.2	5.7
St. Albert 1-10 (2)	Utica Shale	7,731	11.4	3.6	80	5
St. Albert 1-10 (3)	Utica Shale	7,740	12.6	10.7	73.4	3.3
St. Albert 1-10 (4)	Utica Shale	7,752	14.3	2.6	81	2.1
St. Allis 2-30 (1)	Utica Shale	5,291	13.8	4.6	77.7	3.9
St. Allis 2-30 (2)	Utica Shale	5,298	22.4	12	61	4.6
St. Allis 2-30 (3)	Utica Shale	5,307	6.8	47.4	37.3	8.5
St. Allis 2-30 (4)	Utica Shale	5,313	23.7	1.6	70.5	4.2
St. Allis 2-30 (5)	Utica Shale	5,318	10.8	11.5	72.9	4.8
St. Allis 2-30 (6)	Utica/Collingwood	5,319	26.9	14.2	0	58.9
Taylor 1-35 (1)	Utica Shale	3,090	25.4	2.6	67.9	4.1
Taylor 1-35 (2)	Utica Shale	3,094	23.2	12.5	59.9	4.4
Taylor 1-35 (3)	Utica Shale	3,101	10.5	4.5	81.8	3.2
Thompson 1-30 (1)	Utica Shale	2,235.5	27	27	44	2
Thompson 1-30 (2)	Utica Shale	2,246	22	28	47	3
Thompson 1-30 (3)	Utica Shale	2,260	34	27	36	3
Thompson 1-30 (4)	Utica Shale	2,270	25	19	53	3
Thompson 1-30 (5)	Utica Shale	2,286	26	28	43	3
Thompson 1-30 (6)	Utica Shale	2,307	17	26	52	5
Thompson 1-30 (7)	Utica Shale	2,311	23	19	54	4
Thompson 1-30 (8)	Utica Shale	2,321	22	34	42	2
Thompson 1-30 (9)	Utica Shale	2,331	18	41	36	5
Visser 1-27 (1)	Utica Shale	6,705	19.4	4.6	70.6	5.4
Visser 1-27 (2)	Utica Shale	6,720	22	10	64	4
Visser 1-27 (3)	Utica Shale	6,725	32.4	0	54.7	12.9
Visser 1-27 (4)	Utica Shale	6,732	37.1	19.2	34.4	9.3
Visser 1-27 (5)	Utica Shale	6,743	23.5	7.4	63.6	5.5
Visser 1-27 (6)	Utica Shale	6,752	20.8	8	67.1	4.1
Weingartz 1-7A (1)	Utica Shale	10,065	22	3.8	71	3.2
Weingartz 1-7A (2)	Utica Shale	10,082	6	4.6	84.2	5.3
Weingartz 1-7A (3)	Utica Shale	10,089	14.7	7	75	3.3
Winterfield Deep A-1 (1)	Utica Shale	9,885	11.3	11.4	73	4.3
Winterfield Deep A-1 (2)	Utica Shale	9,893	27	8.5	60	4.5

Table 1 (cont): Quantitative mineralogy based on x-ray diffraction results.

A classification scheme was created using a ternary diagram with non-clay siliciclastic, clay and carbonate end members (figure 4-1). This classification scheme was used to subdivide the Utica Shale into various lithofacies.

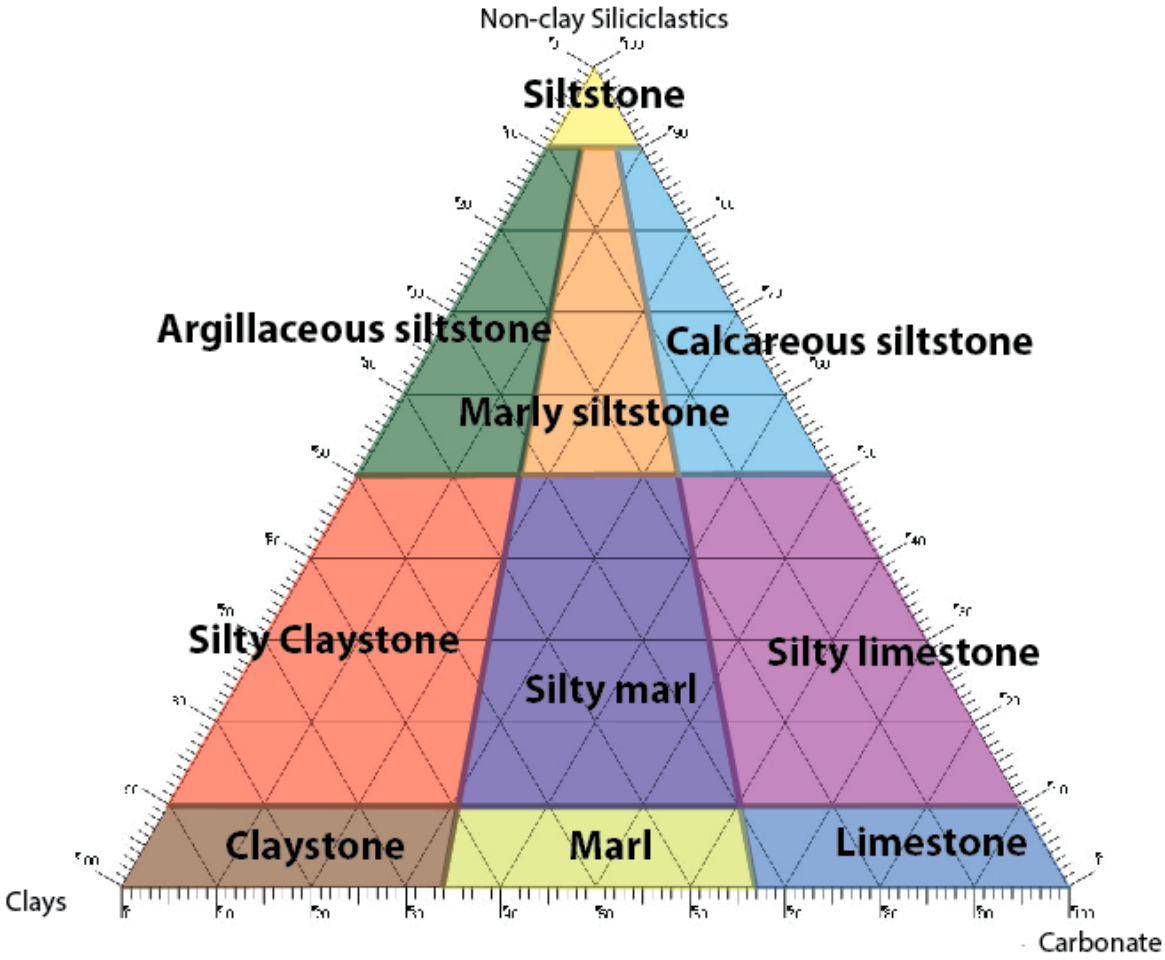

Figure 4- 1: Classification scheme created for the Utica Shale based on quantitative mineralogy

Minerals that would normally be classified in the "other" category (pyrite, anhydrite, fluorapatite etc.) are lumped with the non-clay siliciclastic fraction in this classification scheme. These minerals compose a relatively small (<5%) fraction of most samples, and are not thought to influence results of facies distributions except in the samples taken from the unconformity, which plot as non-clay siliciclastics in this classification scheme. Results are plotted in figure 4-2.

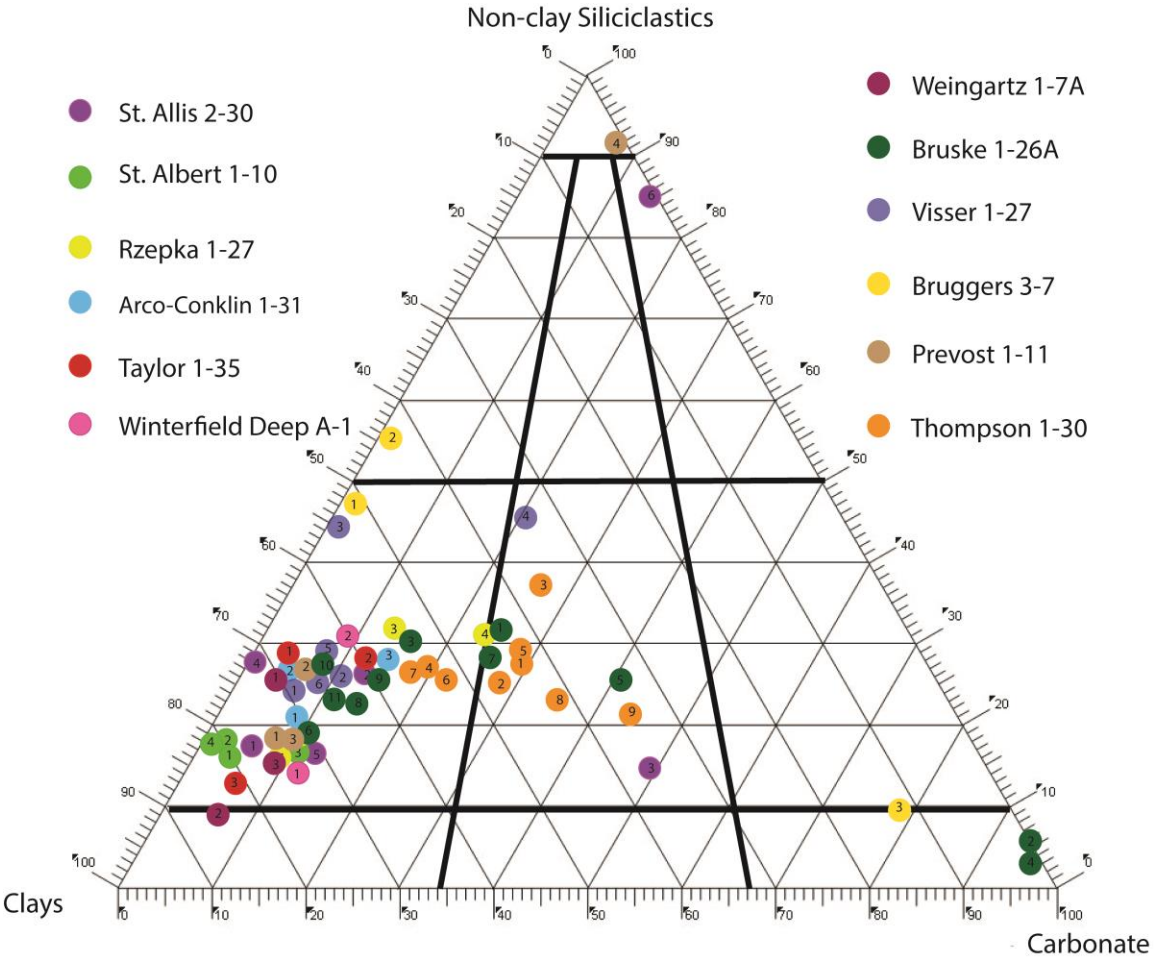

Figure 4- 2: Ternary diagram filled with 12 wells from the Utica Shale in the Michigan basin. Results indicate two distinct lithofacies.

The results indicate two dominant lithofacies are present in the Utica Shale, a Silty Claystone and a Silty Marl. The Silty Marl facies is present in the southeastern sub-basin, in the northern part of the Michigan basin, and in the upper part of the Utica Shale. The upper part of the Utica Shale is represented by the Bruske 1-26A well. The shift to a more carbonate-rich rock is observable in wire-line log analysis. Figure 4-3 shows a W-E trending cross section through the middle of the basin with the cored intervals colored to show the distribution of observed facies. The Bruske 1-26A well shows an alternating Silty Marl facies and Silty Claystone facies in the upper part of the

Utica Shale, while the cores from the lower interval of the Utica are all composed of the Silty Claystone or Claystone facies. Figure 4-4 shows a similar cross section in the southern part of the basin. The Thompson 1-30 well plots primarily as a Silty Marl with some of the sampled interval plotting as a Silty Claystone. The XRD data agrees with the wire-line log signature. In places where the NPHI plots to the left of the PEF curve the Silty Marl facies is present, and where the NPHI plots on top of the PEF curve the Silty Claystone facies is present. Wire-line log signatures are therefore considered reliable for the Utica Shale and suggest the Silty Marl facies is limited to the upper part of the Utica Shale as well as small, localized intervals in the lower part of the Utica, particularly in the subbasin.

The clay size fraction of most samples is dominated by phyllosilicate minerals, primarily illite/muscovite, with varying amounts of chlorite. Quartz, K-feldspar, dolomite and calcite are also commonly observed in x-ray diffraction results. Outliers to the data set are taken from carbonate lenses, where carbonate may compose over 90% of the mineralogy, or from the unconformity found between the Utica Shale and the underlying Trenton/Collingwood which is discussed above.

X-ray diffraction results show that the Utica Shale is composed of a high relative abundance of clay minerals. Most samples analyzed are shown to be composed of greater than 50% clay minerals, with some samples being composed of nearly 80% clay minerals. High clay content generally corresponds to small pore throats and ductile deformation, and is therefore ideal for geologic seals in mudrock formations.

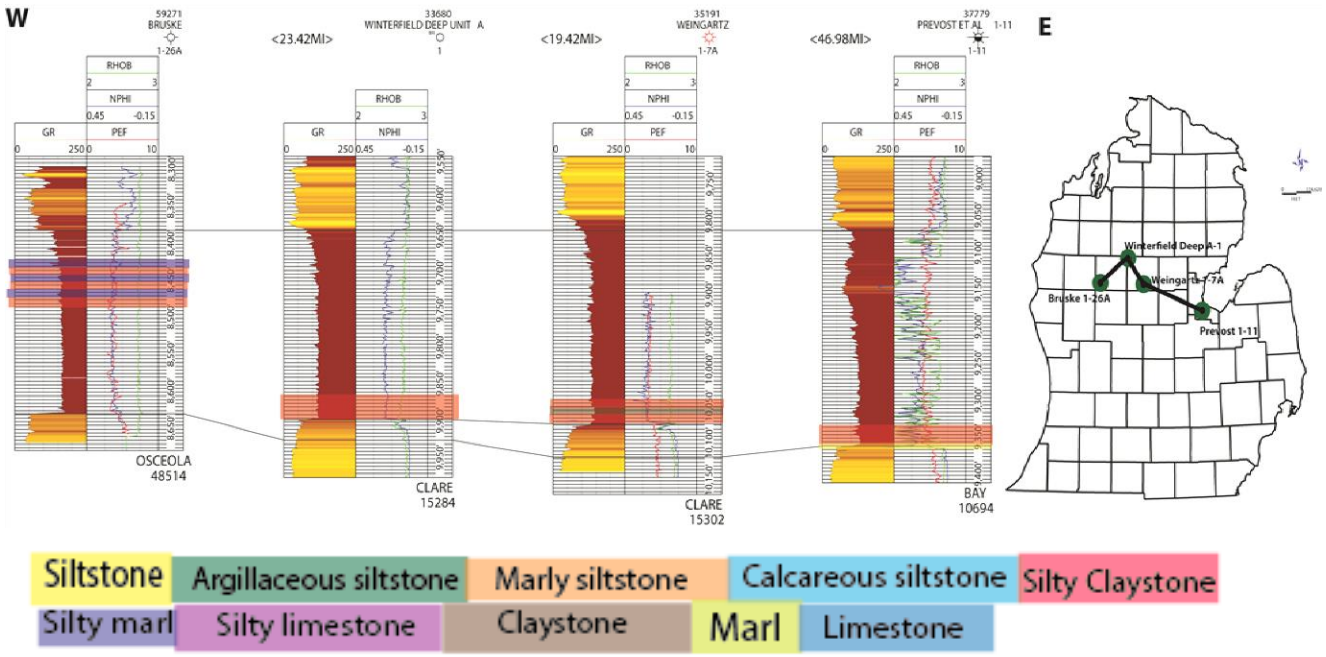

Figure 4- 3: W-E trending cross-section of the Utica Shale with XRD facies superimposed on the log tracks. The Utica Shale is primarily a Silty Claystone in the lower part, and an alternating Silty Claystone/Silty Marl in the upper part.

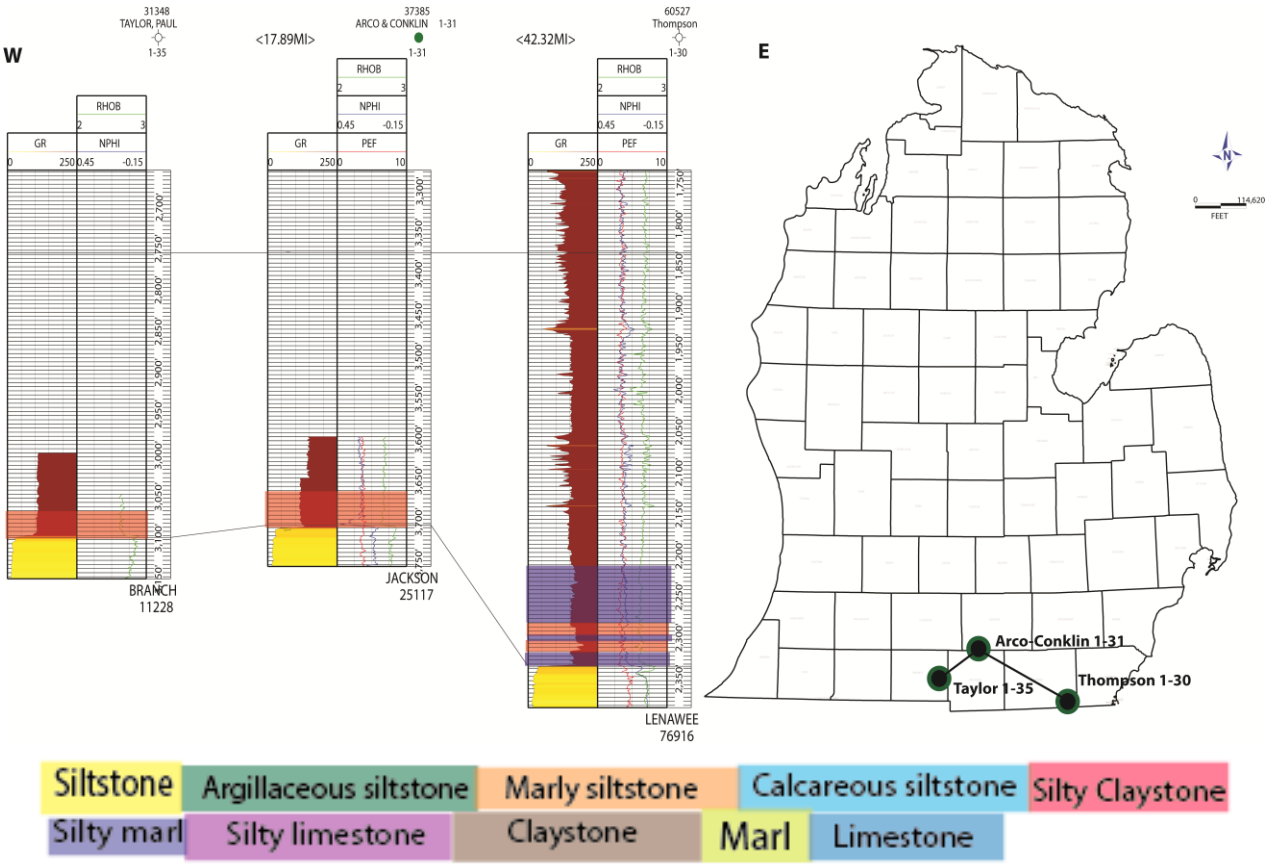

Figure 4- 4: The Utica in the southeastern subbasin. The Thompson 1-30 well is the only core in this study with the Silty Marl facies present in the lower part of the Utica.

5. QEMSCAN/PETROGRAPHIC RESULTS AND ANALYSIS

Microstructure and porosity distribution in mudrocks is an important factor governing subsurface fluid flow properties. Rock strata considered to be potential confining layers may have fracture-dominated flow, from the nano-pore to the macro-pore range. Imaging pore structures and nano-scale pore distribution as well as microfractures is therefore a fundamental characterization tool utilized to investigate seal integrity in mudrock formations. Six samples were analyzed with varying mineralogical properties in 3mm x 3mm fields using QEMSCAN®.

A representative Silty Marl facies sample is shown in figure 5-1 from the Thompson 1-30 well in Lenawee County at 2,277 ft. There are no observed micro-fractures and less than 5% unidentified or background structures. This observation is consistent with observations made in core for the same facies, where marly rocks are generally less prone to fracture than silty (or argillaceous) rocks. The mineralogy consists of 20% quartz, 20% dolomite, 40% illite and 20% other. The high percentage of quartz and dolomite is noteworthy as the Thompson 1-30 sample is the only sample analyzed with such high values of quartz and carbonate content. This well is located in the southeastern sub-basin, likely the first part of the state affected by the influx of clastics following filling of the Taconic foreland basin. Pores observed through QEMSCAN® analysis of the Thompson 1-30 sample are interpreted to be organic porosity (OM), based on the geometry of the pores, and the chemical composition. Composition of pore space is discussed further below. Figures 5-2a and 5-2b show backscattered electron (BSE) images of OM porosity surrounding carbonate grains and near framboidal pyrite. Sulphate-reducing bacteria and associated diagenetic alteration is interpreted to be responsible for OM porosity in this sample based on the proximity of pyrite clusters to organic pore space. Dolomite accounts for 18% of the whole rock mineralogy in the sample. The dolomite is observed to replace calcite as well as

authigenic overgrowths. Calcite is observed with syntaxial overgrowths as well as dolomite cement which formed during diagenesis. Figure 5-3 shows a brachiopod found in a clay matrix, suggesting little to no transport of the fossil. The presence of intact, infaunal brachiopods living in the sediment supports oxygenated conditions, at least near the sediment-water interface.

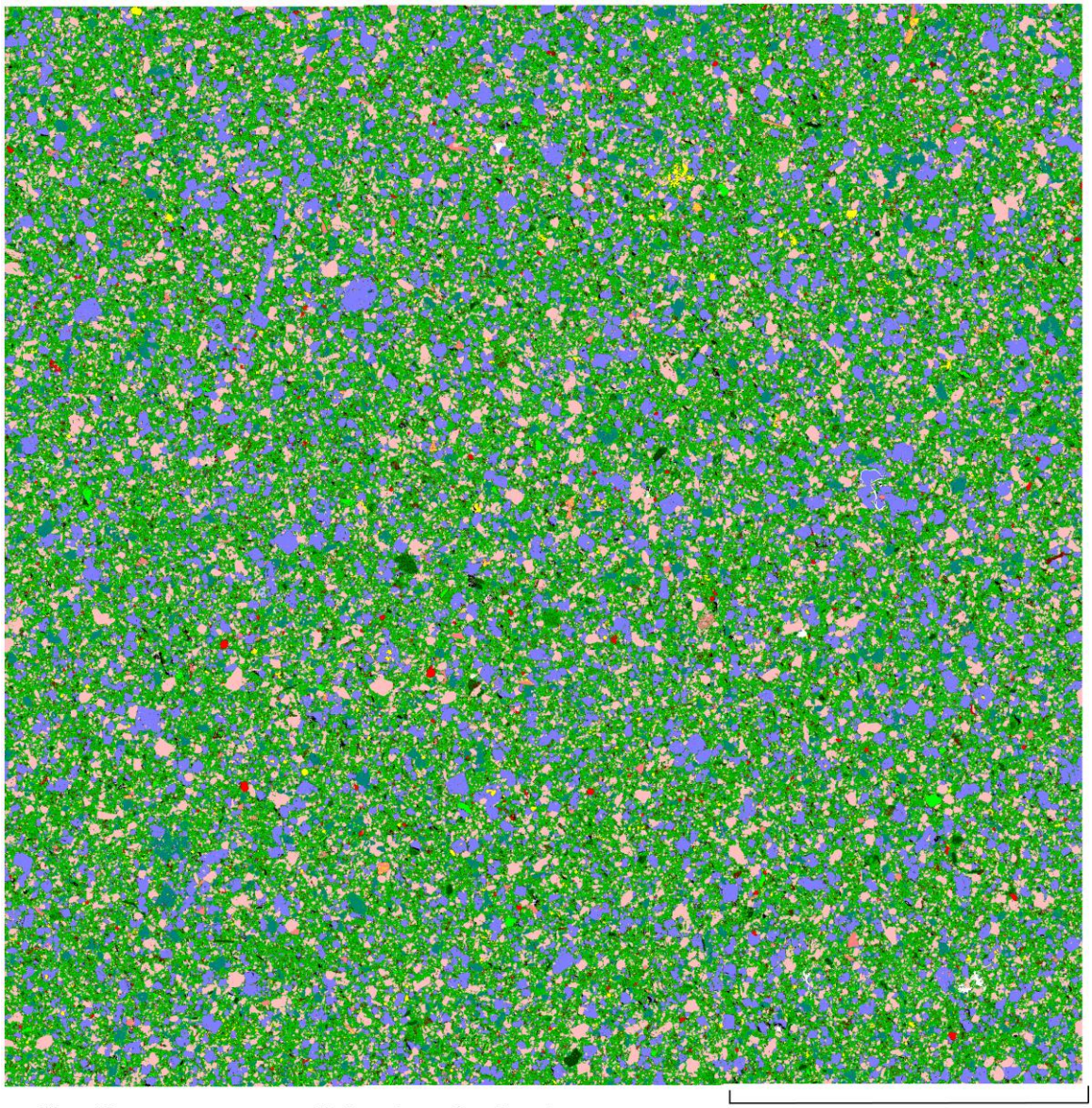

Mineral Name	Pixel counts	Area Percent
Background	39544	0.44
Quartz	1875082	20.93
K-Feldspar	493568	5.51
Rutile	62076	0.69
Dolomite	1648691	18.40
Calcite	7268	0.08
Apatite	66729	0.74
Illite	3701736	41.31
Biotite_Std	367470	4.10
Chamosite	116326	1.30
Muscovite	97834	1.09
Pyrite	118393	1.32
Gypsum/Anhydrite	1949	0.02
Unclassified	403285	4.50

Figure 5- 1: QEMSCAN field of the Thompson 1-30 well at 2,277 ft. The Thompson well consistently plots as a 'Silty Marl' and is rich in carbonate content.

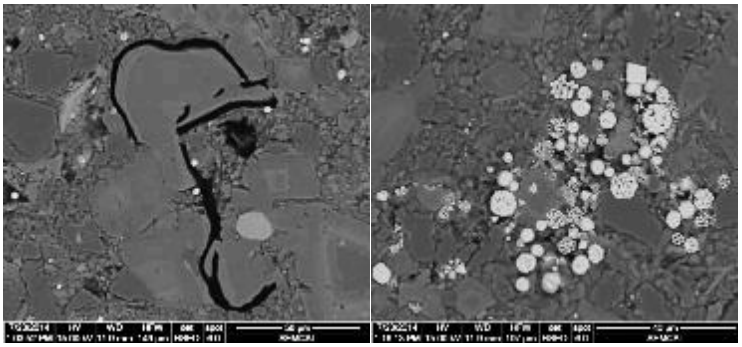

Figure 5- 2a and 5-2b: BSE images of OM porosity in the Thompson 1-30 2,277 ft. sample. OM lines the rim of dolomite grains in figure 5-2a and is within a pyrite cluster in figure 5-2b.

Figure 5- 3: Intact brachiopod fossil found during conventional thin section analysis at 2,255 ft. in the Thompson 1-30 core. The condition of the brachiopod suggests it was living in (infaunal) the sediment. Scale bar reflects 0.4 mm.

A sample from the Bruske 1-26A well in Osceola County at 8,479 ft was analyzed by the QEMSCAN® software and is shown in figure 5-4. Alternating carbonate and clastic lenses with larger grain size suggest varying energy regimes, with larger grains deposited during periods of higher energy. Some small, bedding parallel fractures are observed and cemented with gypsum/anhydrite cement. This is the only thin section examined from the upper part of the Utica Shale. The lenses of coarser grained particles are primarily composed of carbonate, with the geometry of grains suggesting skeletal origin. The increased calcite content in the lenses is interpreted to be locally reworked, fossiliferous debris deposited during higher energy regimes. These observations suggest a shift in depositional environment from what is observed in the lower part of the Utica

Shale. The upper interval of the Utica Shale is commonly observed to have carbonate lenses and bedding structures consistent with deposition above storm weather wave base, indicating an overall shoaling upward trend.

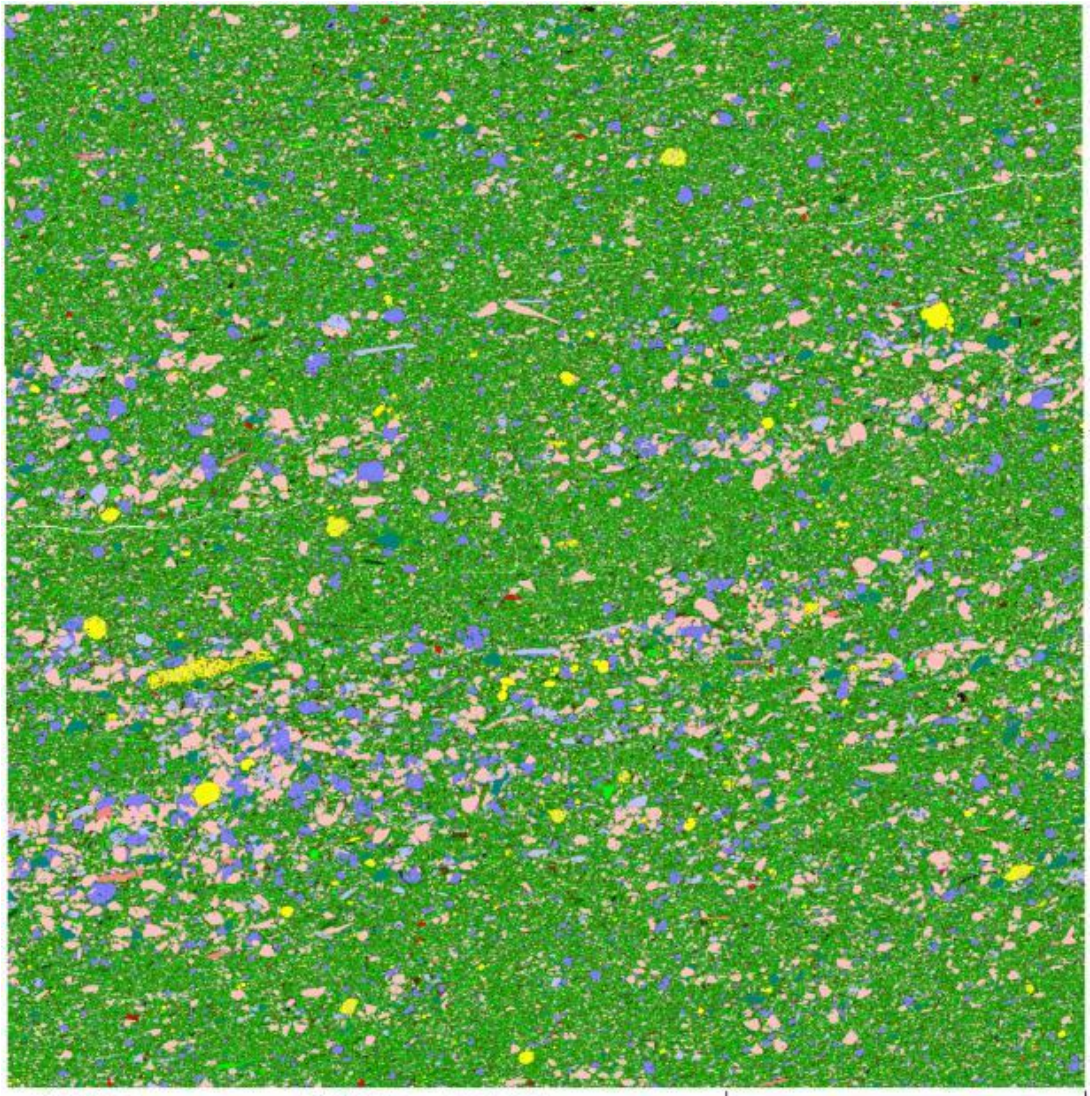

Mineral Name	Pixel counts	Area Percent
Background	52309	0.59
Quartz	1974671	22.11
K-Feldspar	258991	2.90
Rutile	57743	0.65
Dolomite	475162	5.32
Calcite	324314	3.63
Apatite	33979	0.38
Illite	4089496	45.80
Biotite_Std	902549	10.11
Chamosite	200715	2.25
Muscovite	44735	0.50
Pyrite	138024	1.55
Gypsum/Anhydrite	5037	0.06
Unclassified	424029	4.75

Figure 5- 4: QEMSCAN field of the Bruske 1-26A well at 8,479 ft. The Bruske well QEMSCAN field shows that mineralogy varies in bedding parallel lenses. These lenses are composed of larger grains and suggest shifting energy regimes.

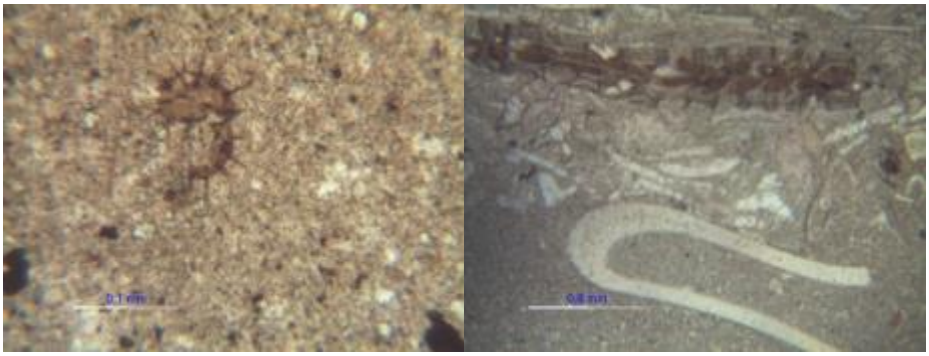

Figure 5- 5a and 5-5b: Acritarch fossil and disarticulated trilobites observed in the Bruske 1-26A well at 8,426 ft. and 8,428 ft. respectively. The scale bars are 0.1 mm and 0.8mm for the images shown.

Standard thin section analysis of samples from the Bruske well was also performed (figures 5-5a, 5-5b). Figure 5-5a is a thin section taken from a structure-less dull gray mudrock section of core (8,426 ft.) with no megascopically visible grains or bedding structures. An intact acritarch fossil surrounded by a mud matrix suggests quiet water conditions during deposition with little or no current-induced transport. Acritarchs are organic-walled microphytoplanktonic organisms that may be very diverse in appearance, and are frequently found in Paleozoic sedimentary rocks. The spikes observed on the wall of the organism are interpreted to have been used as a mechanism to stay afloat or for defense against predators. Disarticulated trilobites, brachiopods and crinoid ossicles are observed in a nearby thin section obtained from a depth of 8,428 ft. (figure 5-5b). This thin section was taken in a carbonate lens where silt to sand sized carbonate grains are common. The thin section analysis reveals the carbonate lens to be composed of disarticulated skeletal fragments. These textures are interpreted as the fossil fragments of marine organisms that lived in nearby environments and were reworked during higher energy events. The acritarch fossil is found in the Utica Shale surrounded by a clay matrix, while the trilobites are present primarily in carbonate lenses. This observation suggests the acritarch lived in a pelagic, open marine environment while the trilobites and crinoids were benthic organisms and

are interpreted to have lived in shallower, well circulated water nearby and deposited as a result of storm activity, where they were reworked and disarticulated.

The Prevost 1-11 core is located within the region of anomalous well log signature in the Saginaw Bay area and was analyzed using SEM technques. Figure 5-6 shows QEMSCAN® analysis from a sample in the Prevost 1-11 well in Bay County at 9,360 ft. This sample contains a high abundance of clay minerals (68%), 20% siliciclastic sediments, and less than 4% carbonate. This sample has numerous bedding parallel fractures with gypsum/anhydrite cement, indicating some amount of fluid flow in open fractures at some point in time.

The log signature observed in the Prevost 1-11 well was originally thought to be the result of elevated coarse siliciclastic content, due to initial XRD analysis. SEM analysis shows that the Prevost 1-11 well does not contain significant amounts of coarse clastic sediments, but instead a high abundance of clay minerals. The wire-line log signature found around the Saginaw Bay area is currently suggested to be the result of overpressure in the formation causing blowouts. The well file for the Prevost 1-11 well indicates that high pressure gas is present in the Utica Shale interval. Clay minerals may hold a large amount of bound water, which may cause the formation to become over-pressured, causing blowouts during drilling. Pyrite clusters are common in the Prevost 1-11 SEM analysis and a cluster of pyrite overprinting micro-fractures is shown in an electron-transfer dissociation (ETD) image as well as a small QEMSCAN® field in figures 5-7 and 5-8.

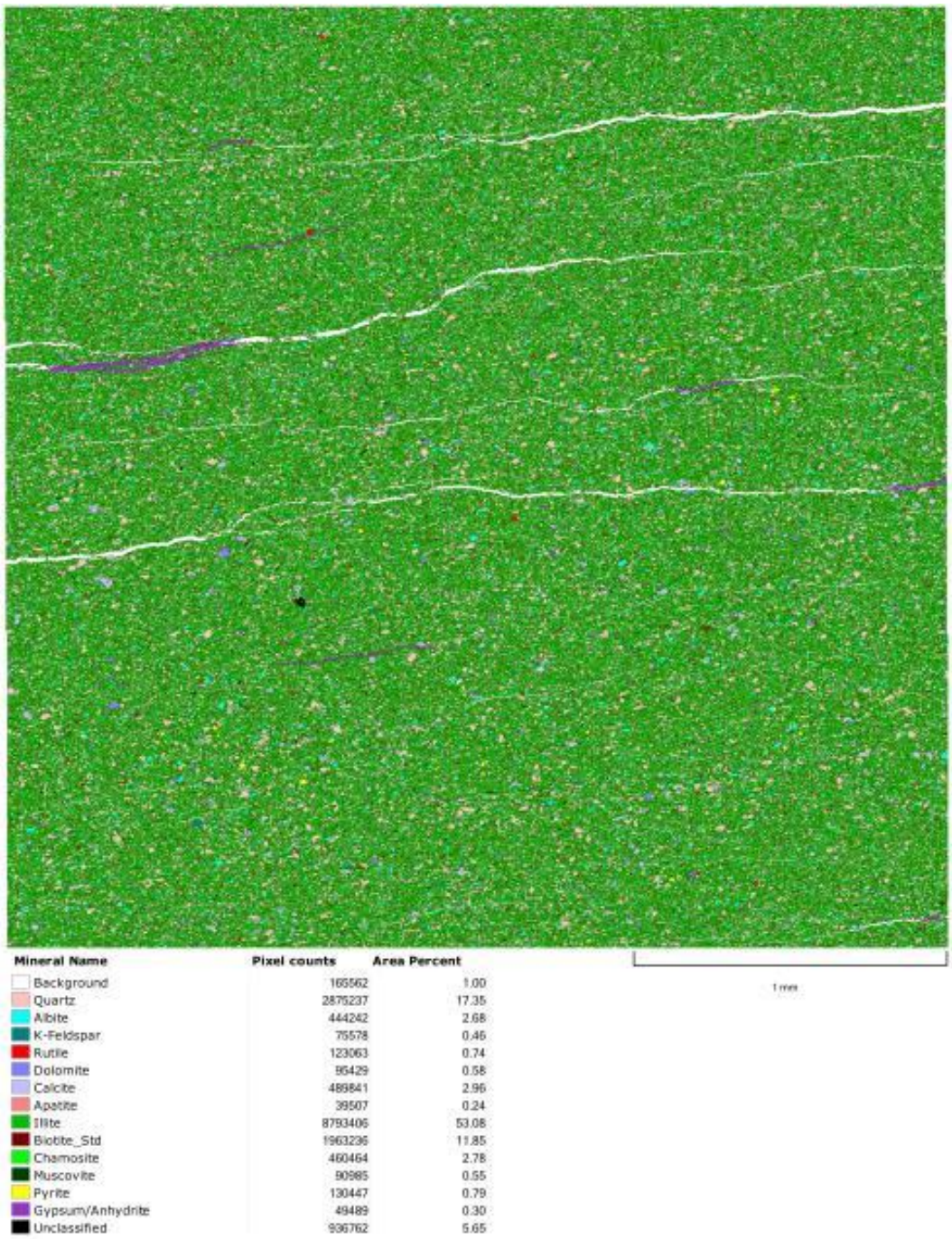

Mineral Name	Pixel counts	Area Percent
Background	165562	1.00
Quartz	2875237	17.35
Albite	444242	2.68
K-Feldspar	75578	0.46
Rutile	123063	0.74
Dolomite	96429	0.58
Calcite	489841	2.96
Apatite	39507	0.24
Illite	8793406	53.08
Biotite_Std	1963236	11.85
Chamosite	460464	2.78
Muscovite	90985	0.55
Pyrite	130447	0.79
Gypsum/Anhydrite	49489	0.30
Unclassified	936762	5.65

Figure 5- 6: QEMSCAN field for the Prevost 1-11 well at 9,360 ft. The Prevost 1-11 well is located in Bay County and is the only well located within the zone containing an anomalous log signature.

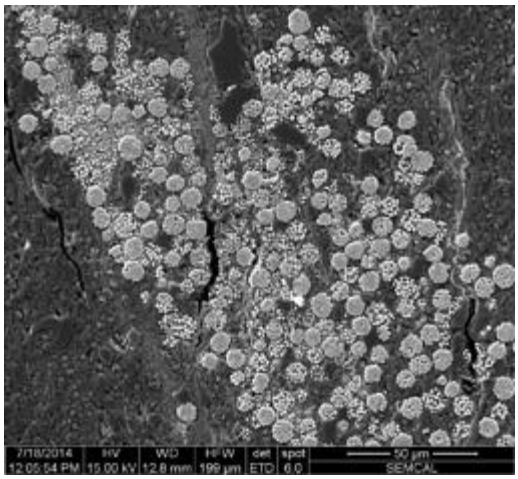

Figure 5- 7: Framboidal pyrite cluster around cemented micro-fractures.

This second QEMSCAN® field (figure 5-8) is generated from the same thin section as the first field, and is not the same size as the other fields generated in this study (the dimensions of the field are 2mm x 2mm). The cementing material observed around the pyrite cluster is gypsum/anhydrite. There appears to be an elevated amount of OM porosity around the pyrite cluster but an elemental spectrum of the composition of the pores could not positively identify increased organic content. The micro-fractures found through the pyrite cluster cross-cut individual framboids, suggesting the pyrite was formed before the microfractures. The black “hair shaped” unidentified mineral near the top of figure 5-10 is extra carbon that is coated on the thin section and is not part of the thin section itself.

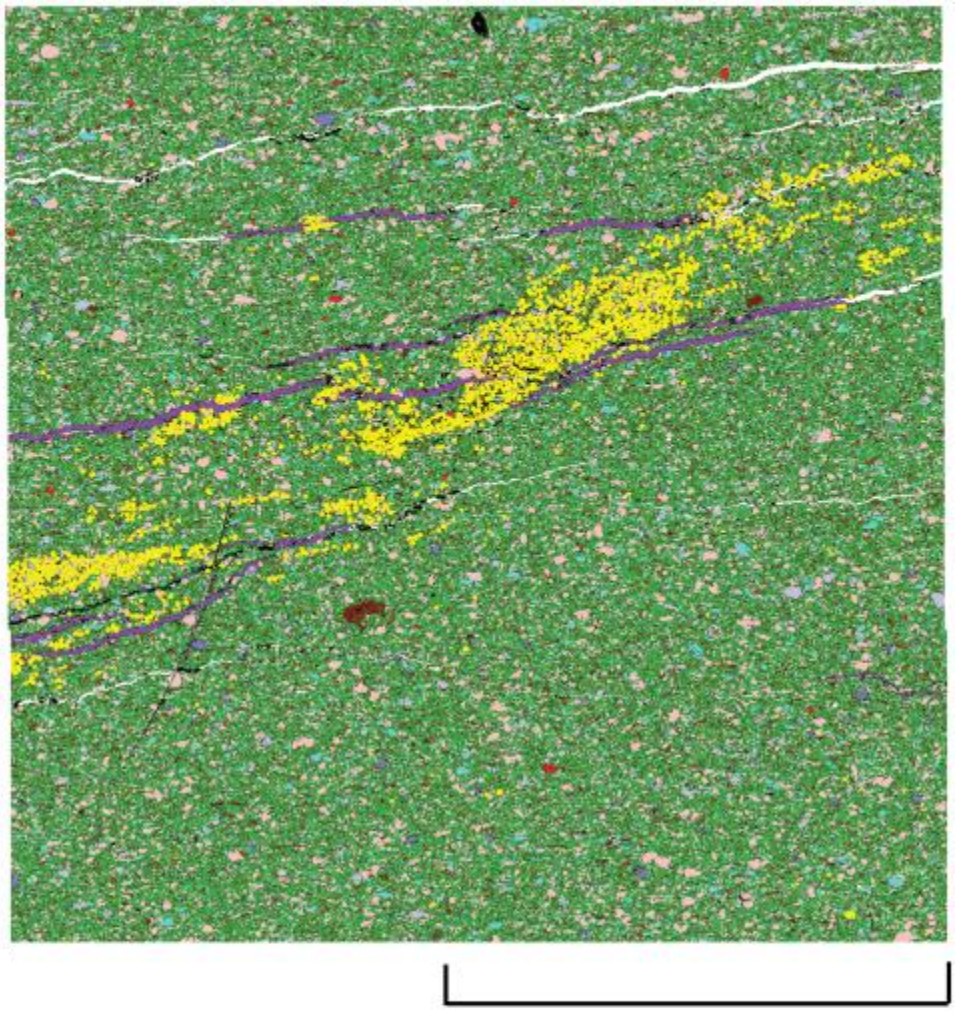

Mineral Name	Pixel counts	Area Percent
Background	18046	0.87
Quartz	348845	16.90
Albite	54697	2.65
K-Feldspar	8999	0.44
Rutile	14338	0.69
Dolomite	9814	0.48
Calcite	55770	2.70
Apatite	4493	0.22
Illite	1023720	49.60
Biotite_Std	233408	11.31
Chamosite	54927	2.66
Muscovite	12156	0.59
Pyrite	84586	4.10
Gypsum/Anhydrite	25789	1.25
Unclassified	132346	6.41

Figure 5- 8: Prevost 1-11 well at 9,360 ft. Pyrite is clustered around an area full of sealed micro-fractures. Cementing material is gypsum/anhydrite.

The State Albert 1-10 well in Montmorency County is studied extensively through SEM analysis. A 3mm x 3mm QEMSCAN® field is generated along with a BSE field of the same dimensions and the same location (figures 5-9 and 5-10).

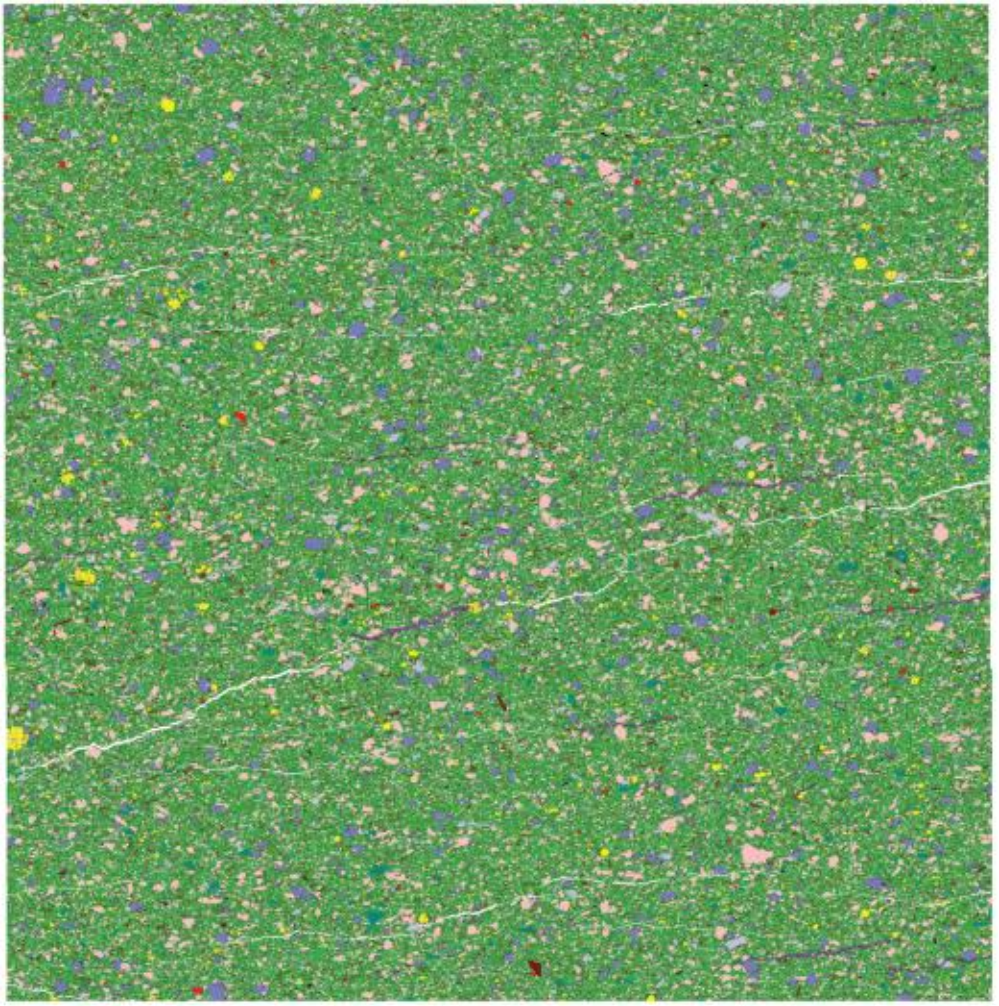

Mineral Name	Pixel counts	Area Percent
Background	56619	1.01
Dolomite	204676	3.64
Calcite	134595	2.39
Gypsum/Anhydrite	13436	0.24
Quartz	1110159	19.72
K-Feldspar	94285	1.68
Rutile	37232	0.66
Illite	3035537	53.93
Biotite_Std	515744	9.16
Chamosite	141906	2.52
Pyrite	87329	1.55
Unclassified	253539	4.50

Figure 5- 9: QEMSCAN field for the St. Albert well at 7,728 ft. The St. Albert 1-10 well was drilled in Montmorency County, in the northeastern part of Lower Michigan. Fractures occur parallel to bedding.

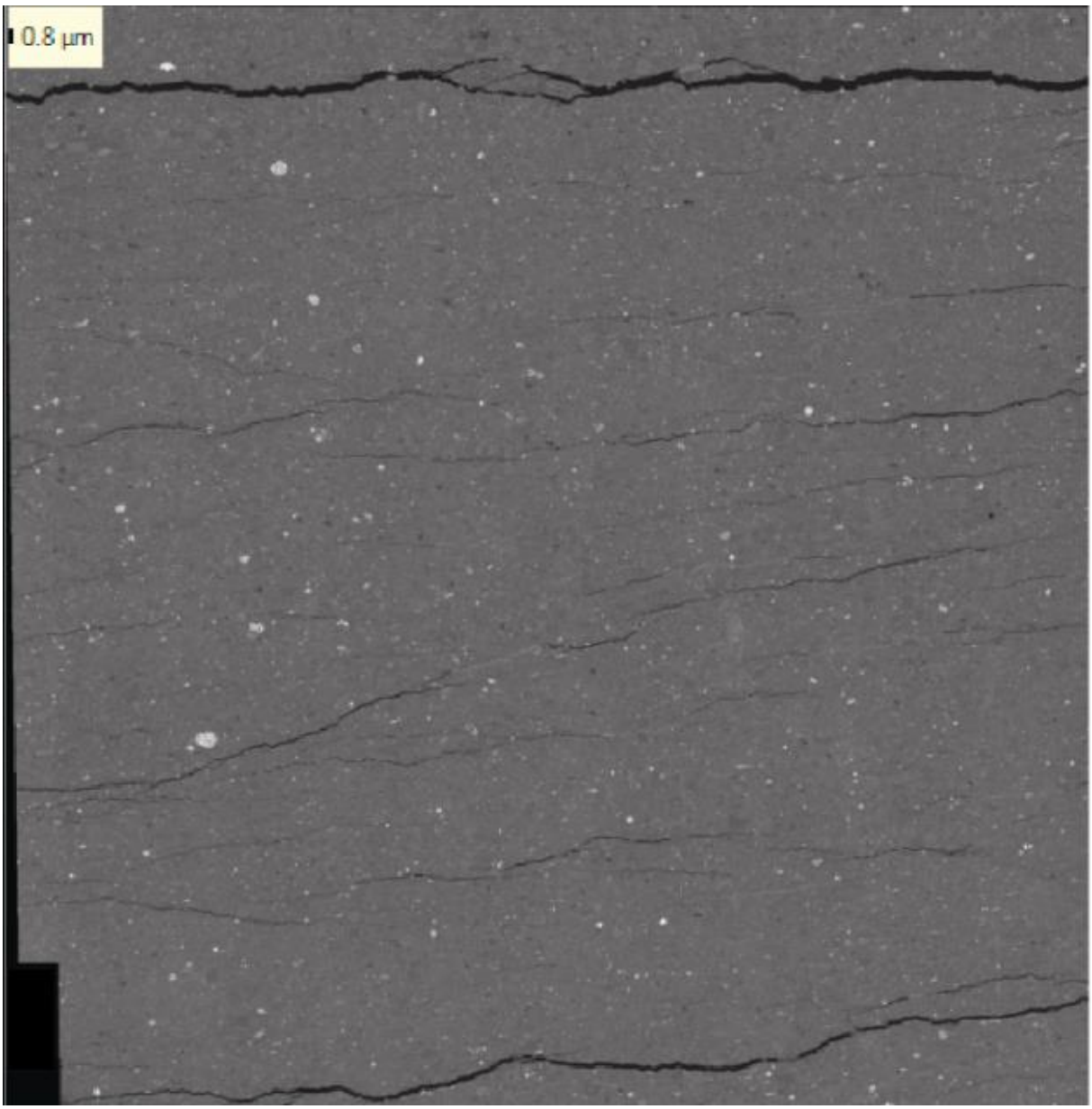

Figure 5- 10: ETD image for the St. Albert well at 7,728 ft. This image can be magnified and is used to check the QEMSCAN® software for accuracy.

The sample analyzed is taken at a depth of 7,728 ft. The resulting fields show a primarily clay matrix with gypsum/anhydrite cemented fractures and silt sized detrital quartz grains. The grains are moderately well rounded and are not the result of authigenic mineralization. Dolomite is observed replacing calcite and interpreted to

have formed in-situ. Montmorency County is located in the northeastern part of the Michigan basin, and the upper interval of the Utica Shale in this location is observed to contain increased carbonate content (discussed in Ch. 3). This sample was taken from the lower interval of the Utica, near the contact with the underlying Collingwood Mbr. The matrix is composed of phyllosilicate minerals, primarily illite with some mica group minerals and chlorite. Chlorite is identified as chamosite (a reduced iron-rich chlorite) by the iDiscover software. Pyrite and K-feldspar are also present in the sample but in low abundance. The State Albert 1-10 well contains numerous bedding parallel fractures typically cemented with gypsum/anhydrite. The BSE image field (figure 5-10) is used to ensure accuracy of the QEMSCAN® software. The resolution and zoom of the field may be increased to accurately depict grains and gives a higher degree of confidence for accurate mineral identification. Figure 5-11 is a high resolution ETD image that shows authigenic clay minerals coating detrital grains. The scale bar in the photo is for 10 µm. These relationships suggest that, at least some clay minerals were formed during diagenesis, further reducing intergranular porosity and permeability.

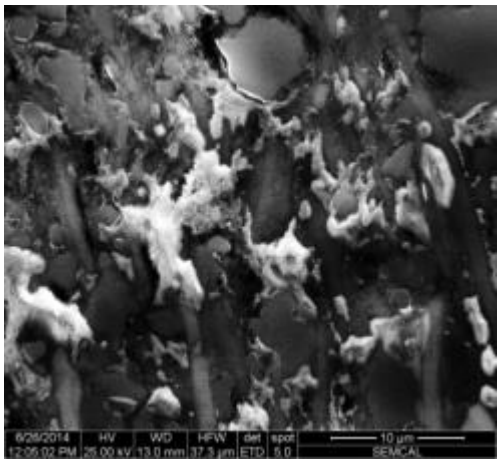

Figure 5- 11: Authigenic mineralization of clay minerals and coating of detrital grains. Scale bar is 10 µm.

The Arco & Conklin 1-31 (Jackson Co.) sample studied was taken at a depth of 3,696 ft. The field generated by QEMSCAN® analysis is shown below in figure 5-12. The field is taken from a section of core with visible grains and cross-bedding. This section of

core was probably deposited above storm weather wave base and is the only QEMSCAN® field to have been taken from an area of core with cross-bedding. The QEMSCAN® results show that the larger grains are quartz and K-feldspar. Authigenic dolomite composes just over 11% of the whole rock mineralogy. Calcite is included into the dolomite fraction because it represented <1% of the field. Minor intergranular cement is primarily gypsum/anhydrite. Clay minerals are the most abundant mineral type observed in this sample although they compose less than 50% of the sample, significantly less than previously analyzed samples.

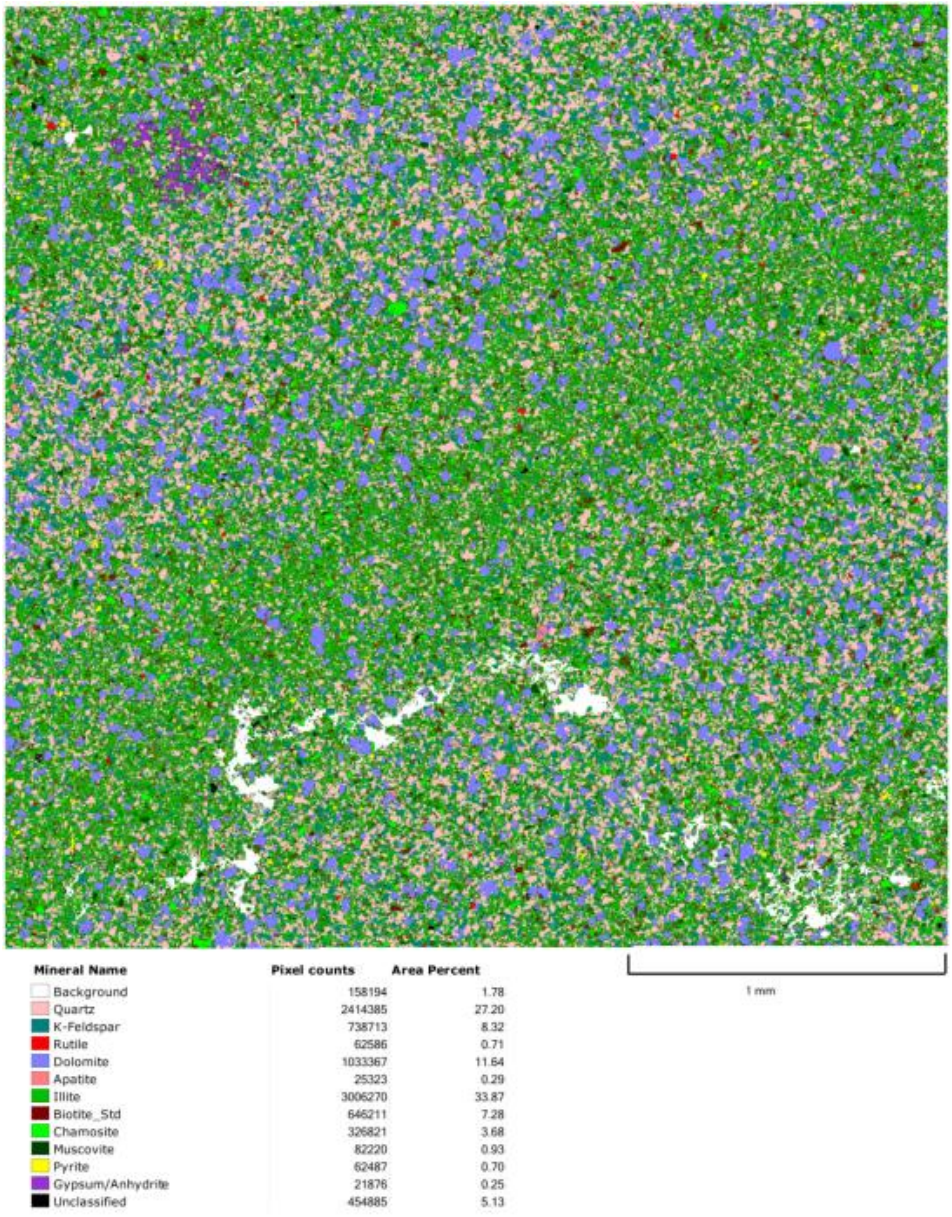

Mineral Name	Pixel counts	Area Percent
Background	158194	1.78
Quartz	2414385	27.20
K-Feldspar	738713	8.32
Rutile	62586	0.71
Dolomite	1033367	11.64
Apatite	25323	0.29
Illite	3006270	33.87
Biotite_Std	646211	7.28
Chamosite	326821	3.68
Muscovite	82220	0.93
Pyrite	62487	0.70
Gypsum/Anhydrite	21876	0.25
Unclassified	454885	5.13

Figure 5- 12: QEMSCAN® field of the Arco-Conklin well at 3,696 ft. Increased siliciclastic content and carbonate grains are observed to occur in a rhythmic pattern.

In sample 3,696 ft a large, irregular and elongate pore occurs in the lower-right part of the field. The origin of this vein-like pore is difficult to analyze with confidence in a standard QEMSCAN® field, however when the QEMSCAN® field is modified to show only pores and OM, the pore is clearly well connected (figure 5-13). The morphology of this porosity is suggestive of origin related to a stylolite. Stylolites form as a result of pressure induced mineral dissolution. High stress associated with dissolution can lead

to the formation of stylolites, and these relationships are present in the Arco-Conklin sample presented in the QEMSCAN® field in figures 5-12 and 5-13. The stylolite would likely have been sealed shut in the subsurface and opened during coring, slabbing, or during the creation of the thin section itself.

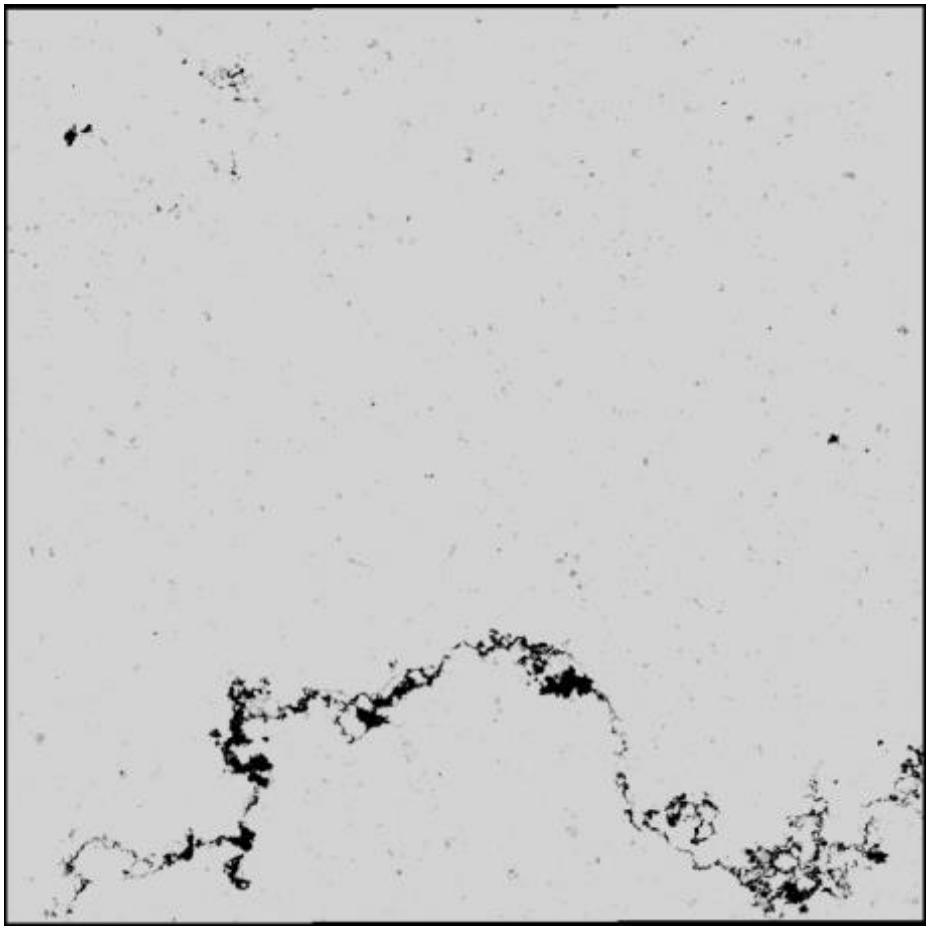

Figure 5- 13: Negative image of porosity in the Arco-Conklin well. The connectivity of pore space is not as easily observed in QEMSCAN® analysis, however here it is shown to be well connected.

The Weingartz 1-7A well located in Clare County is sampled at a depth of 10,076 ft. The QEMSCAN® field reveals a primarily clay matrix with nearly 20% quartz content and some carbonate grains (figure 5-14, below).

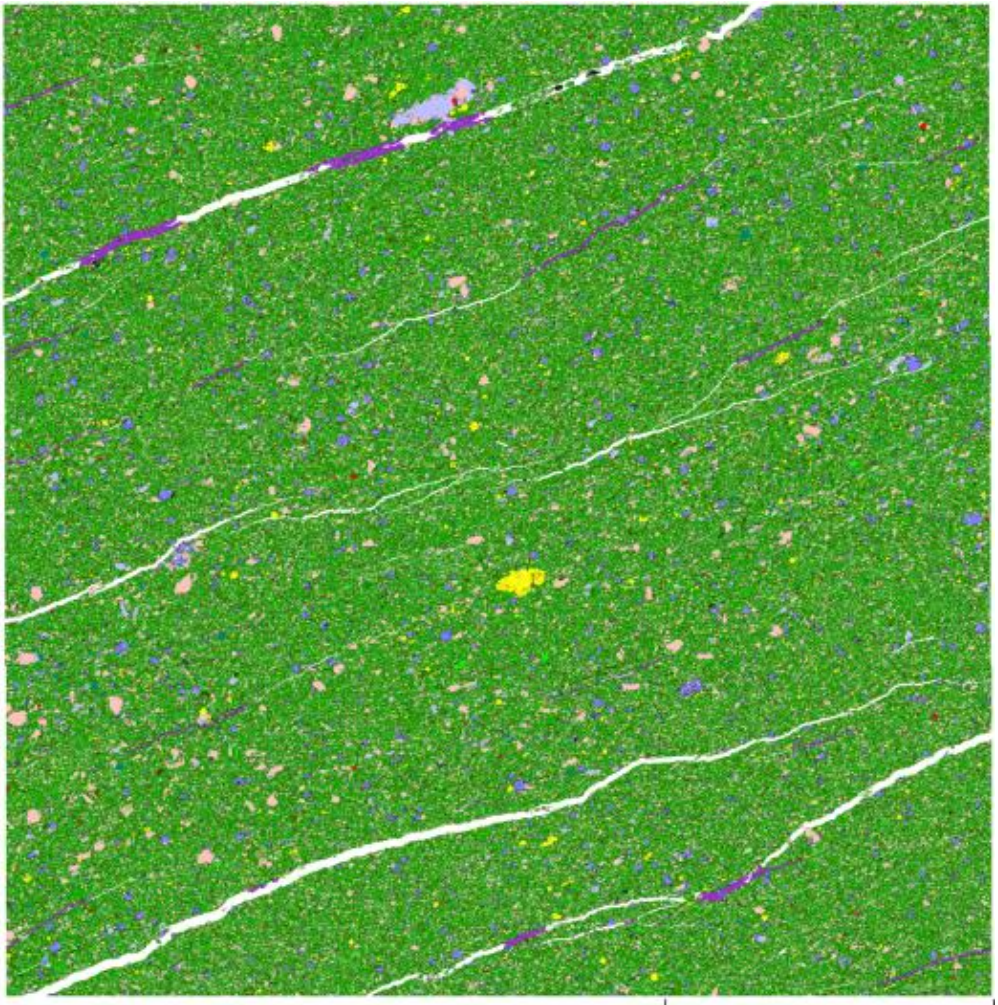

Mineral Name	Pixel counts	Area Percent
Background	101743	1.16
Quartz	1627427	18.52
K-Feldspar	49393	0.56
Rutile	58072	0.66
Dolomite	231446	2.63
Calcite	298902	3.40
Apatite	18530	0.21
Illite	4549612	51.79
Biotite_Std	999834	11.38
Chamosite	184147	2.10
Muscovite	37722	0.43
Pyrite	145040	1.65
Gypsum/Anhydrite	52737	0.60
Unclassified	532694	6.06

Figure 5- 14: QEMSCAN® field of the Weingartz well at 10,076 ft. Note the increased abundance of bedding parallel microfractures. These fractures are interpreted to have been formed as a result of pressure release as the core was taken to the surface and stored.

The rock is highly fractured when compared to previously analyzed samples. Fractures are cemented with gypsum/anhydrite and in some instances cut across large grains. Open fractures observed in the sample likely formed late, possibly as a result of

pressure release as the rock was brought to the surface, while mineralized fractures are of geologic origin. The Utica is buried to significant depth in Clare County and at a pressure gradient of 0.5 psi/ft., it is reasonable to infer that the rock was under a minimum of 5,000 psi in the subsurface. Upon drilling and coring the rock was brought to the surface where only atmospheric pressure conditions exist. Many of the fractures observed in this sample formed during this rapid pressure release when the samples went from being under 5,000 psi to atmospheric pressure conditions (14 psi) and were stored. Figure 5-15 shows a grain cross cut by a fracture and is suggested to have been formed in this fashion.

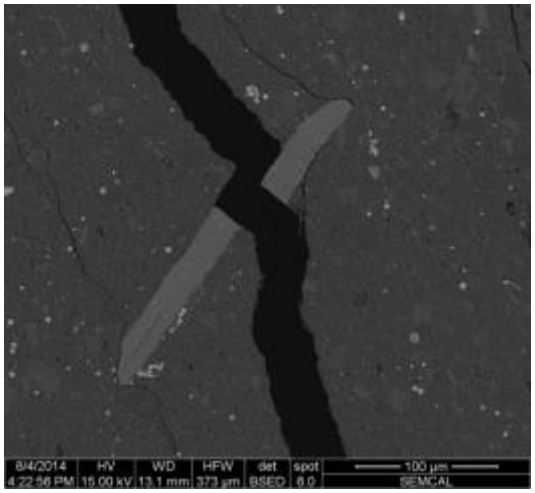

Figure 5- 15: Grain being cross cut by an artificial fracture. The fracture is suggested to not have been open in the subsurface.

The Weingartz 1-7A QEMSCAN® field has small OM pores scattered throughout. Figure 5-16 is one such pore. The irregular shape of the pore and the relationship of the pore to surrounding grains aids in interpretation of OM porosity. To be confident in interpreting the origin of this porosity a spectrum of elemental abundances is required. One such spectrum is shown along with the BSE image and shows an 88.45% carbon signature. Fractures filled with epoxy typically contain Cl along with C and O, and the absence of Cl suggests the spectrum generated is that of organic matter. Pores interpreted as OM are frequently observed to be in close proximity to apatite grains or

pyrite. Pores in this study that have a similar elemental spectrum are considered organic and have been labelled as such (OM).

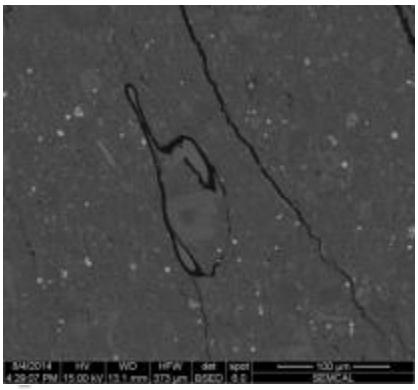

El	AN	Series	unn. C [wt.%]	norm. C [wt.%]	Atom. C [at.%]	Error (1 Sigma) [wt.%]
C	6	K-series	88.45	88.45	93.25	9.90
O	8	K-series	4.67	4.67	3.70	0.83
Si	14	K-series	4.36	4.36	1.96	0.21
Al	13	K-series	1.89	1.89	0.89	0.12
K	19	K-series	0.62	0.62	0.20	0.05
		Total:	100.00	100.00	100.00	

Figure 5- 16: OM porosity within the Weingartz 1-7A well and the chemical composition of the pore. A high carbon signature suggests the pore to be organic. Scale bar is 500 µm.

Results from QEMSCAN® analysis are consistent with quantitative mineralogy results produced by X-ray diffraction analysis (figure 5-17, below). QEMSCAN® analysis of samples from the Thompson 1-30 well and the Bruske 1-26A plot as a 'Silty Claystone' on a ternary composition diagram. The QEMSCAN® results show that the Utica Shale consistently plots as a Silty Claystone in the classification scheme presented in figure 4-1. Several samples with mineralogical analysis from whole rock x-ray diffraction only plot in the Silty Marl or Argillaceous Siltstone facies. Although these facies were not observed in QEMSCAN® analysis, these mineralogical facies are expected to be accurately characterized by the x-ray diffraction analysis. Thin sections selected are interpreted to be representative of the rock at the depth provided. Each thin section was taken from a section of rock that was characteristic of the Utica Shale in the core

provided. The Arco-Conklin sample is the one exception in that it was taken from a cross-bedded section of core with grains visible to the naked eye. The Bruske, Thompson, Prevost, St. Albert, and Weingartz thin sections were all taken from areas of core that appeared to best represent the general core appearance. This was done in order to ensure an accurate depiction of quantitative mineralogy for each well. Of the 9 thin sections generated for use in this study, only 6 were used for QEMSCAN® analysis. Thin sections that were not selected for QEMSCAN® analysis were observed under a standard petrographic microscope and no interpretations of mineralogy were made on such samples. The samples that were selected for QEMSCAN® analysis have the best field size and characteristics (no fractures, artifacts) and are most representative of the core and depth provided.

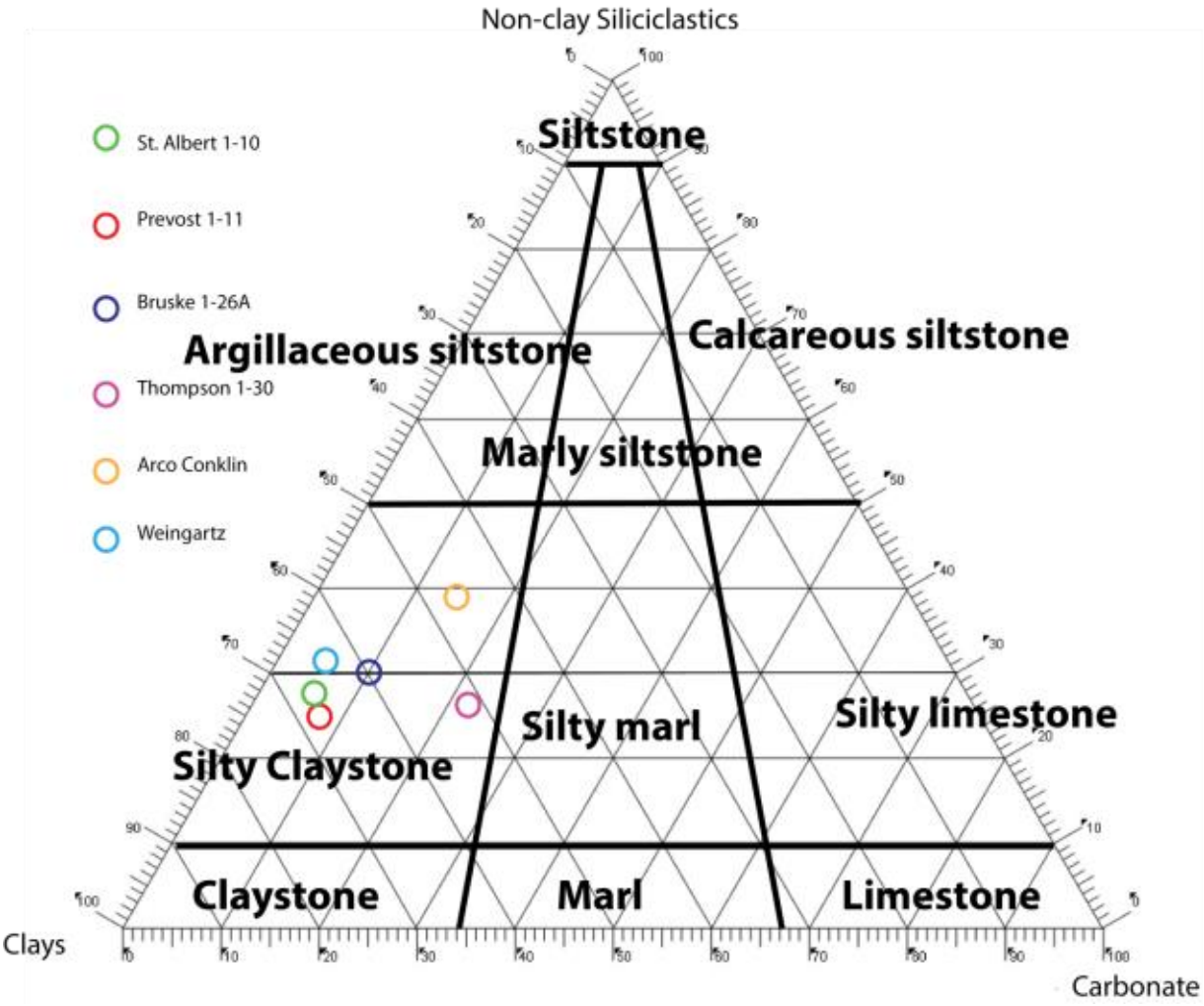

Figure 5- 17: QEMSCAN® results plotted on a ternary diagram. Results confirm XRD analysis on the distribution of lithofacies. The Bruske 1-26A and Thompson 1-30 wells do not plot directly in the 'Silty Marl' facies, but are within expected facies boundaries.

6. MERCURY INJECTION-CAPILLARY PRESSURE TESTING

Mercury injection porosimetery is used to determine porosity, pore connectivity, and pore size for five samples from the Thompson, Bruske, Prevost, Arco & Conklin and Weingartz wells. Each sample with measured porosity and calculated permeability values is shown in table 2.

	Depth (ft.)	Weight (g)	Porosity (%)	Permeability (mD)
Thompson 1-30	2,277	16.251	0.77	0.003
Bruske 1-26A	8,479	16.083	2.66	0.179
Prevost 1-11	9,353	13.329	6.11	5.368
Arco-Conlkin 1-31	3,696	14.214	2.78	14.71
Weingartz 1-7A	10,076	14.539	5.93	89.42

Table 2: Measured porosity and calculated permeability values for each sample analyzed.

The measured outputs given by the mercury porosimeter are total intrusion volume, total pore area, pore diameter, bulk density, apparent (skeletal) density and porosity. The total intrusion volume is the total volume of mercury that is intruded during the experiment. The intrusion volume converted to an area (assuming cylindrical shaped pores) is the total pore area. The pore (throat) diameters are determined by the size at the 50^{th} percentile on the cumulative volume and area graphs. An average is taken from these amounts and is reported as the average pore diameter. The mass of the sample (measured) divided by the bulk volume (penetrometer filled with mercury at 0.5 psia) yields the bulk density. Once the sample in under maximum pressure (assuming 100% pore volume filled with mercury) the mass of the sample divided by the volume yields apparent (skeletal) density of the rock. Porosity can then be calculated by dividing the bulk density by the apparent density. The permeability is calculated based on the first inflection point of rapidly rising mercury intrusion on the intrusion curve. The corresponding pressure for the inflection point corresponds to the pore throat size at which mercury can migrate in a sample.

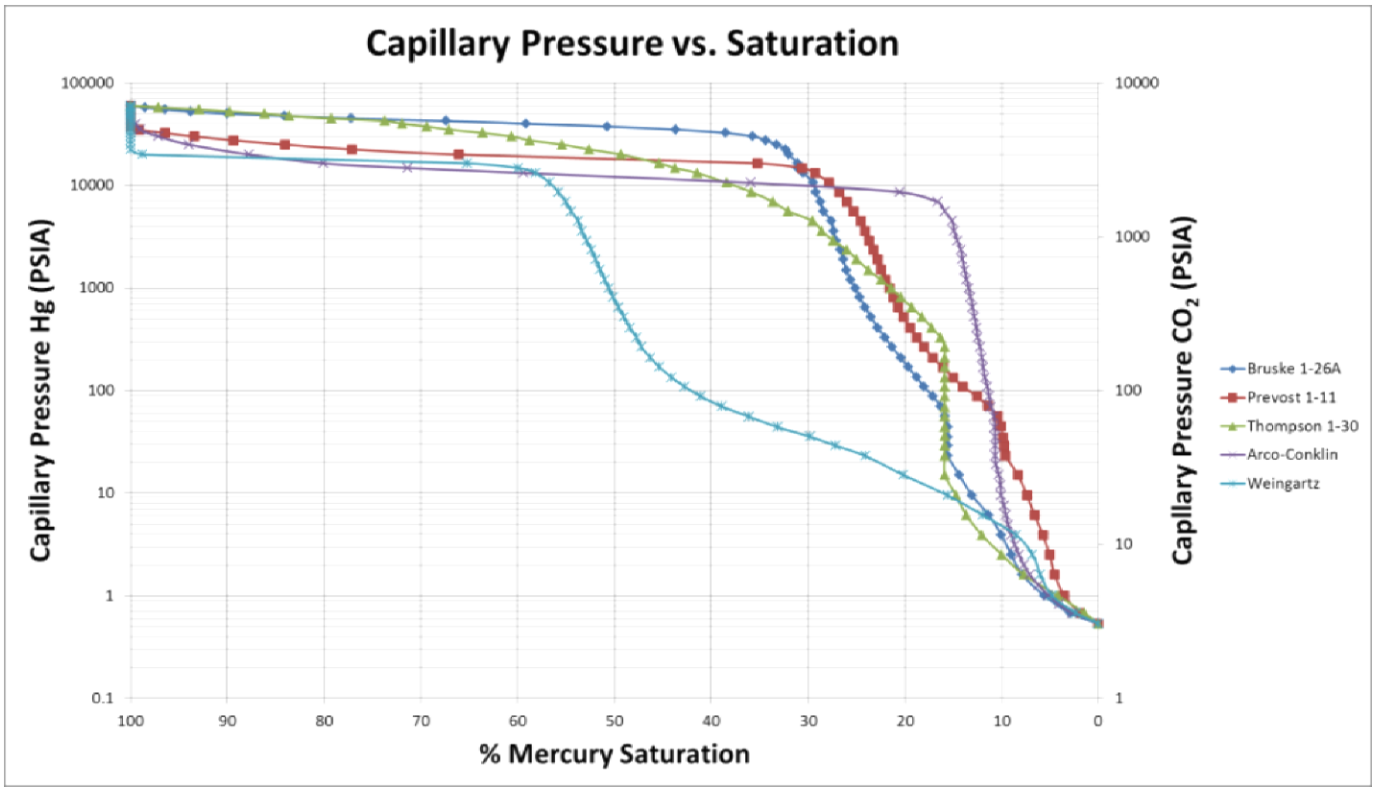

Figure 6- 1: Capillary Pressure vs. Percent Saturation. Note the decrease in pressure required to mobilize the non-wetting fluid phase when reservoir (CO_2) conditions are given.

Mercury injection porosimetery was used in this study to estimate the regional seal capacity for the Utica Shale in the Michigan basin. Figure 6-1 is a plot of capillary pressure vs. pore volume intruded. The y-axis represents pressure and the x-axis mercury saturation. The values for pressure are plotted on a logarithmic scale and the Hg saturation is plotted in reverse order. As pressure is increased more of the sample becomes saturated. When the line that represents each sample moves in a straight line to the left (increased saturation without increased pressure) the sample is readily imbibing the non-wetting fluid phase.

CO_2 and Hg have different surface tensions and therefore contact angles that depend not only on the fluid, but on the surface to which the fluid is contacting. Therefore when calculating in-situ reservoir conditions the properties of the injection fluid must be taken into account. CO_2 breakthrough pressures may be an order of magnitude smaller than breakthrough pressures measured in laboratory experiments using Hg. Estimated CO_2 breakthrough pressures are plotted on the secondary y-axis in figure 6-1. These values are calculated from the conversion equations generated by Hartmann and Beaumont, (1999). The pressures used in this study are accurate for gaseous CO_2 and not supercritical CO_2. The buoyancy forces for gaseous CO_2 should be even higher than supercritical CO_2, and therefore the pressures used in this study are conservative numbers, with the actual pressures required to migrate the non-wetting fluid phase likely to be substantially higher than recorded.

Figure 6-2 shows a plot of cumulative intrusion vs. pore diameter. Pore throat size distributions were calculated from mercury injection capillary pressure (MICP) data using relationships that are dependent on the properties of both mercury and the rock matrix. Pore throats are assumed to be cylindrical allowing for use of the Washburn equation:

$$D = -4 \gamma \cos(\theta) / P$$

D is pore throat diameter, P is mercury intrusion pressure, γ is the surface tension of mercury and θ is the advancing mercury contact angle. The plot shows that a vast majority of the intrusion takes place in pore throats with a diameter of 0.1 µm or less

(nanometer scale). Intrusion in larger pore throats is considered to primarily take place in fractures located in the sample, or as Hg conforms to irregularities at the surface of the sample. This recorded intrusion is not representative of in-situ conditions as pressure release micro-fractures and sample surface irregularities are artifacts that are only encountered in the lab. The Weingartz sample had a significant amount of intrusion at the 10's of µm scale. The sample used for MICP analysis for the Weingartz well is from a depth of 10,076 ft. and therefore has undergone significant pressure changes allowing fractures to form after drilling. The observed intrusion at larger pore throats for the sample may therefore be artifacts, fractures that would not be open and transporting fluids in the subsurface. The remaining samples are observed to have little to no intrusion until the nanometer scale pore space. This observation is consistent with what would be expected in an impermeable geologic seal.

A mercury saturation of 35% corresponds to the pore system that dominated flow through rock (Hartmann and Beaumont, 1999). Figure 6-3 is a plot that takes into account pore throat size, reservoir capillary pressure, mercury saturation and height of non-wetting fluid column required to enter 35% of the pore throat space. The vertical black bar labelled "R_{35} Port" represents 35% mercury saturation in a given sample. This point is traced to the secondary y-axis on the left side of the figure, showing the capillary pressure (of CO_2 in psia) required to access 35% of the pore throats. The corresponding height of CO_2 column is the height of buoyant non-wetting fluids (in this case CO_2) required to overcome the capillary resistance of the pore throat radii. For example, when considering the Thompson 1-30 sample (in green), the pore throat radii that corresponds to 35% mercury saturation is < 0.1 µm (nanopore). A capillary pressure of ≈3,000 psia CO_2 is required to access this amount of pore space, and a CO_2 column 5,200 ft high would be required to overcome the capillary resistance of the pores to actively migrate fluids. The Weingartz sample is an outlier in the data set, with macropore sized pore throats and only 15 psi CO_2 required to access pore throats, corresponding to a CO_2 column height of only 60 ft. The Weingartz sample was previously discussed as having been buried to significant depth (>10,000 ft.) and

artificial fractures may have resulted in inaccurate measurements of porosity, intrusion volume, and pore throat sizes. All other samples from the Thompson, Bruske, Prevost and Arco-Conklin wells have breakthrough pressures over 3,000 psi CO_2 corresponding to CO_2 column height of over 5,000 ft. Therefore the Utica Shale in the Michigan basin will act as a regional geologic seal for a minimum of 5,000 ft. of CO_2, and greater than a 10,000 ft. of CO_2 column (see Bruske sample). The column heights suggested are once again representative of gaseous CO_2. Supercritical CO_2 will have a lower buoyancy force than gaseous CO_2 and therefore the column heights are once again conservative values.

The Arco-Conklin sample is the only sample in this study that used a single piece of rock during MICP testing, and is also the only sample taken from a piece of core with silt-sized grains present. The Arco-Conklin sample is taken through a cross-bedded section of core and has breakthrough pressure at around 3,500 psia CO_2. The capillary resistance of the pore throats in the sample are capable of holding a 7,000 ft. column of CO_2 before transporting fluids. The cross-bedded section of core therefore does behave as a geologic seal. SEM analysis conducted on the Arco-Conklin well shows a primarily clay composition, with the cross-bedding consisting of larger quartz and dolomite grains. This piece of core was chosen to ensure quality control and for experimental results.

MICP analysis is supplemented with SEM, XRD and thin section analysis in order to document mineralogical and textural variations. The results observed during both SEM and MICP analyses are consistent with one another. Fractures are most abundant in the Prevost 1-11 well and MICP analysis confirms this sample has the highest porosity and permeability relative to the other samples. The lowest porosity and permeability values are observed in the Thompson 1-30 well. An absence of connected fractures or fracture-fill cement is also observed with SEM analysis. Pores observed in SEM analysis of the Thompson 1-30 well are thought to originate as organic (OM) porosity in the absence of intergranular pores.

Porosity and permeability values may be in error due to microfractures that developed during or after coring. It is possible stress relief fractures account for some

amount of porosity and mislead permeability calculations. Older cores that have been stored for longer periods of time and that were originally buried at significant (8,000 ft. +) depth tend to have more bedding parallel stress relief fractures than newer, shallower cores. It is possible that older cores, slabbed and stored for multiple decades, may be weaker and therefore subject to error during MICP analysis (microfractures may develop during storage over time).

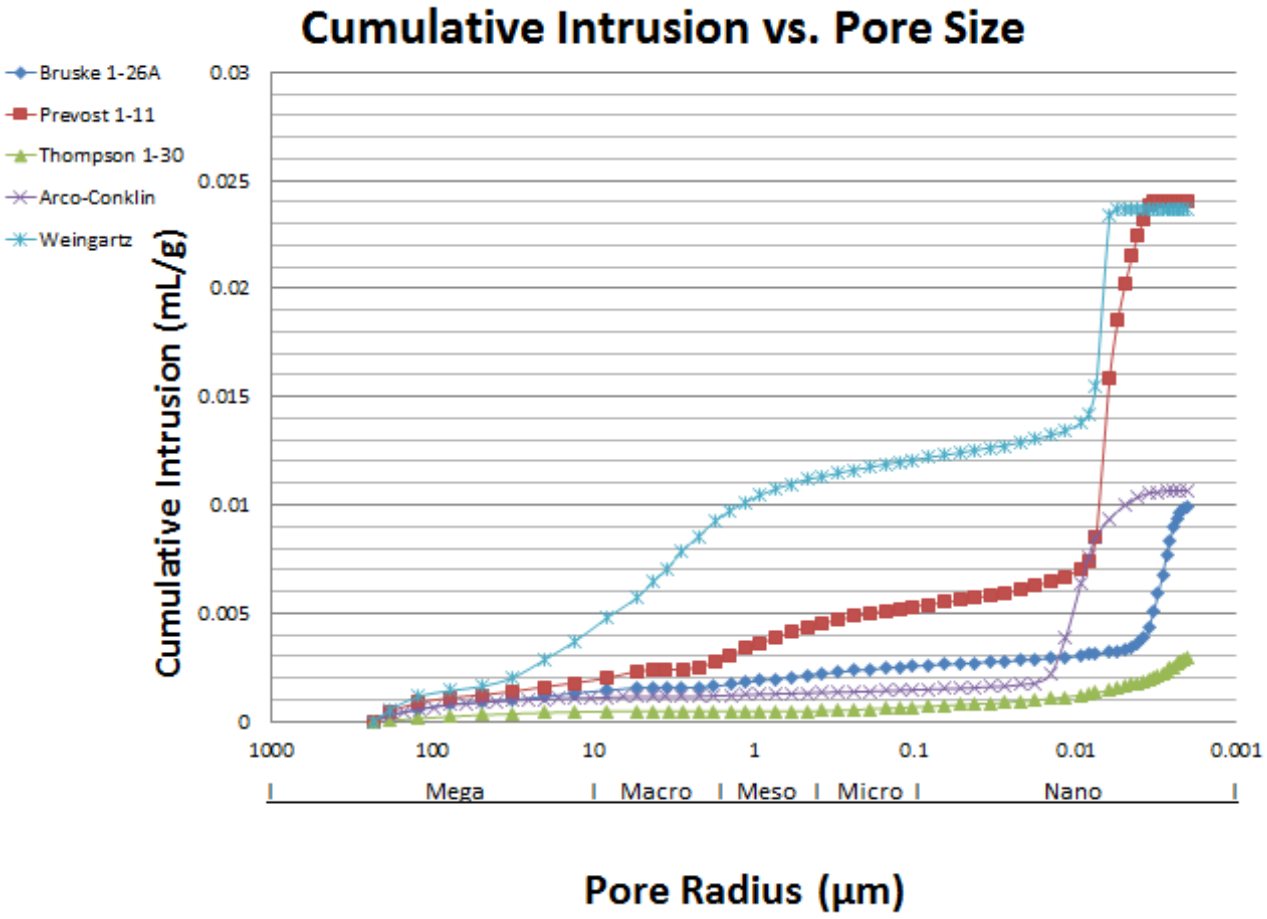

Figure 6- 2: Cumulative Intrusion vs. Pore Size. Each curve shows the majority of intrusion occurring at the nanometer scale pore size.

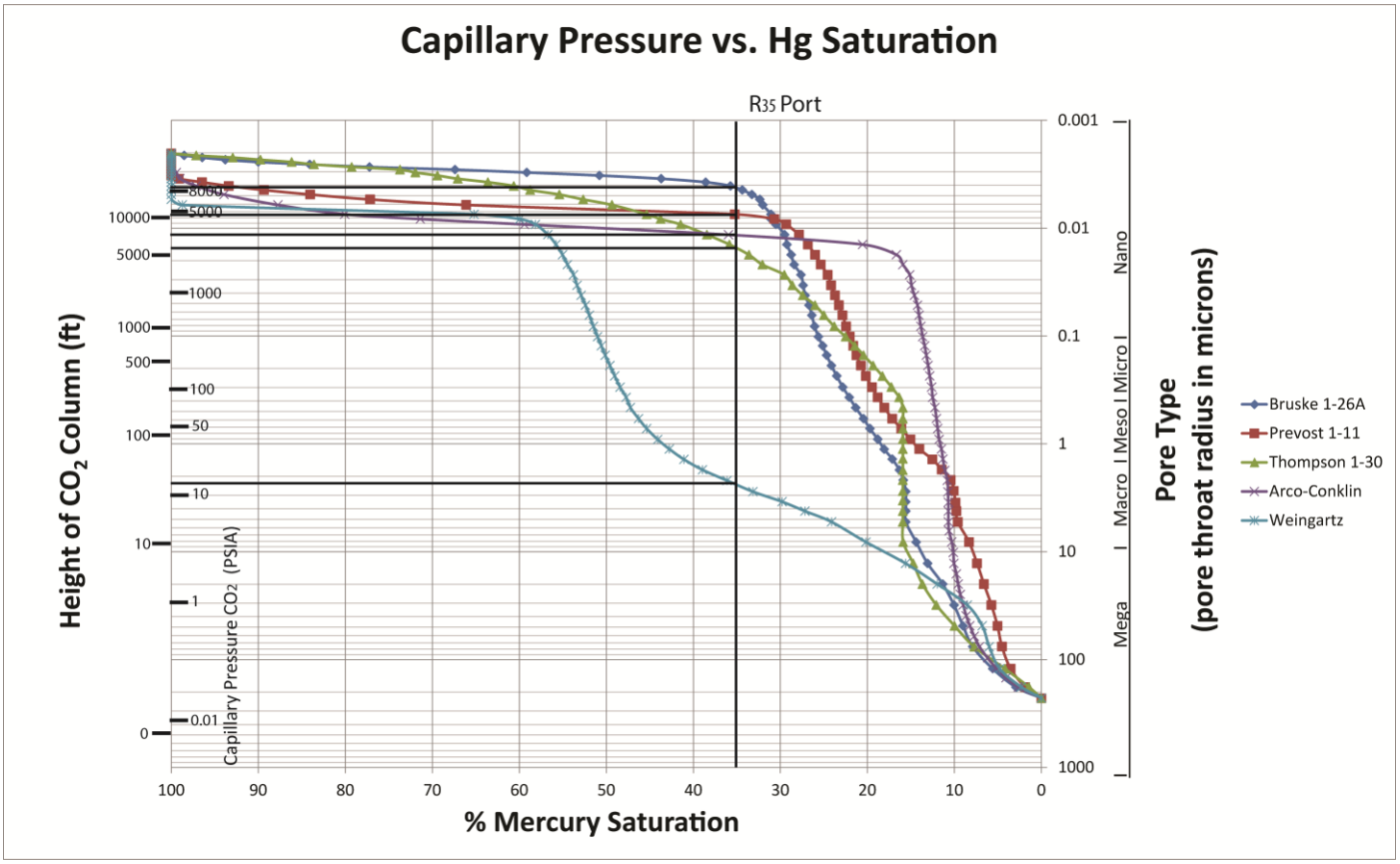

Figure 6- 3: Height of CO_2 column required to overcome capillary resistance.

7. MECHANICAL TESTING

Triaxial strength tests are used to measure the mechanical properties in rocks. Shales that have low density and high ductility are ideal geologic seals. Increased ductility allows for rock to undergo large amounts of strain without giving way to brittle failure, and a loss of seal integrity due to mechanical fracture. Shale with density values greater than 2.1 g/cm^3 will undergo brittle failure given sufficient strain (Hoshino et al., 1972). Ductility is also a function of confining pressure, where increasing confining pressure increases ductility of the rock. Results for triaxial strength tests and testing parameters are shown below in tables 3 and 4.

Sample	Orientation to Bedding	Depth ft.	Mass g	Length in.	Diameter in.	Nominal Density g/cc
Bruske 1-26A #3	⊥	8428.0	68.9	2.0250	0.9855	2.722
Bruske 1-26A #4	⊥	8470.0	63.0	1.8543	0.9852	2.720
Thompson 1-30 #5	⊥	2273.0	58.0	1.7528	0.9838	2.656
Thompson 1-30 #6	═	2273.0	54.8	1.6478	0.9867	2.654
Thompson 1-30 #8	⊥	2293.0	56.2	1.6884	0.9843	2.669
Thompson 1-30 #10	⁄	2288.0	67.7	2.0421	0.9853	2.653

Table 3: Sample names and testing parameters for the six samples used in this study.

Sample No.	Depth (ft)	Confining Pressure (psi)	Compressive Strength (psi)	Static Young's Modulus (x10^6 psi)	Static Poisson's Ratio
1-26A #3	8428.00	4214	40032	7.08	0.28
1-26A #4	8470.00	4235	33150	5.28	0.26
1-30 #5	2273.30	1137	19234	3.21	0.22
1-30 #6	2273.00	1137	14088	5.55	0.22
1-30 #8	2293.00	1147	17888	3.77, 2.93	0.16, 0.36
1-30 #10	2288.00	1144	11591	3.88	0.19

Table 4: Results for each sample including compressive strength, Young's modulus, and Poisson's ratio.

Samples taken from the Bruske well have the higher compressive strength of the two lithologies (Silty Claystone/Silty Marl). Results for all samples are shown in figures 7-1, 7-2, 7-3. The compressive stresses required to cause mechanical failure of the Bruske samples are 40,032 psi and 33,150 psi (table 4). These values are considerably higher than the 11,591 psi to 19,324 psi required to cause mechanical failure for the Thompson samples. Additionally the static Young's Modulus (*ES*) [as determined by mechanical deformation of the sample] of the Bruske samples was generally higher than Thompson samples, (5.28-7.08) $x10^6$ psi as compared to (~3-5.55) $x10^6$ psi. Likewise the static Poisson's Ratio (μ*S*) for the Bruske samples is higher (0.26-0.28) than the Thompson samples (0.16-0.22).

A higher Young's Modulus and a lower Poisson's Ratio means the Bruske samples will deform in a more brittle fashion than the Thompson samples. An interesting note is that while the Bruske samples have higher compressive strength, it is the Thompson samples that fail truly catastrophically, exhibiting significant stress drops upon failure, as opposed to the much more gentle failures shown by the Bruske samples. This increase in ductility shown by the Bruske samples may be explained by the increased depth, as an increase in depth correlates to an increase in confining pressure, and therefore, ductility. The assumed pressure gradient for the Michigan basin in this study is 0.5 psi/ft, and since an increase in confining pressure corresponds to higher ductility, the results are expected. The Bruske samples were expected to fail in a more brittle fashion than the Thompson samples, primarily due to higher porosity in the Bruske samples. The effect of porosity on mechanical behavior is discussed by Lashkaripour, (2002). The results suggest that confining pressure may be a more determining factor in rock ductility than porosity, at least when the change in confining pressure is significant (> 3,000 psi +). It is difficult to compare these samples because they are tested at vastly different confining pressures to mimic in-situ conditions. Both of the samples analyzed are shown to require thousands of psi higher than what the in-situ stresses are at depth in the subsurface, indicating that the Utica Shale is not likely to succumb to brittle fracture in the subsurface in the Michigan basin.

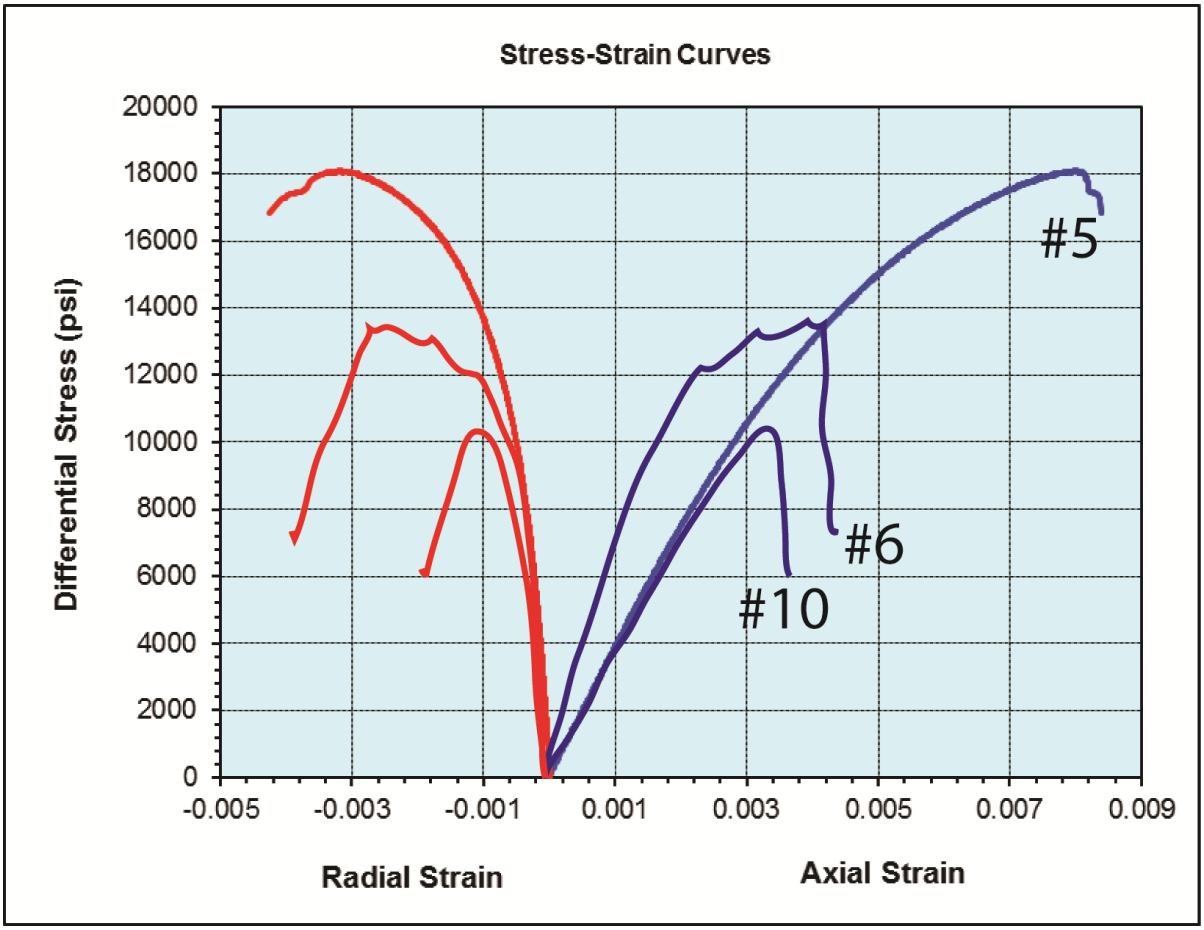

Figure 7- 1: Thompson samples #5, 6 and 10. This graph has been modified in order to quantify anisotropy. A 40% reduction of rock strength is observed at 45% to bedding. Sample #5 is taken at 90^{o} to bedding, sample #6 at 0^{o} to bedding, and sample #10 at 45^{o} to bedding.

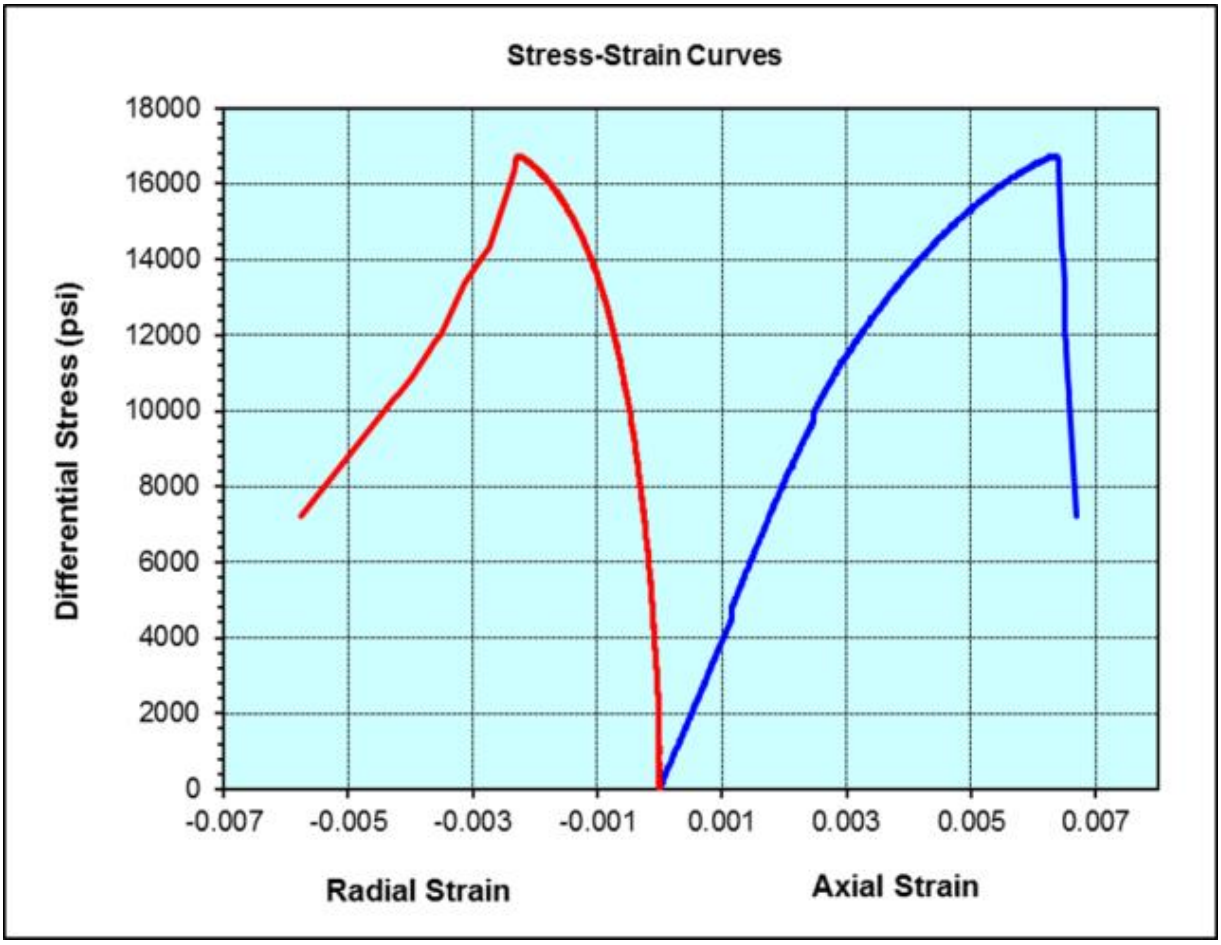

Figure 7- 2: Thompson sample #8. This sample may have errors in the values for elastic parameters due to transducer failure during testing.

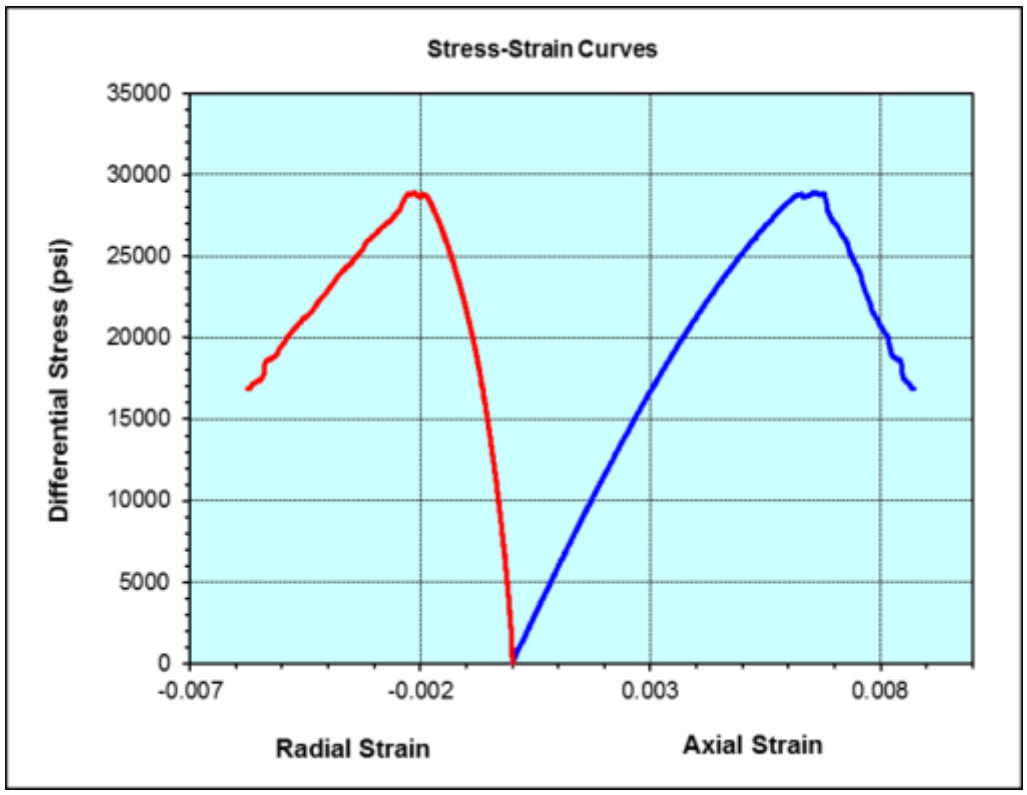

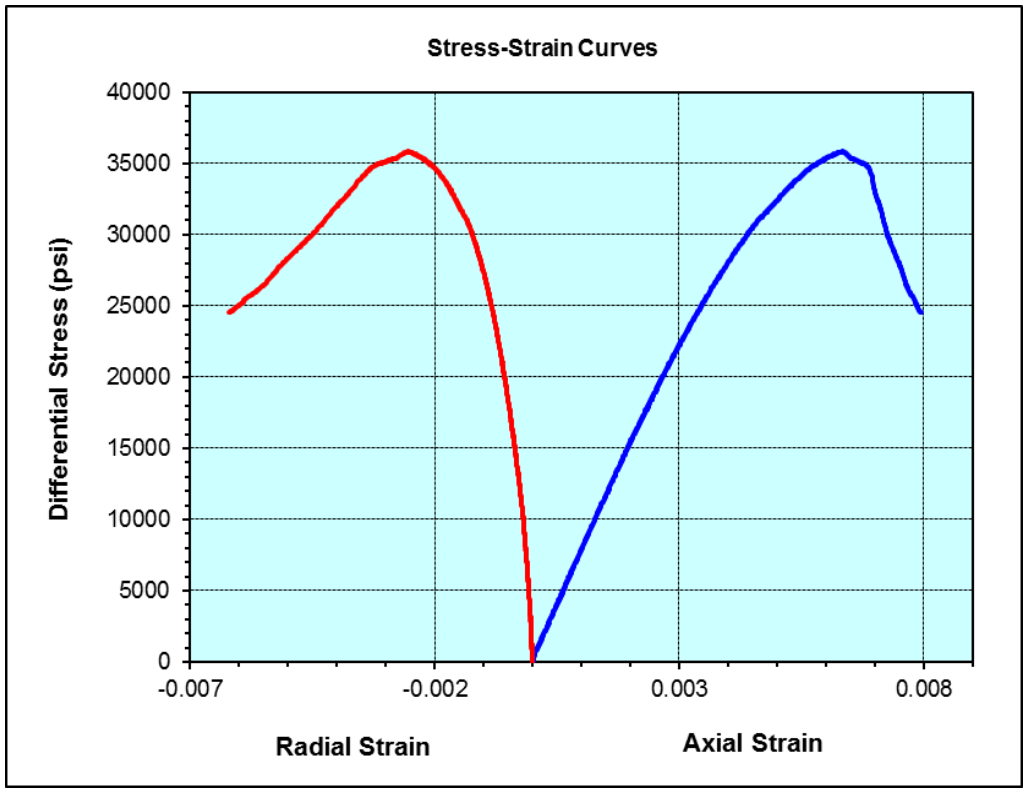

Figure 7- 3a and b: Bruske 1-26A samples #3 and #4. The Bruske samples are seemingly much stronger than the Thompson samples, failing at over 30,000 psi as opposed to

around 15-20k psi. This increase in strength is attributed to testing parameters mimicking in-situ conditions.

Thompson samples 1-30 #6 and #10 were cored parallel to and oblique (45°) to bedding respectively, and they exhibit some mechanical behaviors which can be described as "typical of anisotropic formations". Thompson 1-30 #6 shows a higher value for *ES* ($5.55x10^6$ psi) than the two Thompson samples plugged perpendicular to bedding (#5 & #8), and while the ultimate strength of #6 is slightly lower (14,088 psi) than for the perpendicularly plugged samples, this is likely due to small failures that occurred at ~11,500, 12,500, and 13,000 psi applied differential stress, therefore it is possible that the ultimate strength parallel to bedding is similar to and possibly even in excess of strength perpendicular to bedding. Thompson 1-30 #10, which was plugged oblique to bedding, exhibits a compressive strength (11,591 psi) that is far below the other Thompson samples tested (14,088-19,234 psi), which is a 40% reduction in rock strength at 45^o to bedding. As a result, wellbores drilled at 45^o to bedding are more liable to be subjected to bore hole collapse than wellbores drilled at 90^o to bedding (Kier et al., 2011). The results indicate that while the samples taken at 45^o to bedding are significantly weaker than the samples taken at 90^o or 0^o, the formation is not considered to be highly anisotropic. Highly anisotropic formations may exhibit a loss of strength of up to 85% when tested at 45-55^o to bedding planes (Kier et al., 2011).

Thompson 1-30 sample #8 is shown to have two values of Young's modulus and Poisson's ratio (table 2). During this test one of the axial displacement transducers was reported to have stopped responding at a point when ~26% of failure load was applied, and began responding again when ~60% the failure load was applied. During this time all axial strain measurements were based only on one displacement transducer, and therefore are inaccurate. Before and after this time both transducers were functioning as normal and strain calculations are believed to be correct. Young's modulus and Poisson's ratio are typically measured in the range of 40-50% of failure load. Accurate measurements were therefore not able to be made during the time of 40-50% failure load. The two values provided have been taken during measurements of 21-26% and

60-65% of failure load. These values are then end members of the spectrum for Young's Modulus or Poisson's Ratio.

Measurements of P- and S-wave velocity were conducted on the samples Bruske 1-26A #3 and #4, and Thompson 1-30 #5, all of which were plugged perpendicular to bedding (table 5). The Thompson sample exhibited P- and S-wave velocities of 13,697 ft/s and 8,206 ft/s respectively, and dynamic elastic moduli of E_D=5.86x10^6 psi, K_D=3.52x10^6 psi, and G_D=2.40x10^6 psi, all of which are the lowest of the measured samples, where E_D is the dynamic Young's Modulus, K_D is the dynamic Bulk Modulus, and G_D is the dynamic Shear Modulus. The P-wave (15,758-17,126 ft/s) and S-wave (9,517-10,123 ft/s) velocities of the Bruske samples are slightly higher than those exhibited by the Thompson sample, however the calculated dynamic elastic moduli are markedly higher for the Bruske samples than the Thompson indicating the Bruske samples should behave in a more brittle fashion than the Thompson samples. Dynamic Poisson's ratio for the 3 samples ranges from 0.21 to 0.23, which are within the range of expected values for shale formations with no real variation based on well location.

Sample No.	Depth (ft)	Confining Pressure (psi)	Bulk Density (g/cc)	Ultrasonic Wave Velocity				Dynamic Elastic Parameter			
				Compressional		Shear		Young's Modulus (x10^6 psi)	Poisson's Ratio	Bulk Modulus (x10^6 psi)	Shear Modulus (x10^6 psi)
				ft/sec	µsec/ft	ft/sec	µsec/ft				
1-26A #3	8428.00	4214	2.72	17126	58.39	10123	98.78	9.25	0.23	5.75	3.76
1-26A #4	8470.00	4235	2.72	15758	63.46	9517	105.08	8.02	0.21	4.67	3.31
1-30 #5	2273.30	1137	2.66	13687	73.06	8206	121.86	5.86	0.22	3.52	2.40

Table 5: Results of acoustic velocity testing. Dynamic elastic parameters are within the range of dynamic values calculated through dipole sonic logs.

Triaxial compressive strength tests on 6 samples from the Bruske and Thompson wells indicate that the failure strength of the Bruske samples is in the range of 33,150-40,032 psi at a confining stress of ~4200 psi, as compared to a range of 11,591-19234 psi for the Thompson at a confining pressure of ~1100 psi. Young's Modulus for the Bruske samples ranged from (5.28-7.08) x10^6 psi and the Thompson samples from (2.93-5.55) x10^6 psi.

Measurements of P- and S-wave velocity conducted on 2 Bruske samples and 1 Thompson sample do not show a significant difference, though calculated dynamic elastic parameters would seem to indicate that the Bruske samples are generally stiffer than the Thompson samples. Dynamic Poisson's ratio for all samples was in the narrow range of 0.21-0.23. The dynamic Young's Modulus and Poisson's Ratio values are within range ($\pm 5 \times 10^6$ or ± 0.1) of dynamic values calculated from dipole sonic log data for the Bruske 1-26A well in figure 3-4. This relationship suggests that dipole sonic logs do a reasonable job of estimating dynamic mechanical parameters.

The expected results would be a more brittle deformation for the Bruske samples based on the higher Young's Modulus values, however it is the Thompson samples that have a failure envelope indicating more brittle behavior. This relationship suggests that increasing confining pressure will both increase rock strength and ductility. The primary difference in testing parameter for the Bruske (higher in-situ ambient pressure) and Thompson samples (lower in-situ ambient pressure) is the increase of confining pressure for the Bruske samples. The Thompson samples are buried as shallow as 2,200 ft and were tested with confining pressures as low as 1,137 psi, while the Bruske samples were tested with confining pressures of 4,200+ psi. The typical overburden of the Utica Shale in the Michigan basin is well over 2,600 ft (figure 7-4, below). The in-situ confining pressures for the Utica Shale across most of the Michigan basin will therefore be elevated as compared to the Thompson well.

Results generated by triaxial strength testing and acoustic velocity testing are consistent with those expected in a geologic seal. The compressive strength of the Utica Shale in laboratory testing is well in excess of subsurface in-situ confining pressures. The United States Environmental Protection Agency (EPA) controls regulations for carbon dioxide (Class VI) injection wells. The EPA requires extensive site characterization and operators are restricted to injection pressures such that pressure in the injection zones does not exceed 90% of the fracture pressure of the injection zone. The calculated fracture pressure (injection pressure limit) is based on site-specific geologic and geomechanical data. The pressure would therefore be dependent on the

mechanical properties of the injection zone underlying the Utica. If the injection zone involved the Utica Shale in Lenawee or Osceola counties the fracture pressure that operators would be allowed to inject under would be 90% of the reported results (table 4).

The values for Poisson's ratio and Young's modulus suggest the Utica Shale will deform in a ductile fashion, and is strong enough to withstand in-situ pressure conditions in the Michigan basin. The mechanical properties measured in this study provide evidence that the Utica Shale will not undergo brittle deformation (causing fractures) in the subsurface, and injection pressures (as regulated by the US EPA) would be dependent on the injection zone for each prospective well. Laboratory testing of core plugs from Utica Shale cores suggest that the Utica Shale is a strong and ductile mudrock formation, ideal for a regional geologic seal.

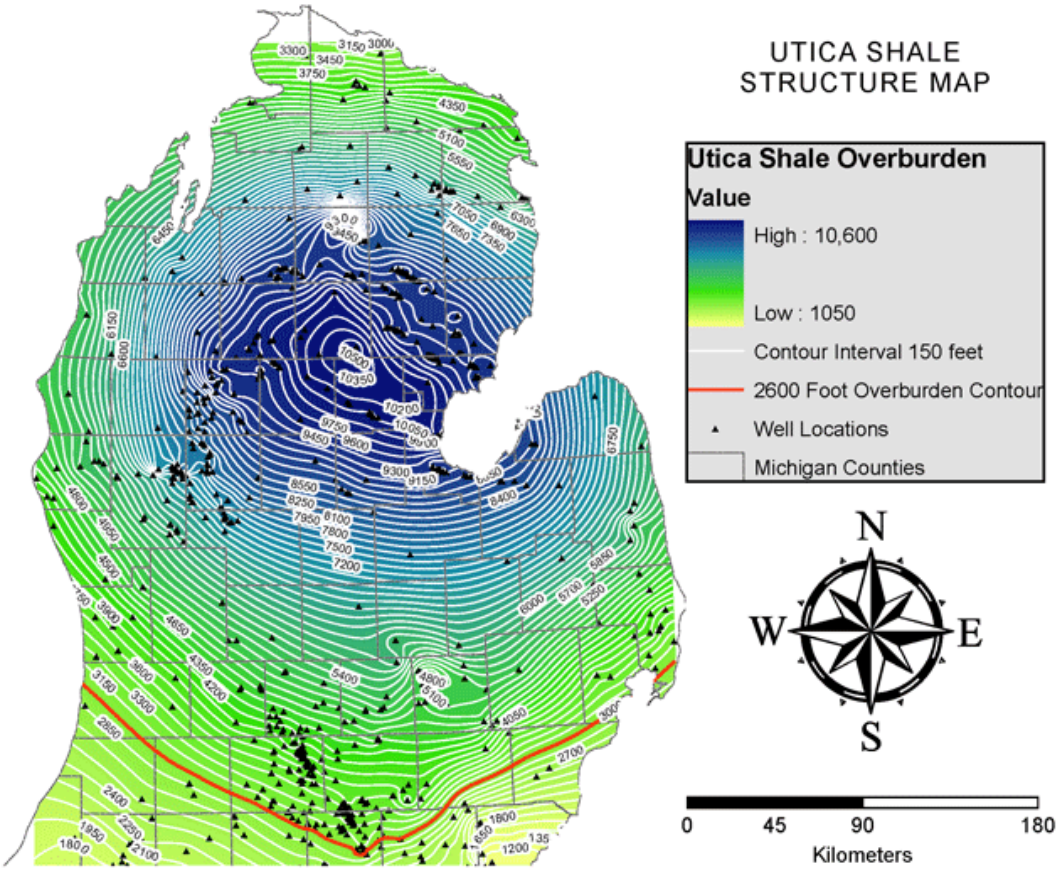

Figure 7- 4: Utica (Shale) Formation overburden. The burial depth of the Utica Shale over much of the Michigan basin suggests it will exhibit ductile deformation, and will require failure pressures much higher than are expected in the subsurface.

Contour interval shown in legend

Modified from Barnes, D.A. (knoxstp.org/mi-strat.htm)

8. DISCUSSION AND CONCLUSIONS

The Utica Shale in the Michigan basin is a thick, mud-rich rock that is laterally persistent through the entire basin. The clay fraction of the Utica frequently makes up over 50% of the whole rock mineralogy, with some samples composed of as high as 70% or more clay minerals. The mineralogy may vary considerably over short distances, as evidenced by the increased carbonate content in the Thompson 1-30 well in Lenawee County which is not observed in the Arco-Conklin well in nearby Jackson County. Dolomite is the most common authigenic carbonate mineral observed in SEM analysis, commonly observed replacing calcite. Pores are observed to be primarily on the nanometer scale, with most of the intrusion of the non-wetting fluid phase likely to take place in pores with breakthrough pressures corresponding to massive (>1,000 ft) CO_2 columns. Mechanical testing suggests ductile deformation for in-situ conditions, with deformation occurring at fracture pressures that are 10's of thousands of pounds per square inch (psi) higher than expected in the subsurface. Increased confining pressures associated with significant burial depth (> 3,000 ft) will result in increased rock strength. Nanometer scale pore space, ductile deformation and significant burial depth allow for subsurface conditions ideal for a regional geologic mudrock seal.

Lack of core availability for much of the state may provide some amount of error. The core used in this study is not distributed equally throughout the state, and therefore there are large areas where no sampling has been done. South of the Saginaw Bay area there are only four cores studied, all located in or around the southeastern subbasin. Wire-line log correlations do not suggest a significant change in mineralogy or rock properties but the absence of data should be noted. Mechanical testing was completed on only 2 wells during this study. The Thompson 1-30 and Bruske 1-26A wells have elevated carbonate content which made plugging the core easier. It was difficult to take plugs from rock with high clay content and lack of full or "butt-end" core made it impossible to sample each core stored at the MGRRE facility. Mercury Injection Capillary Pressure (MICP) analysis provided values for the Weingartz well of

permeability and porosity that may vary significantly from true subsurface conditions due to multiple bedding plane fractures. These fractures (as previously discussed) are not believed to be open in the subsurface. Mercury entering this artificial fracture network is likely being misinterpreted as porosity that would otherwise be unavailable in the subsurface. The MICP results did indicate that at 35% saturation of the pore throats, the required breakthrough pressures for supercritical CO_2 correspond to large buoyant super-critical CO_2 columns.

Various analytical techniques have been utilized in this study in order to characterize the Utica Shale in the Michigan basin. X-ray diffraction, SEM petrography, MICP testing and mechanical testing have been used to determine and predict lithologic properties of the Utica Shale in the subsurface. The results from each technique are compatible, providing concrete evidence that the Utica Shale contains abundant clay minerals, contains mostly nano-scale pore throats, and has enough strength to withstand in-situ pressure condition and not fracture in the subsurface. Quantitative mineralogical analysis that confirms the Utica Shale is composed of greater than 50% clay minerals is consistent with mechanical testing results indicating that the Utica Shale will deform in a ductile fashion at significant burial depths. Mechanical testing also confirms that stresses required to induce failure are significantly higher than in-situ stress conditions and allow for a high frac pressure gradient when injecting into underlying strata. This study confirms that the Utica Shale will behave as a regional geologic seal for the sequestration of supercritical CO_2 into underlying Cambro-Orodovician injection targets.

REFERENCES

Banas, R.M. (2011). A Geophysical and Geological Analysis of the Collingwood Member of the Trenton Formation. Master's Thesis, Michigan Technological University. 74 pp.

Brie, A., Endo, T., Hoyle, D., Codazzi, D., Esmersoy, C., Hsu, S, Denoo, S., Mueller, M.C., Plona, T., Shenoy, R., Sinha, B. (1998). New Directions in Sonic Logging. Oilfield Review pp. 40-55.

Brogly, P.J., Martini, I.P., Middleton, G.V. (1998). The Queenston Formation: shale-dominated, mixed terrigenous-carbonate deposits of Upper Ordovician, semiarid, muddy shores in Ontario, Canada. Canadian Journal of Earth Sciences. V. 35 pp. 702-719.

Buller, D., Hughes, S., Market, J., Petre, E., Halliburton, and Spain, D., Odumosu, T., BP America. (2010). Petrophysical Evaluation for Enhancing Hydraulic Stimulation in Horizontal Shale Gas Wells. SPE Annual Technical Conference. SPE 132990.

Ding, W., Li, C., Li, C., Xu, C., Jiu, K., Zeng, W., Wu, L. (2012). Fracture development in shale and its relationship to gas accumulation. Geoscience Frontiers. V. 3(1) pp. 97-105.

Donald, A., Paxton, A., Keir, D., Koster, K. (2009). Improving seismic calibration and geomechanical models through characterization of anisotropy using single and multi well data: Case Study in Forties Field, UK. SEG Houston 2009 International Exposition and Annual Meeting pp. 557-561.

Eberl, D. D. (2003). User's Guide to RockJock—A Program for Determining Quantitative Mineralogy from Powder X-Ray Diffraction Data. U.S. Geological Survey. Open-File Report 03-78.

Faill, R. T. (1997). A geologic history of the north-central Appalachians, Part 1. Orogenesis from the Mesoproterozoic through the Taconic orogeny. American Journal of Science. Vol. 297. pp. 551-619.

Harrison III, W. B., Grammer, G. M., Barnes, D.A. (2009). Reservoir characteristics of the Bass Islands dolomite in Otsego County, Michigan: Results for a saline reservoir CO_2 sequestration demonstration. Environmental Geosciences. V. 16 pp. 139-151.

Hartmann, D. J., and E. A. Beaumont, (1999). Predicting reservoir system quality and performance, in E. A. Beaumont and N. H. Foster, eds., Exploring for oil and gas traps: AAPG Treatise of Petroleum Geology, Handbook of Petroleum Geology, pp. 9-1– 9-154.

Hiattt, C. R., (1985). A Petrographic, Geochemical, and Well Log Analysis of the Utica Shale-Trenton Limestone Transition in the Northern Michigan Basin. Master's Thesis. Michigan Technological University. 204 p.

Horsrud, P. (2001). Estimating Mechanical Properties of Shale From Empirical Correlations. SPE SINTEF Petroleum Research. pp 68-73.

Hoshino, K., Koide, H., Inami, K., Iwamura, S., Mitsui, S., (1972). Mechanical properties of Japanese Tertiary sedimentary rocks under high confining pressures: Geological Survey of Japan Report 244, pp. 200

Howell, P.D., Van der Pluijm, B.A., (1990). Early history of the Michigan basin: Subsidence and Appalachian tectonics. Geology. V. 18. pp. 1195-1198.

Howell, P.D., Van der Pluijm, B.A., (1999). Structural sequences and styles of subsidence in the Michigan Basin: Geological Society of America Bulletin; July 1999; v.111; no. 7; pp. 974-991.

IEAGHG, "Caprock Systems for CO_2 Geological Storage", 2011/01, May, 2011

Keir, D., McIntyre, B., Hibbert, T., Dixon, R.,Koster, K., Mohamed, F., Donald, A., Syed, A., Liu, S., O'Rourke, T., Paxton, A., Horne, S., Knight, E. (2011). Correcting sonic logs for shale anisotropy: a case study in the Forties field. Rock Physics and Formation Evaluation. First Break vol. 29 pp. 81-86.

Kuila, U., et al., Stress anisotropy and velocity anisotropy in low porosity shale, Tectonophysics (2010), doi:10.1016/j.tecto.2010.09.023 11 pp

Lashkaripour, G.R. (2002). Predicting mechanical properties of mudrock from index parameters. Bulletin of Engineering Geology and the Environment. V. 61. pp. 73-77.

"Michigan Stratigraphy." *Michigan Stratigraphy*. University of Illinois Board of Trustees, n.d. Web. 29 Aug. 2013. http://www.knoxstp.org/mi-strat.htm

Miller, D.E., Plumb, R., Boitnott, G. (2012). Compressive strength and elastic properties of a transversely isotropic calcareous mudstone. Submitted to Geophysical Prospecting 1IWRP Special Issue. 29 pp.

Moore, D.M., Reynolds, R.C. Jr. (1989). X-Ray Diffraction and the Identification and Analysis of Clay Minerals. Oxford University Press pp.332

Mullen, M., Roundtree, R., Halliburton and Barree, B., and Assocs. (2007). A Composite Determination of Mechanical Rock Properties for Stimulation Design (What To Do When You Don't Have a Sonic Log). SPE 108139 pp 13.

Nygaard, R. (2010). Geomechanical Analysis: Wabamun Area CO_2 Sequestration Project (WASP). Energy and Environmental Systems Group; Institute for Sustainable Energy, Environment and Economy (ISEEE). University of Calgary 14 pp.

Rancourt, C. (2009). "Collingwood" Strata in South-Central Ontario – A Petrophysical Chemostratigraphic Approach to Comparison and Correlation Using Geophysical Borehole Logs. Master's Thesis, University of Toronto, 65 pp.

Rickman, R., Mullen, M., Petre, E., Grieser, B., and Kundert, D., SPE and Halliburton. (2008). A Practical Use of Shale Petrophysics for Stimulation Design Optimization: All Shale Plays Are Not Clones of the Barnett Shale. SPE 115258. pp 11.

Rodgers, J. (1971). The Taconic Orogeny. Geological Society of America Bulletin. No 5; pp. 1141-1178

Rupp, J. A. (1997). Tectonic features of Indiana: Indiana Geological Survey Web page, <http://igs.indiana.edu/Geology/structure/tectonicfeatures/index.cfm>, date accessed September 07, 2013.

Preibisch, S., Saalfeld, S., Tomancak, P. (2009). Globally Optimal Stitching of Tiled 3D Microscopic Image Acquisitions. Systems Biology. Vol. 23 no. 11 pp. 1463-1465.

Sharma, S. (2004). Geochemistry and Sedimentology of Upper Ordovician Mudrocks and Limestones, Eastern Ontario: A New Sedimentary Framework for the Distal Taconic Foreland. Master's Thesis. Carleton University. 240 pp.

Sharma, S., Dix, G.R., Riva, J.F.V. (2003). Late Ordovician platform foundering, its paleoceanography and burial, as preserved in separate (eastern Michigan Basin, Ottawa Embayment) basins, southern Ontario. Canadian Journal of Earth Science. V. 40. pp. 135-148.

Środoń, J., Drits, V.A., McCarty, D.K., Hsieh, J.C.C. Eberl, D.D. (2001). Quantitative X-Ray Diffraction Analysis of Clay-Bearing Rocks from Random Preperations. Clays and Clay Minerals. V. 49, No. 6, pp. 514-528.

Swift, A.M., Anovitz, L.M., Sheets, J.M., Cole, D.R., Welch, S.A., Rother, G. (2014). Relationship between Mineralogy and Porosity in Seals Relevant to Geologic CO_2 Sequestration. The Ohio State University. pp. 49

Tucker, M.E. (2001). Sedimentary Petrology 3rd edition. An Introduction to the Origin of Sedimentary Rocks. Blackwell Publishing. pp. 262

"USGS Releases First Assessment of Shale Gas Resources in the Utica." Targeted News ServiceOct 04 2012. ProQuest. Web. 13 Aug. 2013 .

United States Geological Survey. (2003). “The Highlands Province”. ProQuest. July 22 2003. Web. 01 Oct. 2014.

Wicander, R., Monroe, J.S., (2000). Historical Geology: Evolution of Earth and Life Through Time. 3rd edition. Brooks/Cole Thomson Learning.